Bioengineering approaches in immunotherapy: from basic to translational applications

THÈSE N^{O} 6909 (2016)

PRÉSENTÉE LE 15 MARS 2016

À LA FACULTÉ DES SCIENCES DE LA VIE
CHAIRE MERCK-SERONO EN TECHNOLOGIES D'ADMINISTRATION DE MÉDICAMENTS
PROGRAMME DOCTORAL EN BIOTECHNOLOGIE ET GÉNIE BIOLOGIQUE

ÉCOLE POLYTECHNIQUE FÉDÉRALE DE LAUSANNE

POUR L'OBTENTION DU GRADE DE DOCTEUR ÈS SCIENCES

PAR

Martina DAMO

acceptée sur proposition du jury:

Prof. F. G. van der Goot Grunberg, présidente du jury
Prof. J. A. Hubbell, directeur de thèse
Prof. D. Speiser, rapporteur
Prof. S. Turley, rapporteuse
Prof. N. Harris, rapporteuse

ÉCOLE POLYTECHNIQUE
FÉDÉRALE DE LAUSANNE
Suisse
2016

Abstract

Immunotherapies have been developed with the aim of modulating the components of the immune system to provide therapeutic benefit.

Vaccination has been regarded to as the most attractive immunotherapy for cancer because of its ability to instruct immune cells to recognize and kill tumor cells. Exosomes are one of the most recent discoveries translated from basic biology into experimental vaccine therapy of cancer. Exosomes are 30-150 nm membrane vesicles released by many cell types. In particular, dendritic cell (DC)-derived exosomes (Dexo) inherit the molecules that make DCs able to activate antigen-specific immunity. As a consequence, Dexo have been tested in clinical trials for the vaccination of melanoma and lung carcinoma patients, however resulting in poor therapeutic outcomes due to weak immunogenicity. We therefore developed a protocol for the production of Dexo with improved immunogenic properties by exploiting the physiological ability of DCs to mature into immunostimulatory cells in the presence of antigens and immunogenic signals. We cultured Dexo-producing DCs with a murine melanoma cell lysate, that provided tumor antigens, and poly(I:C), a synthetic nucleic acid analog that provided immunogenic signals. The result was a Dexo vaccine capable of eliciting robust tumor-specific immunity in melanoma-bearing mice, leading to significantly reduced tumor growth and enhanced survival of experimental mice. These data indicate our strategy as a valuable improved alternative to currently available protocols for the production of potent tumor-tailored Dexo vaccines.

A healthy immune system recognizes and eliminates potentially harmful agents avoiding collateral damage to normal self tissues, which are spared from immune aggression via the establishment of immune tolerance to self antigens. Tolerance is developed in both central lymphoid organs (central tolerance) and peripheral lymphoid and non-lymphoid organs (peripheral tolerance). The liver has recently been attributed an important role in peripheral tolerogenesis to circulating extracellular antigens, mainly due to the antigen scavenging properties of liver sinusoid endothelial cells. However, even though hepatocytes are the most abundant cell type of the liver and possess enzymatic activities necessary for processing of blood-borne molecules, their ability to take up and induce tolerance to extracellular antigens has yet to be explored. In this thesis we show for the first time *in vitro* and *in vivo* that hepatocytes efficiently take up, process and present extracellular antigens on MHC-I complexes inducing $CD8^+$ T cell tolerance. We also show that the negative regulatory PD-1/PD-L1 pathway is involved in hepatocyte-dependent tolerogenesis. Therefore, we propose

that hepatocytes are instrumental in the establishment and maintenance of liver-mediated peripheral tolerance towards extracellular antigens reaching the liver through the bloodstream.

In addition, this thesis also provides evidence that hepatocytes are capable of directly expressing antigens specific of other peripheral tissues, a process known as promiscuous gene expression. Promiscuous gene expression allows to broaden the pool of self antigens presented to T lymphocytes in central and peripheral lymphoid organs, thus increasing the likelihood of inducing T cell tolerance to self antigens. We describe here for the first time that Deaf1, a transcription factor involved in promiscuous gene expression, is significantly expressed in murine hepatocytes, together with other well characterized peripheral tissue-restricted antigen-coding genes, such as insulin. Even though preliminary, these data further suggest a central role of hepatocytes in peripheral tolerogenesis and confirm the relevance of hepatocyte-targeted approaches as valuable immunotherapy candidates for the treatment of autoimmunity and hepatic chronic infections.

Key words: immunotherapy, cancer, exosomes, hepatocyte, tolerance, peripheral tissue-specific antigen.

Riassunto

L'immunoterapia è stata introdotta allo scopo di modulare il sistema immunitario e fornire beneficio terapeutico.

La vaccinazione è considerata l'immunoterapia più interessante per il cancro grazie alla sua capacità di istruire le cellule immunitarie a riconoscere ed uccidere le cellule tumorali. Gli exosomi sono tra le scoperte più recenti della biologia cellulare ad essere state applicate come vaccini sperimentali per il cancro. Gli exosomi sono vescicole membranose di 30-150 nm rilasciate da molteplici tipi cellulari. In particolare, gli exosomi derivati da cellule dendritiche (CD) (Dexo) ereditano le molecole che permettono alle CD di attivare risposte immunitarie antigene-specifiche. Di conseguenza, i Dexo sono entrati in sperimentazione clinica per la vaccinazione di pazienti affetti da melanoma e carcinoma del polmone, dando tuttavia scarsi risultati terapeutici a causa della loro debole immunogenicità. Abbiamo quindi messo a punto un protocollo per la produzione di Dexo più immunogenici sfruttando la capacità fisiologica delle CD di maturare in cellule immunogeniche in presenza di antigeni e segnali immunostimolatori. Le CD sono state coltivate con un lisato di cellule di melanoma murino, fonte di antigeni tumorali, e poly(I:C), un analogo sintetico degli acidi nucleici usato come segnale immunogenico. Ne è risultato un Dexo vaccino capace di stimolare una robusta risposta immunitaria anti-tumorale in topi affetti da melanoma, di ridurre significativamente la crescita tumorale e aumentare la sopravvivenza dei topi trattati. I dati indicano che la nostra strategia è una valida alternativa ai protocolli attualmente disponibili per la produzione di Dexo vaccini efficaci e specifici.

Un sistema immunitario sano riconosce ed elimina agenti potenzialmente pericolosi evitando danni collaterali ai tessuti normali, risparmiati dall'aggressione immunitaria grazie alla tolleranza verso gli antigeni del self. La tolleranza si sviluppa sia in organi linfoidi centrali (tolleranza centrale) che in organi linfoidi e non-linfoidi periferici (tolleranza periferica). Di recente, al fegato è stato riconosciuto un ruolo importante nello sviluppo di tolleranza periferica verso antigeni extracellulari circolanti nel sangue, soprattutto per le proprietà fagocitiche delle cellule endoteliali sinusoidali epatiche. Tuttavia, anche se gli epatociti sono le cellule epatiche più numerose e possiedono attività enzimatiche per la degradazione di molecole derivanti dal sangue, la loro capacità di endocitare antigeni extracellulari e indurre tolleranza non è ancora stata esplorata. In questa tesi si dimostra per la prima volta sia *in vitro* che *in vivo* che gli epatociti endocitano, degradano e presentano sull'MHC-I antigeni extracellulari inducendo tolleranza nelle cellule T $CD8^+$. Inoltre, si dimostra che le interazioni

tra PD-1 e PD-L1 sono coinvolte nel processo tollerogenico da parte degli epatociti. Proponiamo quindi che gli epatociti svolgono un ruolo di primaria importanza nello sviluppo e nel mantenimento della tolleranza periferica nei confronti di quegli antigeni che raggiungono il fegato attraverso la circolazione sanguinea.

Inoltre, in questa tesi si dimostra anche che gli epatociti sono capaci di esprimere antigeni specifici di altri tessuti periferici, un processo noto come espressione genica promiscua e che permette di aumentare la capacità di presentazione di antigeni del self ai linfociti T negli organi linfoidi centrali e periferici, incrementando di conseguenza la probabilità di indurre tolleranza delle cellule T agli antigeni del self. Riportiamo qui per la prima volta che Deaf1, un fattore di trascrizione coinvolto nell'espressione genica promiscua, è espresso dagli epatociti, assieme ad altri geni che esprimono antigeni tissutali periferici, come l'insulina. Anche se preliminari, questi dati contribuiscono all'ipotesi che gli epatociti abbiano un ruolo centrale nello sviluppo di tolleranza periferica e confermano l'importanza di approcci che targhettano gli epatociti come validi candidati per l'immunoterapia delle malattie autoimmuni e delle infezioni epatiche croniche.

Parole chiave: immunoterapia, cancro, exosomi, epatocita, tolleranza immunologica, antigene tissutale periferico.

Résumé

L'immunothérapie a été développée dans le but de moduler les composants du système immunitaire et de fournir ainsi des bénéfices thérapeutiques.

La vaccination est considérée comme l'immunothérapie la plus attractive contre le cancer, de par sa capacité à éduquer les cellules immunitaires à reconnaître et tuer les cellules tumorales. Les exosomes sont parmi les plus récentes découvertes de la biologie cellulaire ayant été appliquées comme vaccin expérimental contre le cancer. Ce sont des vésicules membranaires de 30-150 nm sécrétées par plusieurs types cellulaires. En particulier, les exosomes dérivés des cellules dendritiques (CD) (Dexo) héritent des molécules permettant aux CDs d'activer une immunité spécifique à l'antigène. De ce fait, les Dexo ont été testés en essais cliniques sur des patients atteints de mélanomes et carcinomes pulmonaires, avec des résultats thérapeutiques limités en raison de leur faible immunogénicité. Par conséquent, nous avons développé un protocole permettant la production de Dexo plus immunogènes en exploitant la capacité physiologiques des CDs à mûrir en cellules immunostimulantes en présence d'antigènes et de signaux immunogéniques. Nous avons cultivé les CDs avec un lysat cellulaire de mélanome murin, fournissant les antigènes tumoraux, et poly(I :C), un analogue synthétique d'acides nucléiques utilisé comme signal immunogénique. Il en résulte un Dexo vaccin capable de stimuler une réponse immunitaire robuste dans des souris atteintes de mélanome, réduisant significativement la croissance tumorale et augmentant l'espérance de vie des souris traitées. Ces données montrent que notre stratégie est une alternative valide aux protocoles actuels de production de vaccins Dexo efficaces et spécifique à la tumeur.

Un système immunitaire sain reconnaît et élimine les agents dangereux en évitant les dommages collatéraux sur les tissus, qui sont épargnés grâce l'établissement d'une tolérance immunitaire aux antigènes du soi. La tolérance est développée à la fois dans les organes lymphoïdes centraux (tolérance centrale) et les organes lymphoïdes et non-lymphoïdes périphériques (tolérance périphérique). Le foie a récemment été attribué d'un rôle important dans la tolérogénèse périphérique aux antigènes extracellulaires circulants dans le sang, principalement dû aux propriétés phagocytiques des cellules endothéliales sinusoïdales hépatiques. Cependant, bien que les hépatocytes soient le type cellulaire le plus abondant du foie et possèdent des activités enzymatiques nécessaires à la dégradation des molécules et des antigènes, leur aptitude à endocytoser les antigènes et induire de la tolérance reste à explorer. Dans cette thèse, nous avons montré pour la première fois *in vitro* et *in vivo* que les hépatocytes endocytosent, dégradent et présentent efficacement les antigènes extracellulaires

sur les complexes MHC-I, ce qui induit la tolérance des cellules T $CD8^+$. Nous avons également montré que la régulation négative de la voie de signalisation PD-1/PD-L1 est impliquée dans la tolérogénèse dépendante des hépatocytes. Ainsi, nous suggérons que les hépatocytes sont essentiels dans l'établissement et la maintenance de la tolérance périphérique médiée par le foie contre les antigènes extracellulaires provenant du sang.

De plus, cette thèse démontre également que les hépatocytes sont capables d'exprimer directement des antigènes spécifiques d'autres tissus périphériques. Ce processus est appelé « l'expression promiscuitaire de gènes», et permet d'élargir la collection des antigènes du soi présentés aux lymphocytes T dans les organes lymphoïdes centraux et périphériques ; il permet donc d'accroître la probabilité d'induire la tolérance des cellules T aux antigènes du soi. Nous décrivons ici pour la première fois que Deaf1, un facteur de transcription impliqué dans l'expression génique promiscuitaire, est significativement exprimé dans les hépatocytes murins, parmi d'autres gènes codant pour des antigènes spécifiques des tissus périphériques, tel que l'insuline. Bien que préliminaires, ces données appuient le rôle central des hépatocytes dans la tolérogénèse périphérique et confirme la pertinence des approches ciblées sur les hépatocytes dans le développement d'immunothérapies pour les maladies auto-immunes et les infections hépatiques chroniques.

Mots clés: immunothérapie, cancer, exosomes, hépatocyte, tolérance immunitaire, antigène spécifique d'autres tissus périphériques.

Table of contents

Chapter 1

Thesis overview & Introduction

1.1 Motivation

Immunotherapies comprise several therapeutic approaches that aim at providing benefits by modulating the immune system. The unique advantage of using the immune system for therapeutic purposes over other therapies derives from its intrinsic capacity to discriminate self from non-self, thus providing a tool able to specifically attack and eliminate harmful agents limiting collateral damage to healthy tissues [1]. Basic and translational research for the development of immunotherapies have significantly improved the treatment of two major classes of diseases, cancer and autoimmune pathologies.

Cancer is a heterogeneous group of diseases that arise when normal cells acquire a phenotype characterized by abnormal and uncontrolled growth and invasiveness as a result of progressive accumulation of genetic mutations [2]. In 2012, 14.1 million people were diagnosed with cancer and 8.2 million people died because of cancer worldwide. While the incidence of cancer has been increasing, the death rate among cancer patients has been constantly declining since the early 90's [3]. The reduction of cancer deaths is the result of multiple factors. Most importantly, oncological research has provided new insights into the mechanisms of carcinogenesis and has allowed the translation of such knowledge into novel therapies. In particular, the role of the immune system in the control of tumor development has been recognized and exploited for the development of therapies aimed at enhancing anti-cancer immunity. Unlike pre-clinical research, clinical trials for cancer immunotherapy have given disappointing results, and thus oncological research and novel therapies are greatly needed [1,4]. In this Ph. D. thesis we applied bioengineering approaches to improve the immunogenicity of dendritic cell-derived exosome-based vaccines, that had been previously tested in clinical trials for the immunotherapy of cancer [7,8]. The data presented here show encouraging results obtained in a murine model of melanoma treated with the improved exosome formulation we developed. Due to the positive therapeutic outcomes we observed as compared to previous publications and the ease of manufacturing of our system, the exosome immunotherapy approach described in this thesis could be easily translated into human application.

Autoimmune diseases are a group of more than 80 pathologies characterized by abnormal and exaggerated immunity against self tissues. Type 1 diabetes, rheumatoid arthritis, multiple sclerosis and systemic lupus erythematosus represent some of the most common autoimmune pathologies. It is calculated that 3 to 8% of the population worldwide is affected by an autoimmune disease [5]. The pathogenesis of autoimmunity is the direct consequence of an immune dysfunction. Therefore, immunotherapy aimed at suppressing

immunity and resetting immune homeostasis has been considered the most straightforward treatment for affected individuals [1]. Even though research has provided a wealth of new information on the physiology of the immune system and on some of the mechanisms of autoimmunity, clinical applications of autoimmune disease immunotherapies have resulted in incomplete therapeutic benefits for the patients [1,6]. Therefore, it is imperative to develop new knowledge and possibly novel therapeutic tools for autoimmunity.

For this Ph. D. thesis, we took advantage of engineering strategies to modify model protein antigens and study how hepatocytes, previously thought to contribute poorly to the modulation of immune responses towards extracellular antigens [9], instead, play an important role in the establishment of immune tolerance towards exogenous antigens. These results are of particular interest in light of the fact that the liver, mostly known for its blood-filtering and metabolic functions, has been recently associated with immunomodulatory functions [10]. The observations described in this thesis not only contribute to a better understanding of immune physiology, but also open the way to the development of hepatocyte-targeting therapeutic strategies for the treatment of autoimmune diseases, immunity against protein therapeutics and hepatic chronic viral infections.

Last, this Ph. D. thesis also provides new insights into basic mechanisms of immune tolerance involving the liver, which we found to contain cells expressing peripheral tissue-specific antigens, suggesting that hepatic cells might have a role similar to other cells located in lymphoid tissues in the maintenance of self tolerance [11-15]. These data further support liver-targeting therapeutics as promising candidates for novel autoimmune disease immunotherapies.

1.2 Background

1.2.1 Immunity vs. Tolerance: the two sides of the same system

The immune system is responsible for maintaining the integrity of the organism both against exogenous insults (pathogen infections) and endogenous threats (cancer). The capability of the immune system to eliminate harmful agents is the result of a delicate balance between immunity and tolerance, as the activation of an immune response (immunity) should occur after recognition of non-self or mutated-self components leading to their elimination but avoiding damage to normal self components (tolerance). This capacity to discriminate self from non-self or mutated-self is the fundamental feature of a healthy immune system and, as such, it is established early during the development of adaptive immune cells in central lymphoid organs and continuously guaranteed by immune regulatory mechanisms and check-points in peripheral lymphoid and non-lymphoid organs [16].

Unlike innate immune responses, that are elicited by conserved pathogen-associated molecular patterns (PAMPs) and that lead to the activation of general innate host defense mechanisms such as inflammation, adaptive responses are tailored for specific non-self components, resulting in the production of antibodies and cellular responses targeted to that particular intruder [17-20]. The specificity and magnitude of adaptive immune responses, especially for T lymphocytes, are the result of three types of signal that need to be co-delivered to adaptive immune cells in order to induce their functional activation: antigen presentation, co-stimulation and secreted mediators (cytokines) (Fig. 1.1) [21].

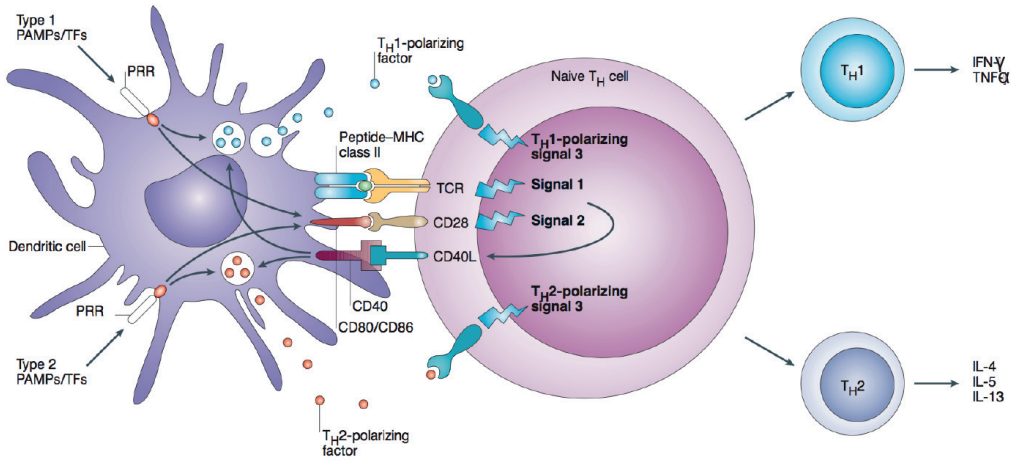

Figure 1.1 Signals leading to T cell activation. Antigen presentation (peptide/MHC), co-stimulation (CD28, CD80 and CD86) and secreted factors (cytokines) are the three signals that altogether shape and orchestrate the type of immune response necessary to protect our body from a specific threat (adapted from Kapsenberg, M. L., *Nat. Rev. Immunol.*, 2003).

T lymphocytes express T cell receptors (TCRs) able to recognize an antigen loaded onto major histocompatibility complex (MHC) molecules on the surface of antigen-presenting cells (APCs). MHC class I (MHC-I) molecules are expressed by every nucleated cell of the organism and allow the display of cellular peptides derived from intracellular protein turnover (direct presentation) and, in some subsets of cells, endocytosis of extracellular antigens (cross-presentation). In both cases, cognate peptide/MHC-I complexes are recognized by $CD8^+$ T lymphocytes (Fig. 1.2a,b) [22,23]. MHC class II (MHC-II) molecules, instead, are expressed by dedicated cell subsets with professional APC functions, including cells of the innate immune system like dendritic cells (DCs) and some non-hematopoietic cells with enhanced antigen-presenting properties. Antigen presentation on the MHC-II requires antigen uptake from the extracellular environment, followed by lysosomal degradation and complexing of the antigen-derived epitopes to MHC-II molecules, which are then translocated

to the cell membrane. Cognate peptide/MHC-II complexes are recognized by the TCR of $CD4^+$ T lymphocytes (Fig. 1.2c) [22].

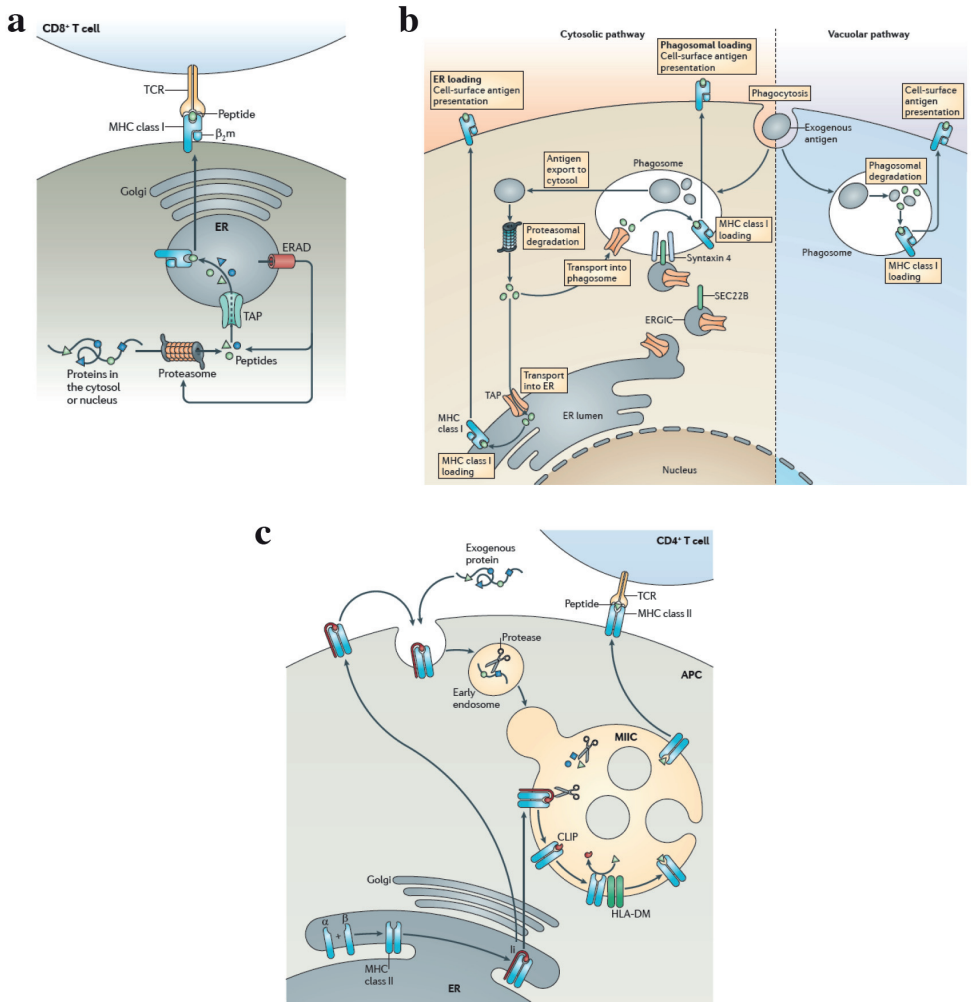

Figure 1.2 Antigen presentation pathways. (a) Direct antigen presentation: intracellular antigens are processed by the proteasome and loaded on MHC-I molecules to be presented to $CD8^+$ T lymphocytes. (b) Antigen cross-presentation: extracellular antigens are phagocytosed and processed by proteasomal degradation for presentation to $CD8^+$ T cells in the context of the MHC-I. (c) Extracellular antigens are endocytosed, digested in endosomes and loaded on MHC-II complexes for presentation to $CD4^+$ T lymphocytes (adapted from Neefjes, J. *et al*, *Nat. Rev. Immunol*., 2011 and Joffre, O. P. *et al*., *Nat. Rev. Immunol*., 2012).

In case of ongoing infections, tissue damage or developing cancerous lesions, danger signals are shed and sensed by innate immune cells, especially DCs. Pathogen-derived danger signals, such as PAMPs, and cell-derived danger signals, such as death-associated molecular patterns (DAMPs), bind to and trigger the activation of pattern recognition receptors (PRRs), among which Toll-like receptors (TLRs). Signal transduction originated from PRR triggering induces several changes in the phenotype of APCs, resulting in their maturation [21]. One of the

hallmarks of DC maturation is the improvement of antigen-presenting and adaptive immune cell stimulatory capabilities, exemplified by the upregulation of MHC-I and II molecules and of surface co-stimulatory molecules, such as CD80 and CD86. CD80 and CD86, in turn, bind to and activate CD28, which is constitutively expressed on T lymphocytes and whose activation promotes T cell survival and migration towards inflamed tissues [24-26].

The cytokine microenvironment in which T cells recognize their cognate antigens and are co-stimulated determines the nature of the immune response developed against that antigen. Cytokines are initially secreted by APCs in response to the danger signals received and shape the type of immune response necessary to clear that particular invading agent. As an example, interleukin-12 (IL-12) is secreted during infections by intracellular pathogens and is crucial for the skewing of naïve $CD4^+$ T cells into pro-inflammatory T helper 1 (Th1) lymphocytes. Th1-polarized lymphocytes, in turn, participate in the orchestration of cellular immunity, mainly by further stimulating APC maturation via CD40L upregulation and by releasing interferon-γ (IFN-γ), IL-2 and tumor necrosis factor-α (TNF-α) [21] (Fig. 1.1). These latter cytokines stimulate cellular immunity by inducing T cell expansion and acquisition of cytotoxic functions by $CD8^+$ T lymphocytes that, upon recognition of their cognate antigen presented on the MHC-I of infected cells, lyse their targets by secretion of perforin and Granzyme-B [27].

1.2.2 Anatomy and physiology of central and peripheral tolerance

The antigen specificity of the TCR is the result of gene recombination and selection processes occurring during the development of T cell precursors in the thymus. As progenitors migrate from the bone marrow into the thymus to begin their maturation into naïve T lymphocytes, expression of recombination-activating gene 1 and 2 (*RAG1* and *RAG2*) activates somatic recombination of the genes coding for the TCR α and β chains [28]. Somatic recombination allows random rearrangements of the segments composing the TCR-coding genes and is therefore responsible for the diversity of the TCR repertoire. It is calculated that the TCR repertoire can reach approximately 10^{18} possible rearrangements, which guarantee the development of T cell clones potentially able to recognize any non-self antigen presented on the MHC [29,30].

As a side effect of TCR random rearrangements, thymocytes unable to bind peptide/MHC ligands with proper affinity (defined "useless") or, most importantly, potentially dangerous auto-reactive thymocytes recognizing self peptides presented on the MHC with too strong affinity are also developed. To maximize the functional diversity of the TCR repertoire and minimize the risk of autoimmune T cell clones reaching peripheral tissues, TCR affinity is tested during thymocyte development by binding to self peptide/MHC

complexes presented on the surface of thymic APCs. Thymocytes with a useless TCR die by neglect, and only those thymocytes whose TCR has a certain affinity for self peptide/MHC molecules receive survival signals and complete their maturation process (positive selection) (Fig. 1.3) [31-33]. On the contrary, binding of a TCR to a self antigen/MHC complex with too strong affinity induces clonal deletion by apoptosis of the corresponding thymocyte (negative selection), since strong binding capacity is recognized as a sign of auto-reactivity (Fig. 1.3) [34-38]. Moreover, some other potential auto-reactive T cell clones can be deviated towards a regulatory phenotype, giving rise to natural T regulatory (Treg) cells instead of being deleted (Fig. 1.3) [39].

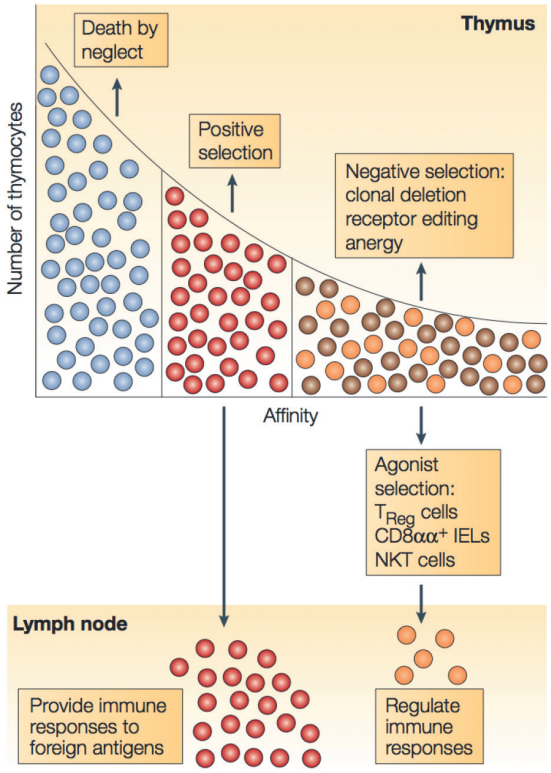

Figure 1.3 Selection processes undergone by T cell progenitors in the thymus. The TCR repertoire generated by recombination of the TCR-coding genes is carefully scanned in the thymus. As a result, precursors bearing a TCR unable to ligate self antigen/MHC complexes are eliminated as "useless" clones by death by neglect, while survival of those thymocytes able to recognize self antigen/MHC complexes with moderate affinity is promoted (positive selection). Deletion or skewing towards a regulatory phenotype is instead established for the potential auto-reactive T cell precursors bearing a TCR binding self antigen/MHC complexes with too high affinity (negative selection) (adapted from Hogquist, K. A. *et al.*, *Nat. Rev. Immunol.*, 2005).

Positive selection, clonal deletion and clonal deviation occur in discrete thymic microenvironments and are made possible by the interaction of thymocytes with APCs of the thymic stroma, especially thymic epithelial cells (TECs) and thymic DCs [40]. Processing and

presentation of self intracellular and extracellular antigens on MHC-I and MHC-II molecules, respectively, by cortical TECs (cTECs) allows for positive selection of functional thymocyte clones. About 10% of the T cell precursors are positively selected and can thus migrate towards the thymic medulla, where medullary TECs (mTECs) and DCs are mainly responsible for antigen presentation (Fig. 1.4a) [31-33].

The thymic medulla is considered the specialized compartment for the establishment of central tolerance, as highlighted by the autoimmune phenotype of murine models bearing thymic medullary defects. A common feature of these murine strains is the high susceptibility to autoimmunity or inflammation, as a result of impaired clonal deletion of T cell precursors and reduced frequency of Treg cells. The immune dysfunctions observed in these mice have been associated to reduced expression of the autoimmune regulator gene (*AIRE*) in mTECs [41-43].

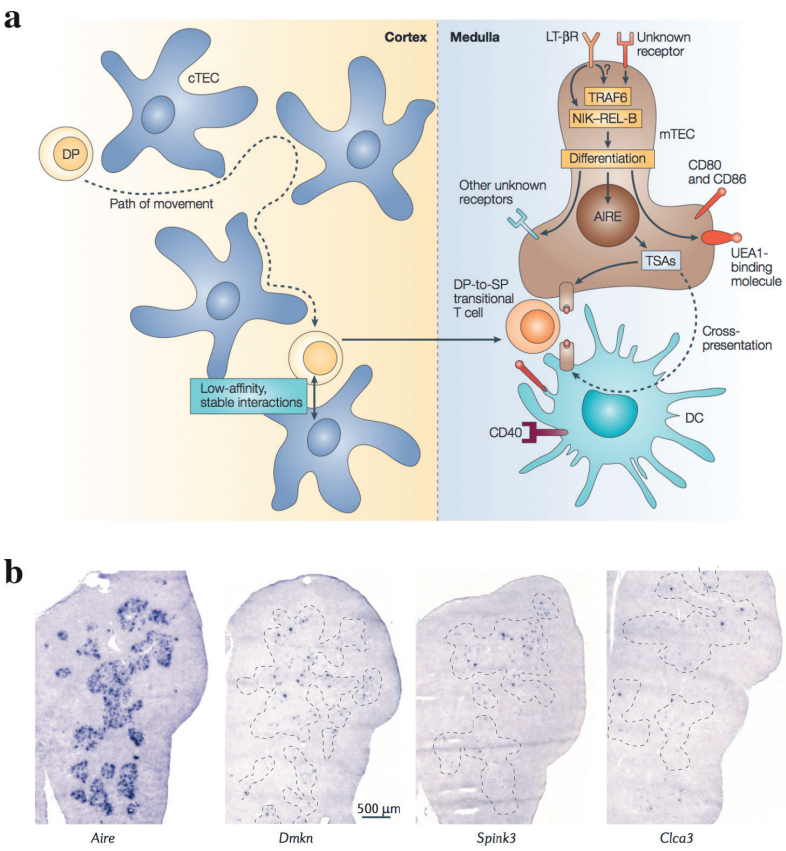

Figure 1.4 Molecular mechanisms of central tolerance. (a) T cell precursors expressing a TCR capable of binding self antigen/MHC complexes displayed on cTECs are positively selected and migrate from the thymic cortex to the medulla. In the thymic medulla, promiscuous expression of peripheral tissue-specific antigens (PTAs) induced by *AIRE* in mTECs and antigen presentation by both mTECs and DCs allows for negative selection of potential auto-reactive thymocytes. (b) *In situ* hybridization of a murine thymic section showing spread distribution of *AIRE* transcripts in the medulla but anatomically restricted localization of the mRNA from 3 representative PTAs (dermokine, *Dmkn*; serine protease inhibitor Kazal-type 3, *Spink3*; calcium-activated chloride channel family

member 3, *Clca3*) (adapted from Hogquist, K. A. *et al*., *Nat*. *Rev*. *Immunol*., 2005 and Klein, L. *et al*., *Nat*. *Rev*. *Immunol*., 2014).

As a transcription factor, AIRE is responsible for the promiscuous gene expression in mTECs of otherwise peripheral tissue-specific antigens (PTAs). Expression of PTAs in the thymic medulla allows for a broad representation of self antigens expressed at different sites or at different times in the organism, and it is thus crucial in determining which thymocyte clones might need to be deleted or deviated because of their TCR specificity and affinity [44-46]. The key role of *AIRE* in the establishment of tolerance is further underscored by the onset of the human autoimmune disease autoimmune polyendocrinopathy-candidiasis-ectodermal dystrophy (APECED) in individuals with mutations in the *AIRE* gene *locus*. Mouse models have confirmed that *AIRE* deficiencies cause increased numbers of activated T cells in the periphery and consequential autoimmune phenotype [47].

The molecular mechanisms by which *AIRE* promotes promiscuous gene expression in mTECs are still under investigation, even though the expression pattern of PTAs in the thymic medulla clearly indicates that AIRE is only one of the molecules involved in the process. For example, even though *AIRE* expression is widely distributed in mTECs, the thymic medulla appears to be organized in discrete areas where expression of clustered PTAs is anatomically restricted (Fig. 1.4b). Moreover, AIRE expression is localized to mTECs, but PTAs are efficiently presented by thymic DCs, probably as a consequence of antigen spreading from mTECs to DCs via gap junctions, exosomes or apoptotic bodies (Fig. 1.4a) [40,48,49].

There are limits to the ability of central tolerance of purging the T cell repertoire of all the possible auto-reactive clones in development. In fact, not every PTA is expressed in the thymic medulla and deletion or deviation typically occur for high-affinity TCR-bearing cells but not for lower affinity self-reactive T cell clones. As a result, potential auto-reactive T cells still reach peripheral tissues, thus requiring additional peripheral tolerogenic mechanisms to preserve the organism from self aggression. Moreover, additional peripheral tolerance is necessary to avoid immunity against innocuous non-self antigens to which our body is continuously exposed, such as environmental antigens, food molecules, metabolic products, or protein therapeutics [48].

One of the most intuitive ways peripheral tolerance can be achieved is antigen ignorance by antigen-specific T lymphocytes. Antigen ignorance is achieved for those auto-antigens expressed and presented on the MHC at levels that are below the activation threshold of naïve self-reactive T cells, since only T cell clones bearing a TCR with low affinity for self peptide/MHC complexes manage to escape clonal deletion in the thymus. Antigens anatomically restricted to immunologically privileged sites where T cells do not have access,

like the eye and the testis, are also ignored by lymphocytes [50]. Naïve T cells, in fact, recirculate between blood and secondary lymphoid organs after exiting the thymus.

In secondary lymphoid organs, T lymphocytes are continuously exposed to antigens presented on the MHC by migratory lymphoid organ-homing DCs or by resident APCs presenting antigens derived from lymphatic or blood drainage from local tissues or direct expression *in situ* [51,52]. In the lymph nodes (LNs), for example, multiple subsets of resident cells of both hematopoietic lineage, such as DCs, or non-hematopoietic lineage, such as lymphatic endothelial cells of the stroma, are capable of antigen presentation to T cells [52,53]. Importantly, since antigen drainage or migratory DCs would only provide presentation of local antigens, *in situ* expression of PTAs and their presentation on the MHC is also employed by LN resident hematopoietic and stromal cells as a way to increase the pool of presented self antigens [11-15,52]. Of note, non-lymphoid organs, especially the liver, have also been attributed important immunological functions. In the liver, for example, both sinusoid endothelial cells and hepatocytes have direct access to the large amount of circulating extracellular antigens, that can be scavenged, processed and presented on the MHC to T lymphocytes [9,54-56].

In the absence of an ongoing infection, antigen presentation without co-stimulatory signals and pro-inflammatory mediators results in tolerance rather than immunity, as a consequence of suboptimal stimulation of the antigen-specific T cells, leading to their deletion, anergy or skewing towards an induced Treg phenotype. Unlike deleted cells, anergic T cells survive antigen exposure in a hyporesponsive nonproliferative state. The faith decision of peripherally tolerized T cells between deletion or anergy is dependent upon antigen persistence, dose and localization. Limited exposure to small doses of antigen is likely to induce clonal deletion, while prolonged exposure to high-dose antigens has been associated to anergy induction [57-59].

T cells with immune suppressive functions, Treg cells, are also important players in the maintenance of peripheral tolerance. Identified as $CD4^+CD25^+FoxP3^+$, Tregs originate either from the thymus as a result of central tolerance and clonal deviation (natural Tregs) or from peripheral tissues as a consequence of suboptimal stimulation and phenotypic skewing (inducible Tregs) [60]. Treg cells expand and activate in response to TCR triggering in an antigen-specific manner, but their suppressive functions appear to be non-specific as they locally interfere with inflammatory responses by releasing suppressive cytokines (IL-10 and transforming growth factor- β, TGF-β), consuming IL-2, exerting cytotoxic functions on APCs and T cells or dampening APC maturation [61-64]. The result of Treg-driven suppressive activity on T cells is hypoproliferation, reduced survival and defective effector functions.

1.2.3 The enemy inside: cancer, autoimmunity and the logic of immunotherapy

Cancer and autoimmune diseases are both pathologic manifestations occurring when the immune system fails to maintain functional homeostasis in the organism. Inadequate immunity and escape of immunosurveillance are considered crucial steps for transformed cells to be able to grow into clinically apparent tumors. In contrast, autoimmune diseases are a heterogenous group of pathologies characterized by self-reactive immunity, which develops when tolerance towards self components is broken. Aberrant immune responses against protein therapeutics are often also included in the group of autoimmune diseases [1,65]. Due to the fundamental role played by the immune system in the development of autoimmunity and cancer, therapeutic approaches manipulating the components of the immune system (immunotherapy) have been proposed and developed with the aim of targeting pathogenic cells, either auto-reactive lymphocytes or cancerous cells, while limiting the damage to healthy tissues [1].

1.2.3.1 The enemy inside (I): cancer

Cancer cells originate from normal cells in which multiple genetic lesions accumulate over time, leading to the wide range of metabolic, phenotypic and antigenic alterations that differentiate tumor cells from their healthy counterparts [2]. Since precursor cancer cells derive from normal tissues, they express antigens to which the immune repertoire has been tolerized and are thus spared from immune attack. As soon as mutations accumulate in the DNA of transformed cells, aberrant antigens (tumor-associated antigens, TAAs) can be expressed, thus making cancerous cells recognizable by the immune system [66]. The ability of the immune system to detect and eliminate cells bearing pre-tumoral alterations is referred to as immunosurveillance and is vital in preventing cancer precursors from growing into established cancers. When immunosurveillance fails, either because of the selective pressure exerted by the immune system promoting the survival of non-immunogenic tumor cell clones (immunoselection) or because of active immune suppression (immunosubversion), tumors become clinically detectable [67,68].

Cancer cells and immune cells are in a close relationship, as they are two of the major components of the tumor microenvironment [69]. In particular, different populations of immune cells in the tumor microenvironment significantly shape the balance between pro-tumor and anti-tumor immunity. On one hand, DCs, natural killer (NK) and NK-T cells, $CD4^+$ T lymphocytes and effector $CD8^+$ T lymphocytes contribute to immune recognition of the tumor cells and to their elimination, mainly by the activation of cytotoxic functions. On the other hand, myeloid-derived suppressor cells, Treg cells and exhausted T lymphocytes negatively affect anti-tumor immunity. Therefore, immunotherapy approaches have been

applied for the treatment of cancer with the aim of eliciting anti-cancer immunity, reducing tumor growth and invasion, and ultimately eradicating tumors [4,70].

Cancer immunotherapy has taken advantage of several treatment possibilities in the past decades. Vaccination has been regarded to as the most attractive immunotherapy for the treatment of cancer, because of its ability to stimulate all the components of the anti-tumor response, including $CD8^+$ and $CD4^+$ T lymphocytes, NK and NK-T cells, and to counteract the recruitment of immunosuppressive cells. Moreover, vaccination can induce both effector $CD8^+$ T lymphocytes, recognizing tumor cells, and long-lasting memory $CD8^+$ T lymphocytes, controlling tumor relapse [71-73] (Fig. 1.5). Several vaccine protocols have been tested in clinical trials, including the use of tumor cells (either autologous or allogeneic), peptides or whole proteins and DNA vaccines. However, these approaches have generated tumor regression in a limited number of patients [58]. *Ex vivo*-generated DCs loaded with tumor antigens have also been exploited as vaccination tool to improve anti-tumor immunity [74-76]. Even though promising, DC vaccines display important disadvantages, including manufacturing limitations, safety issues associated with the use of cell-based therapies and variable immunological outcomes of *ex vivo* manipulation on the DC phenotype. In fact, DC vaccines have shown limited therapeutic efficacy in clinical trials [77].

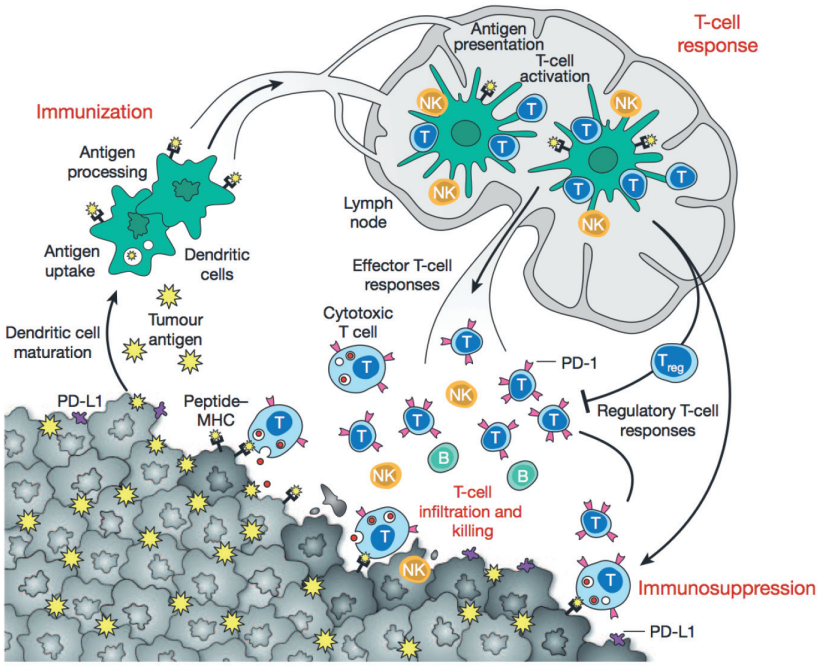

Figure 1.5 Generation and regulation of anti-tumor immunity. Immune cells are actively involved in the recognition and elimination of tumor cells. When transformed cells manage to escape immunosurveillance, they grow into established tumors. Vaccination is a promising therapy to enhance anti-tumor immunity by activating tumor-specific $CD4^+$ and $CD8^+$ T lymphocytes, B lymphocytes, NK and NK-T cells and counteracting the immunosuppressive effects of myeloid-derived suppressor and Treg cells (adapted from Mellman, I., Coukos, G. & Dranoff, G., *Nature,* 2011).

The reasons for the limited clinical efficacy of cancer vaccines are several, in line with the complexity of tumor diseases. In order for a vaccine to elicit eradicating immunity, tumor antigens must be presented by APCs under immunogenic conditions to tumor antigen-specific T cells and anti-tumor immune cells must be able to reach the tumor site where transformed cells can be recognized and destroyed. Therefore, the immunogenic profile of a cancer vaccine dramatically affects its capability to stimulate an anti-cancer immune response [1]. In addition, tumor cells can develop mechanisms to escape or suppress immunity. For example, cancer cells have been shown to downregulate the expression of MHC-I molecules, thus avoiding engagement of $CD8^+$ T lymphocytes, or to directly promote inactivation of immune cells via the expression of the inhibitory receptor PD-1 ligand 1 (PD-L1) or the secretion of inhibitory mediators. Suppressive immune cells also play a significant role in counteracting anti-tumor immunity [69].

1.2.3.2 Exosomes in cancer immunotherapy

Exosomes are 30-150 nm extracellular membrane vesicles released by most nucleated cells and derived from the endocytic compartment. Exosomes have been shown to selectively incorporate both proteins and nucleic acids from the cells of origin and are thus considered to participate in intercellular communication. In fact, exosomes can both engage in receptor-ligand interactions with the surface of their target cells initiating signal transduction and fuse with or be endocytosed by their targets transferring new membrane and cytosolic material (Fig. 1.6) [78,79].

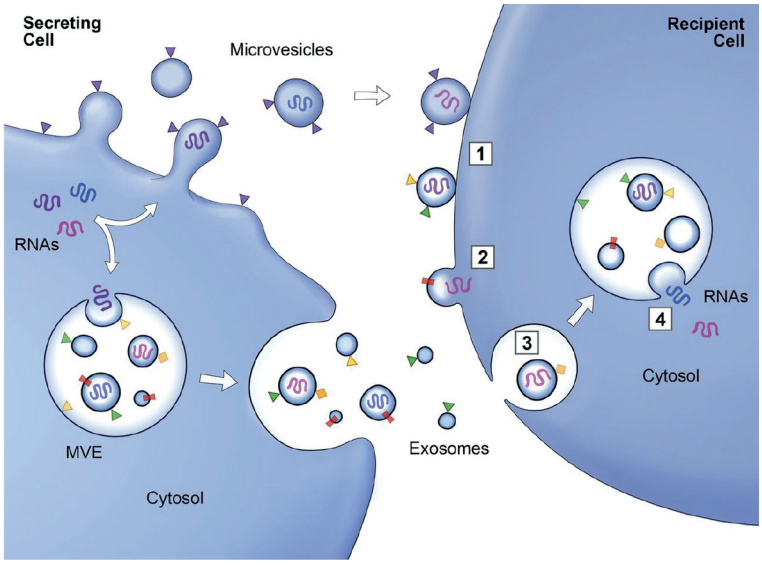

Figure 1.6 Transfer of proteins and nucleic acids via exosomes. Exosomes participate in intercellular communication systems by interacting directly with ligands on the surface of target cells

or by delivering their cargo of proteins and nucleic acids into target cells upon membrane fusion or endocytosis (adapted from Raposo, G. & Stoorvogel, W., *J. Cell Biol.*, 2013).

Since exosomes originating from either hematopoietic or non-hematopoietic cells have shown immune modulating properties, they have been proposed for the development of vaccine protocols in immunotherapy applications. DC-derived exosomes (Dexo) have elicited particular interest as vaccines since they carry key immunologically relevant DC-derived components (antigens, MHC-I and II molecules, co-stimulatory molecules, cellular adhesion molecules and integrins) and their immunological properties can be modified according to the activation state of the producing DCs [79-81].

Research in the field of cancer immunotherapy has benefited the most from the development of Dexo-based vaccines, proposed as one possible alternative to DC vaccines. Several studies showed that DCs pulsed with tumor peptides could secrete exosomes able to stimulate peptide-specific cytotoxic responses and to negatively affect tumor growth in murine models [78,82,83]. In an attempt to replicate the promising findings of the pre-clinical tests, phase I clinical trials have been conducted to evaluate the efficacy of subcutaneous immunization with Dexo derived from DCs pulsed with tumor-derived peptides in melanoma and lung carcinoma patients. Even though these trials have provided useful information on the manufacturing and safety of Dexo vaccine therapies in humans, therapeutic efficacy was poor, mainly because of weak immunogenicity [7,8].

Novel strategies to enhance the immunogenicity of Dexo are currently under investigation. The most promising approach tested in pre-clinical models so far has been the purification of Dexo from DCs loaded with whole tumor antigens instead of peptides and matured in the presence of danger signals, since multiple antigenic epitopes (either free peptides or peptide/MHC complexes), co-stimulatory signals and cytokines can be generated in the DCs, incorporated into exosomes and delivered into the vaccinated host [83-85].

1.2.3.3 The enemy inside (II): autoimmunity

Immunotherapy of autoimmune diseases is focused on the suppression of aberrant or exaggerated immune responses. For many autoimmune diseases the pathogenic mechanisms and the antigens recognized by the immune system have yet to be identified. For this reason, non-specific immunotherapies have been adopted in the clinics, such as immunosuppressive cytokines or monoclonal antibodies aimed at modulating immune cell functions. Due to their non-specific nature, all of these therapies have been associated with important toxicity and side effects, mainly represented by increased susceptibility to infections and cancer [1].

Only for those few autoimmune diseases for which the self antigens involved have been identified, such as type 1 diabetes, multiple sclerosis and rheumatoid arthritis, safer antigen-specific tolerogenic immunotherapies have been proposed. Intravenous infusion of soluble peptides, oral or nasal administration of peptides and intravenous administration of antigen-coupled apoptotic cells have been attempted in pre-clinical models with the goal of providing antigen presentation in the absence of immunogenic stimuli. Results have been disappointing, either because of lack of efficacy or because of severe toxic side effects [86-88].

As a better understanding of the basic mechanisms leading to immune tolerance is acquired, novel and safer therapeutic technologies can be developed. For example, the discovery that an organ such as the liver, which is easily targettable via the intravenous route, contains cells capable of presenting antigens to $CD4^+$ and $CD8^+$ T lymphocytes without co-stimulation [89], has opened the way to the search for immunotherapies employing liver-targeted antigens.

1.3 Accomplishments

In this Ph. D. thesis we addressed distinct biological questions on immune physiology and immunotherapy applications by taking advantage of bioengineering approaches.

The aim of the project presented in Chapter 2 was to develop an improved vaccine formulation based on Dexo for the treatment of melanoma, recently published in Scientific Reports. Dexo have elicited a great amount of interest in the cancer immunotherapy community because of their immunogenicity and potential adaptability to different cancer diseases. In fact, Dexo have previously entered clinical trial as therapeutic vaccines for melanoma and lung carcinoma [7,8]. Since the Dexo vaccines tested in these clinical trials resulted in poor therapeutic benefits due to limited anti-tumor immune responses, we propose an approach to increase the immunogenicity of Dexo that takes advantage of the intrinsic capacity of DCs to acquire immunostimulatory functions upon antigen loading and danger signal sensing. With this strategy, we obtained a Dexo vaccine capable of stimulating anti-melanoma immunity, significantly reducing tumor growth and enhancing the survival of melanoma-bearing mice.

In the project described in Chapter 3, we took a step back from direct translational applications and employed bioengineering techniques to obtain a version of a model antigen (ovalbumin) with enhanced binding to endocytotic receptors. We used this modified version of ovalbumin we the aim of studying the biology of extracellular antigen uptake in

hepatocytes and the immunological consequences of such mechanism. We were able to observe that, unlike in previous reports [9], hepatocytes are efficient antigen cross-presenting cells leading to antigen-specific $CD8^+$ T cell tolerance in mice. Since hepatocytes represent the most abundant cell type of the liver and are involved in the metabolic and detoxification functions of the liver, we suggest that hepatocyte cross-presentation is a key mechanism by which tolerance is maintained towards blood-borne harmless molecules to which our body is continuously exposed. These findings could be helpful in the development of novel tolerogenic therapies taking advantage of hepatocyte-targeted strategies for the treatment of autoimmunity or immunity against protein therapeutics. These data have been included in two manuscripts that will be soon sent for peer review.

In the project presented in Chapter 4, we continued investigating the role of the liver in the establishment of peripheral tolerance. Previous reports have shown that non-hematopoietic stromal cells of the LNs express PTAs that induce T cell tolerance upon antigen presentation on the MHC [11-15]. Since the liver contains cells that phenotypically resemble lymphoid endothelial cells of the LNs, the aim of this project was to investigate whether non-hematopoietic cells of the liver express tissue-restricted antigens and participate in active tolerance induction. Here, we describe preliminary findings that confirm our hypothesis. Sorted murine liver cells, both hepatocytes and liver sinusoid endothelial cells, were found to be negative for the expression of *AIRE* but hepatocytes were found to be positive for another transcription factor-coding gene (deformed epidermal autoregulatory factor 1, *Deaf1*), that has been recently associated with promiscuous gene expression and regulation of immunity and autoimmunity [15,90]. Expression of some of the best characterized PTAs was also detected in hepatocytes, suggesting that active peripheral tolerance via promiscuous gene expression might be occurring in the liver. Even though we have not yet investigated the correlation between the expression of *Deaf1* and PTAs in hepatocytes and we are only beginning to study whether MHC presentation of such antigens occurs and influences immune cell fate, we propose the liver as the first non-lymphoid organ to be described to express PTAs and to participate in active peripheral tolerance through promiscuous gene expression.

1.4 References

1. Caspi, R. R. Immunotherapy of autoimmunity and cancer: the penalty for success. *Nat. Rev. Immunol*. **8,** 970–976 (2008).
2. Hanahan, D. & Wenberg, R. A. The hallmarks of cancer. *Cell*. **100,** 57–70 (2000).

3. Cancer Research UK. *Cancer incidence statistics*. (2015) Available at: http://www.cancerresearchuk.org/health-professional/cancer-statistics/incidence. (Accessed on: 13th November 2015)
4. Zitvogel, L., Tesniere, A. & Kroemer, G. Cancer despite immunosurveillance: immunoselection and immunosubversion. *Nat. Rev. Immunol.* **6,** 715–727 (2006).
5. National Institutes of Health. Autoimmune diseases coordinating committee. Autoimmune dieases research plan. (2002) Available at: http://www.niaid.nih.gov/topics/autoimmune/documents/adccreport.pdf. (Accessed on: 13th November 2015)
6. Miller, S. D., Turley, D. M. & Podojil, J. R. Antigen-specific tolerance strategies for the prevention and treatment of autoimmune disease. *Nat. Rev. Immunol.* **7,** 665–677 (2007).
7. Escudier, B. *et al.* Vaccination of metastatic melanoma patients with autologous dendritic cell (DC) derived-exosomes: results of the first phase I clinical trial. *J. Transl. Med.* **3,** 10–13 (2005).
8. Morse, M. A. *et al.* A phase I study of dexosome immunotherapy in patients with advanced non-small cell lung cancer. *J. Transl. Med.* **3,** 9–8 (2005).
9. Ebrahimkhani, M. R., Mohar, I. & Crispe, I. N. Cross-presentation of antigen by diverse subsets of murine liver cells. *Hepatology.* **54,** 1379–1387 (2011).
10. Thomson, A. W. & Knolle, P. A. Antigen-presenting cell function in the tolerogenic liver environment. *Nat. Rev. Immunol.* **10,** 753–766 (2010).
11. Lee, J. W. *et al.* Peripheral antigen display by lymph node stroma promotes T cell tolerance to intestinal self. *Nat. Immunol.* **8,** 181–190 (2006).
12. Yip, L. *et al.* Deaf1 isoforms control the expression of genes encoding peripheral tissue antigens in the pancreatic lymph nodes during type 1 diabetes. *Nat. Immunol.* **10,** 1026–1033 (2009).
13. Cohen, J. N. *et al.* Lymph node-resident lymphatic endothelial cells mediate peripheral tolerance via Aire-independent direct antigen presentation. *J. Exp. Med.* **207,** 681–688 (2010).
14. Fletcher, A. L. *et al.* Lymph node fibroblastic reticular cells directly present peripheral tissue antigen under steady-state and inflammatory conditions. *J. Exp. Med.* **207,** 689–697 (2010).
15. Yip, L., Creusot, R. J., Pager, C. T., Sarnow, P. & Fathman, C. G. Reduced DEAF1 function during type 1 diabetes inhibits translation in lymph node stromal cells by suppressing Eif4g3. *J. Mol. Cell Biol.* **5,** 99–110 (2013).
16. Iwasaki, A. & Medzhitov, R. Regulation of adaptive immunity by the innate immune

system. *Science*. 327, 291–295 (2010).

17. Kawai, T. & Akira, S. The role of pattern-recognition receptors in innate immunity: update on Toll-like receptors. *Nat. Immunol.* **11,** 373–384 (2010).
18. Rathinam, V. A. K., Vanaja, S. K. & Fitzgerald, K. A. Regulation of inflammasome signaling. *Nat. Immunol.* **13,** 333–332 (2012).
19. Wu, J. & Chen, Z. J. Innate immune sensing and signaling of cytosolic nucleic acids. *Annu. Rev. Immunol.* **32,** 461–488 (2014).
20. Iwasaki, A. & Medzhitov, R. Control of adaptive immunity by the innate immune system. *Nat. Immunol.* **16,** 343–353 (2015).
21. Kapsenberg, M. L. Dendritic-cell control of pathogen-driven T-cell polarization. *Nat. Rev. Immunol.* **3,** 984–993 (2003).
22. Neefjes, J., Jongsma, M. L. M., Paul, P. & Bakke, O. Towards a system understanding of MHC class I and MHC class II antigen presentation. *Nat. Rev. Immunol.* **11,** 823–836 (2011).
23. Joffre, O. P., Segura, E., Savina, A. & Amigorena, S. Cross-presentation by dendritic cells. *Nat. Rev. Immunol.* 12, 557–569 (2012).
24. Boise, L. H., Noel, P. J. & Thompson, C. B. CD28 and apoptosis. *Curr. Opin. Immunol*. **7,** 620–625 (1995).
25. Lenschow, D. J., Walunas, T. L. & Bluestone, J. A. CD28/B7 system of T cell costimulation. *Annu. Rev. Immunol*. **14,** 233–258 (1997).
26. Sallusto, F. The role of chemokines and chemokine receptors in T cell priming and Th1/Th2-mediated responses. *Haematologica*. **84,** 28–31 (1999).
27. Barry, M. & Bleackley, R. C. Cytotoxic T lymphocytes: all roads lead to death. *Nat. Rev. Immunol*. 2, 401–409 (2002).
28. Hogquist, K. A., Baldwin, T. A. & Jameson, S. C. Central tolerance: learning self-control in the thymus. *Nat. Rev. Immunol.* **5,** 772–782 (2005).
29. Kyewski, B. & Klein, L. A central role for central tolerance. *Annu. Rev. Immunol.* **24,** 571–606 (2006).
30. Klein, L., Kyewski, B., Allen, P. M. & Hogquist, K. A. Positive and negative selection of the T cell repertoire: what thymocytes see (and don't see). *Nat. Rev. Immunol.* **14,** 377–391 (2014).
31. Huesman, M., Scott, B., Kisielow, P. & von Boehmer, H. Kinetics and efficacy of positive selection in the thymus of normal and T cell receptor transgenic mice. *Cell*. **66,** 533–540 (1991).
32. Shortman, K., Vremec, D. & Egerton, M. The kinetics of T cell antigen receptor expression by subgroups of CD4+8+ thymocytes: delineation of CD4+8+3(2+)

thymocytes as post-selection intermediates leading to mature T cell. *J. Exp. Med*. **173,** 323–332 (1991).

33. Surh, C. D. & Sprent, J. T-cell apoptosis detected in situ during positive and negative selection in the thymus. *Nature*. **372,** 100–103 (1994).
34. Ignatowicz, L., Kappler, J. & Marrack, P. The Repertoire of T cells shaped by a single MHC/peptide ligand. *Cell*. **84,** 521–529 (1996).
35. Fukui, Y. *et al*. Positive and negative CD4+ thymocyte selection by a single MHC class II/peptide ligand affected by its expression level in the thymus. *Immunity*. **6,** 401–410 (1997).
36. Tourne, S. *et al*. Selection of a broad repertoire of CD4+ T cells in H-2Ma0/0 mice. *Immunity*. **7,** 187–195 (1997).
37. van Meerwijk, J. P. *et al*. Quantitative impact of thymic clonal deletion on the T cell repertoire. *J. Exp. Med.* **185,** 377–383 (1997).
38. Anderson, G., Partington, K. M. & Jenkinson, E. J. Differential effects of peptide diversity and stromal cell type in positive and negative selection in the thymus. *J. Immunol*. **161,** 6599–6603 (1998).
39. Takahashi, T. *et al*. Immunologic self-tolerance maintained by CD25+CD4+ naturally anergic and suppressive T cells: induction of autoimmune disease by breaking their anergic/suppressive state. *Int. Immunol*. **10,** 1969–1980 (1998).
40. Gallegos, A. M. Central tolerance to tissue-specific antigens mediated by direct and indirect antigen presentation. *J. Exp. Med.* **200,** 1039–1049 (2004).
41. Weih, F. *et al*. Multiorgan inflammation and hematopoietic abnormalities in mice with a targeted disruption of RelB, a member of the NF-kappa B/Rel family. *Cell*. **80,** 331–340 (1995).
42. Boehm, T., Scheu, S., Pfeffer, K. & Bleul, C. C. Thymic medullary epithelial cell differentiation, thymocyte emigration, and the control of autoimmunity require lympho-epithelial cross talk via LTbetaR. *J. Exp. Med.* **198,** 757–769 (2003).
43. Kajiura, F. *et al.* NF-kappa B-Inducing kinase establishes self-tolerance in a thymic stroma-dependent manner. *J. Immunol.* **172,** 2067–2075 (2004).
44. Smith, K. M., Olson, D. C., Hirose, R. & Hanahan, D. Pancreatic gene expression in rare cells of thymic medulla: evidence for functional contribution to T cell tolerance. *Int. Immunol*. **9,** 1355–1365 (1997).
45. Derbinski, J., Schulte, A., Kyewski, B. & Klein, L. Promiscuous gene expression in medullary thymic epithelial cells mirrors the peripheral self. *Nat. Immunol.* **2,** 1032–1039 (2001).
46. Avichezer, D. *et al.* An immunologically privileged retinal antigen elicits tolerance:

major role for central selection mechanisms. *J. Exp. Med.* **198,** 1665–1676 (2003).

47. Villasenor, J., Benoist, C. & Mathis, D. AIRE and APECED: molecular insights into an autoimmune disease. *Immunol. Rev*. **204,** 156–164 (2005).
48. Kyewski, B. & Derbinski, J. Self-representation in the thymus: an extended view. *Nat. Rev. Immunol.* **4,** 688–698 (2004).
49. Gillard, G. O. Contrasting models of promiscuous gene expression by thymic epithelium. *J. Exp. Med.* **202,** 15–19 (2005).
50. Forrester, J. V., Xu, H., Lambe, T. & Cornall, R. Immune privilege or privileged immunity? *Mucosal Immunol.* **1,** 372–381 (2008).
51. Redmond, W. L. & Sherman, L. A. Peripheral Tolerance of CD8 T lymphocytes. *Immunity.* **22,** 275–284 (2005).
52. Zehn, D. & Bevan, M. J. More promiscuity resulting in more tolerance. *Nat. Immunol.* **8,** 120–122 (2007).
53. Hirosue, S. *et al.* Steady-state antigen scavenging, cross-presentation, and cd8+ t cell priming: a new role for lymphatic endothelial cells. *J. Immunol.* **192,** 5002–5011 (2014).
54. Diehl, L. *et al.* Tolerogenic maturation of liver sinusoidal endothelial cells promotes B7-homolog 1-dependent CD8+ T cell tolerance. *Hepatology.* **47,** 296–305 (2007).
55. Holz, L. E., Warren, A., Le Couteur, D. G., Bowen, D. G. & Bertolino, P. CD8+ T cell tolerance following antigen recognition on hepatocytes. *J. Autoimmun.* **34,** 15–22 (2010).
56. Böttcher, J. P. *et al.* Liver-primed memory t cells generated under noninflammatory conditions provide anti-infectious immunity. *Cell Rep.* **3,** 779–795 (2013).
57. Aichele, P., Brduscha-Riem, K., Zinkernagel, R. M., Hengartner, H. & Pircher, H. T cell priming versus t cell tolerance induced by synthetic peptides. *J. Exp. Med*. **182,** 261–266 (1995).
58. Rocha, B., Grandien, A. & Freitas, A. A. Anergy and exhaustion are independent mechanisms of peripheral T cell tolerance. *J. Exp. Med*. **181,** 993–1003 (1995).
59. Zinkernagel, R. M. Localization dose and time of antigens determine immune reactivity. *Semin. Immunol.* **12,** 163–171 (2000).
60. de Lafaille, M. A. C. & Lafaille, J. J. Natural and adaptive FoxP3+ regulatory T cells: more of the same or a division of labor? *Immunity.* **30,** 626–635 (2009).
61. Herrath, von, M. G. & Harrison, L. C. Regulatory lymphocytes: antigen-induced regulatory t cells in autoimmunity. *Nat. Rev. Immunol.* **3,** 223–232 (2003).
62. la Rosa, de, M., Rutz, S., Dorninger, H. & Scheffold, A. Interleukin-2 is essential for CD4+CD25+ regulatory T cell function. *Eur. J. Immunol.* **34,** 2480–2488 (2004).

63. Grossman, W. J. *et al.* Human T regulatory cells can use the perforin pathway to cause autologous target cell death. *Immunity*. **21,** 589–601 (2004).
64. Sakaguchi, S. Naturally arising Foxp3-expressing CD25+CD4+ regulatory T cells in immunological tolerance to self and non-self. *Nat. Immunol.* **6,** 345–352 (2005).
65. Cho, J. H. & Feldman, M. Heterogeneity of autoimmune diseases: pathophysiologic insights from genetics and implications for new therapies. *Nat. Med.* **21,** 730–738 (2015).
66. Boon, T., Cerottini, J. C., Van den eynde, B., van der Bruggen, P. & Van Pel, A. Tumor antigens recognized by T lymphocytes. *Annu. Rev. Immunol.* **12,** 337–365 (1994).
67. Dunn, G. P., Old, L. J. & Schreiber, R. D. The three Es of cancer immunoediting. *Annu. Rev. Immunol.* **22,** 329–360 (2004).
68. Dunn, G. P., Old, L. J. & Schreiber, R. D. The Immunobiology of cancer immunosurveillance and immunoediting. *Immunity.* **21,** 137–148 (2004).
69. Mellman, I., Coukos, G. & Dranoff, G. Cancer immunotherapy comes of age. *Nature.* **480,** 480–489 (2011).
70. Banchereau, J. & Palucka, A. K. Dendritic cells as therapeutic vaccines against cancer. *Nat. Rev. Immunol.* **5,** 296–306 (2005).
71. Cerwenka, A. & Lanier, L. L. Natural killer cells, viruses and cancer. *Nat. Rev. Immunol*. **1,** 41–49 (2001).
72. Northrop, J. K. & Shen, H. CD8+ T-cell memory: only the good ones last. *Curr. Opin. Immunol.* **16,** 451–455 (2004).
73. Kronenberg, M. Toward an understanding of NKT cell biology: progress and paradoxes. *Annu. Rev. Immunol.* **23,** 877–900 (2005).
74. Palucka, K. & Banchereau, J. Cancer immunotherapy via dendritic cells. *Nat. Rev. Cancer* **12,** 265–277 (2012).
75. Anguille, S., Smits, E. L., Lion, E., van Tendeloo, V. F. & Berneman, Z. N. Clinical use of dendritic cells for cancer therapy. *Lancet Oncol.* **15,** e257–e267 (2014).
76. Mac Keon, S., Ruiz, M. A. S., Gazzaniga, S. & Wainstok, R. Dendritic cell-based vaccination in cancer: therapeutic implications emerging from murine models. *Front. Immunol.* **6,** 1–18 (2015).
77. Gilboa, E., Nair, S. K. & Lyerly, H. K. Immunotherapy of cancer with dendritic-cell-based vaccines. *Cancer Immunol. Immunother*. **46,** 82–87 (1998).
78. Théry, C. *et al.* Indirect activation of naïve CD4+ T cells by dendritic cell–derived exosomes. *Nat. Immunol.* **3,** 1156–1162 (2002).
79. Robbins, P. D. & Morelli, A. E. Regulation of immune responses by extracellular

vesicles. *Nat. Rev. Immunol.* **14,** 195–208 (2014).

80. Théry, C. *et al*. Molecular characterization of dendritic cell-derived exosomes: selective accumulation of the heat shock protein hsc73. *J. Cell Biol.* **147,** 599–610 (1999).
81. Pitt, J. M. *et al.* Dendritic cell-derived exosomes as immunotherapies in the fight against cancer. *J. Immunol.* **193,** 1006–1011 (2014).
82. Segura, E. ICAM-1 on exosomes from mature dendritic cells is critical for efficient naive T-cell priming. *Blood.* **106,** 216–223 (2005).
83. Näslund, T. I., Gehrmann, U., Qazi, K. R., Karlsson, M. C. I. & Gabrielsson, S. Dendritic cell-derived exosomes need to activate both T and B cells to induce antitumor immunity. *J. Immunol.* **190,** 2712–2719 (2013).
84. Sobo-Vujanovic, A., Munich, S. & Vujanovic, N. L. Dendritic-cell exosomes cross-present Toll-like receptor-ligands and activate bystander dendritic cells. *Cell. Immunol.* **289,** 119–127 (2015).
85. Damo, M., Wilson, D. S., Simeoni, E. & Hubbell, J. A. TLR-3 stimulation improves anti-tumor immunity elicited by dendritic cell exosome-based vaccines in a murine model of melanoma. *Sci. Rep*. (2015). *In press*
86. Monetini, L. *et al.* Cytokine profile and insulin antibody IgG subclasses in patients with recent onset Type 1 diabetes treated with oral insulin. *Diabetologia.* **47,** 1795–1802 (2004).
87. Staeva-Vieira, T., Peakman, M. & Herrath, Von, M. Translational mini-review series on type 1 diabetes: immune-based therapeutic approaches for type 1 diabetes. *Clin. Exp. Immunol.* **148,** 17–31 (2007).
88. Getts, D. R. *et al.* Tolerance induced by apoptotic antigen-coupled leukocytes is induced by PD-L1+ and IL-10-producing splenic macrophages and maintained by T regulatory cells. *J. Immunol.* **187,** 2405–2417 (2011).
89. Crispe, I. N. Liver antigen-presenting cells. *J. Hepatol.* **54,** 357–365 (2011).
90. Reed, D. E., Huang, X. M., Wohlchlegel, J. A., Levine, M. S. & Senger, K. DEAF-1 regulates immunity gene expression in Drosophila. *Proc. Natl. Acad. Sci. U. S. A.* **105,** *8351*–8356 (2008).

Chapter 2

TLR-3 stimulation improves anti-tumor immunity elicited by dendritic cell exosome-based vaccines in a murine model of melanoma

Adapted from publication:

Damo, M., Wilson, D.S., Simeoni, E. & Hubbell, J.A. TLR-3 stimulation improves anti-tumor immunity elicited by dendritic cell exosome-based vaccines in a murine model of melanoma. *Scientific Reports*. 2015. Dec 3; 5:17622. doi: 10.1038/srep17622.

2.1 Abstract

Dendritic cell (DC)-derived exosomes (Dexo) contain the machinery necessary to activate potent antigen-specific immune responses. As promising cell-free immunogens, Dexo have been tested in previous clinical trials for cancer vaccine immunotherapy, yet resulted in limited therapeutic benefit. Here, we explore a novel Dexo vaccine formulation composed of Dexo purified from DCs loaded with antigens and matured with either the TLR-3 ligand poly(I:C), the TLR-4 ligand LPS or the TLR-9 ligand CpG-B. When poly(I:C) was used to produce exosomes together with ovalbumin (OVA), the resulting Dexo vaccine strongly stimulated OVA-specific $CD8^+$ and $CD4^+$ T cells to proliferate and acquire effector functions. When a B16F10 melanoma cell lysate was used to load DCs with tumor antigens during exosome production together with poly(I:C), we obtained a Dexo vaccine capable of inducing robust activation of melanoma-specific $CD8^+$ T cells and the recruitment of cytotoxic $CD8^+$ T cells, NK and NK-T cells to the tumor site, resulting in significantly reduced tumor growth and enhanced survival as compared to a Dexo vaccine formulation similar to the one previously tested on human patients. Our results indicate that poly(I:C) is a particularly favorable TLR agonist for DC maturation during antigen loading and exosome production for cancer immunotherapy.

2.2 Introduction

Immunotherapy for cancer aims at stimulating tumor-specific immune responses to prevent, treat or eradicate malignancies [1,2]. Several approaches have been exploited clinically for cancer immunotherapy, including the use of DCs for therapeutic vaccination. As professional APCs, DCs represent a favorable candidate for immunotherapy purposes due to their ability to take up, process and present antigens and to sense danger signals to initiate an effective cancer-specific immune response. However, DC-based therapies are far from optimal, since *ex vivo* or *in vivo* manipulation of patient-derived DCs is still time-consuming, costly and associated with risks and a high rate of failure [3,4].

In recent years, alternative approaches to the use of DCs in cancer vaccination have been investigated, including the use of exosomes. Exosomes are 30-150 nm membrane vesicles originating from intracellular multivesicular bodies and secreted into the extracellular space by most eukaryotic cell types [5,6]. In particular, exosomes originating from DCs (Dexo) contain several immunologically relevant components, such as antigens, MHC class I and II molecules (often complexed with antigenic epitopes), co-stimulatory molecules (e.g., CD80, CD86, CD40), cellular adhesion molecules (e.g., ICAM-1) and integrins [7,8]. Since exosomes can transfer their protein and nucleic acid content from a secreting cell to a target cell, Dexo are considered to be important intercellular communication vehicles exploited by DCs in the orchestration of immune responses [7-10].

Murine Dexo have been shown to be able to stimulate antigen-specific $CD4^+$ and $CD8^+$ T cells both *in vitro* and *in vivo* and to enhance anti-cancer immunity *in vivo* [11-17]. Antigen-loaded Dexo derived from the DCs of cancer patients have been tested in phase I clinical trials for the treatment of melanoma and non-small cell lung carcinoma. Those clinical trials proved the feasibility and safety of Dexo-based vaccination in human cancer patients but did not show significant tumor growth control or regression in the treated candidates [18-20]. One hypothesis is that these antigen-loaded Dexo did not contain the activation signals required to elicit and activate cytotoxic effector cells that would be able to recognize and kill transformed cells.

Maturation of DCs via treatment with TLR ligands as adjuvants to activate danger signal-sensing pathways coupled to antigen loading of DCs instead of exosomes has been proposed as a possible solution to improve the immunogenic profile of Dexo. Recently, it was shown that treatment of DCs with LPS (a TLR-4 ligand) or Pam_3 (a TLR-1/2 ligand) leads to secretion of Dexo with an increased ability to stimulate cytotoxic NK and $CD8^+$ T cells and to significantly affect tumor growth *in vivo* [16,21,22]. However, LPS is not clinically viable and the effect of other adjuvants, already proposed for clinical use in immunotherapies, has yet to be explored in the development of Dexo-based vaccines.

In this project, in an attempt to further improve the immune stimulatory properties of Dexo and to provide a vaccination tool easily transferrable to clinical development for both infectious diseases and cancer, we compared poly(I:C) (a TLR-3 ligand) and CpG-B (a TLR-9 ligand) to LPS as adjuvants for DC maturation during Dexo production [23-28]. Our results indicate that Dexo produced upon treatment of DCs with the model antigen ovalbumin (OVA) and poly(I:C) (Dexo(OVA+pIC)) robustly activate OVA-specific Th1 immune responses, characterized by the release of the pro-inflammatory cytokines IFN-γ and TNF-α by $CD4^+$ T lymphocytes and associated with the stimulation of OVA-specific cytotoxic $CD8^+$ T cells but negligible production of OVA-specific antibodies. Most importantly, therapeutic vaccination targeted to the tumor-draining lymph nodes (tdLNs) of B16F10 melanoma-bearing mice with Dexo released by DCs co-cultured with oxidized necrotic B16F10 cells as source of melanoma antigens and matured with poly(I:C) (Dexo(B16+pIC)) raised both melanoma-specific effector $CD8^+$ T cells in the tdLNs, spleen and tumor mass and tumor-infiltrating NK and NK-T cells, significantly reducing tumor growth and increasing the survival rate of diseased mice.

2.3 Results

2.3.1 Characterization of DC-derived exosomes produced in the presence of LPS, CpG-B or poly(I:C)

DCs express a wide range of pattern-recognition receptors, among which TLR-3, TLR-4 and TLR-9 are good candidates as adjuvant targets to elicit potent cytotoxic T cell responses in mice and humans for cancer as well as infectious disease vaccination [25-29]. In an attempt to improve the immunogenic profile of Dexo and test their ability to raise antigen-specific immune responses against the model antigen OVA, Dexo were harvested from the supernatant of bone marrow-derived DCs (BMDCs) either left untreated (Dexo(unt)), treated with OVA (Dexo(OVA)) or treated with OVA and matured with either the TLR-4 ligand LPS (Dexo(OVA+LPS)), the synthetic oligonucleotide CpG-B ligand of TLR-9 (Dexo(OVA+CpGB)) or the synthetic dsRNA analog poly(I:C) ligand of TLR-3 (Dexo(OVA+pIC)).

Transmission electron microscopy and dynamic light scattering (DLS) analysis of Dexo(unt), Dexo(OVA), Dexo(OVA+LPS), Dexo(OVA+CpGB) and Dexo(OVA+pIC) samples confirmed the presence of 30-150 nm cup-shaped vesicles, proving that TLR stimulation of exosome-secreting DCs does not affect Dexo physical characteristics (Fig. 2.1a,b). While typical exosomal markers such as the regulators of vesicular trafficking Alix and Tsg101 were revealed by western blot in all the Dexo preparations, full-length OVA

could not be detected, suggesting the presence of only processed OVA peptides (Fig. 2.1c). In fact, OVA-related peptides, measured by mass spectrometry as albumin peptides, could be detected more abundantly in those Dexo formulations prepared from OVA-treated BMDCs as compared to Dexo(unt) samples (Fig. 2.1d).

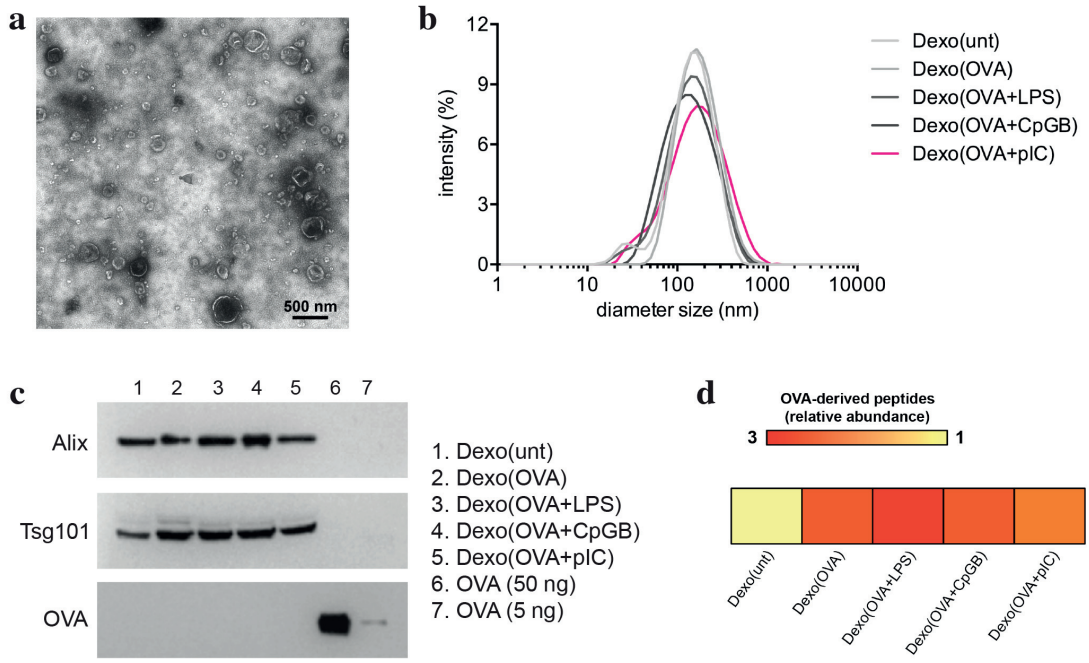

Figure 2.1 Exosomes are purified from the supernatant of DCs cultured in the presence of the model antigen ovalbumin and activated with different Toll-like receptor ligands. Exosomes were purified from the supernatant of untreated BMDCs (Dexo(unt)) or of BMDCs treated with OVA (Dexo(OVA)) or from the supernatant of BMDCs treated with OVA and matured with LPS (Dexo(OVA+LPS)), CpG-B (Dexo(OVA+CpGB) or poly(I:C) (Dexo(OVA+pIC)). (a) Example of transmission electron microscopy of one of the Dexo samples after purification from the supernatant of BMDCs confirms the expected physical characteristics of exosomal vesicles. (b) Diameter of exosomes was measured by DLS analysis of the different Dexo samples. (c) Presence of the exosome-specific markers Alix (100 kDa) and Tsg101 (46 kDa) and of full-length OVA protein (45 kDa) was detected by western blot to confirm the identity of *bona-fide* exosomes and loading of intact OVA in Dexo samples. 50 ng and 5 ng of OVA were used as positive control for detection of full-length OVA. (d) Presence of OVA-derived peptides was detected in Dexo samples by mass spectrometry. Abundance of OVA-related peptides in Dexo(OVA), Dexo(OVA+LPS), Dexo(OVA+CpGB) and Dexo(OVA+pIC) samples is normalized to the background abundance of OVA-related peptides detected in Dexo(unt) samples (relative abundance).

2.3.2 Screening of the immunogenic profile of Dexo(unt), Dexo(OVA), Dexo(OVA+LPS), Dexo(OVA+CpGB) and Dexo(OVA+pIC) in an OT-I adoptive transfer model of vaccination

Antigen-specific cytotoxic $CD8^+$ T cells play a major role in anti-cancer immunity by directly recognizing and killing transformed cells. To compare the ability of the Dexo formulations produced from BMDCs incubated in the presence of LPS, CpG-B or poly(I:C) to activate an antigen-specific cellular immune response *in vivo*, we took advantage of an OT-I adoptive transfer model of vaccination (Fig. 2.2a). Recipient mice were vaccinated either intravenously (i.v.) or intradermally (i.d.) in the four footpads with 50 μg of either Dexo(unt), Dexo(OVA), Dexo(OVA+LPS), Dexo(OVA+CpGB) or Dexo(OVA+pIC) 1 day after receiving i.v. 10^6 CFSE-labeled naïve OT-I cells, transgenic $CD8^+$ T cells specific for the $OVA_{257–264}$ immunodominant epitope SIINFEKL. 6 days after adoptive transfer, OT-I cells were harvested from the spleens and brachial, axillary ad inguinal LNs of recipient mice and analyzed by flow cytometry for proliferation and expression of markers indicative of the acquisition of T cell effector functions.

Proliferation of the OT-I cells, measured by flow cytometric analysis of CFSE dilution, was significantly increased both in the spleen and the LNs of those mice vaccinated with a Dexo(OVA+pIC) formulation (62.8% and 57.7% of proliferated OT-I cells in the spleens and 46.4% and 44.7% in the LNs of mice vaccinated i.v. or i.d., respectively) as compared to those mice vaccinated i.v. or i.d. with the other Dexo formulations (Fig. 2.2b). Both i.v. and i.d. vaccination with Dexo(OVA+pIC) also increased the percentage of $CD62L^-$ $CD44^+$ effector memory OT-I cells up to 14.1% and 12.1%, respectively, in the spleens and up to 21.4% and 20.0%, respectively, in the LNs (Fig. 2.2c). Acquisition of effector functions by adoptively transferred OT-I cells was further confirmed by their expression of IFN-γ (Supplementary Fig. 2.1).

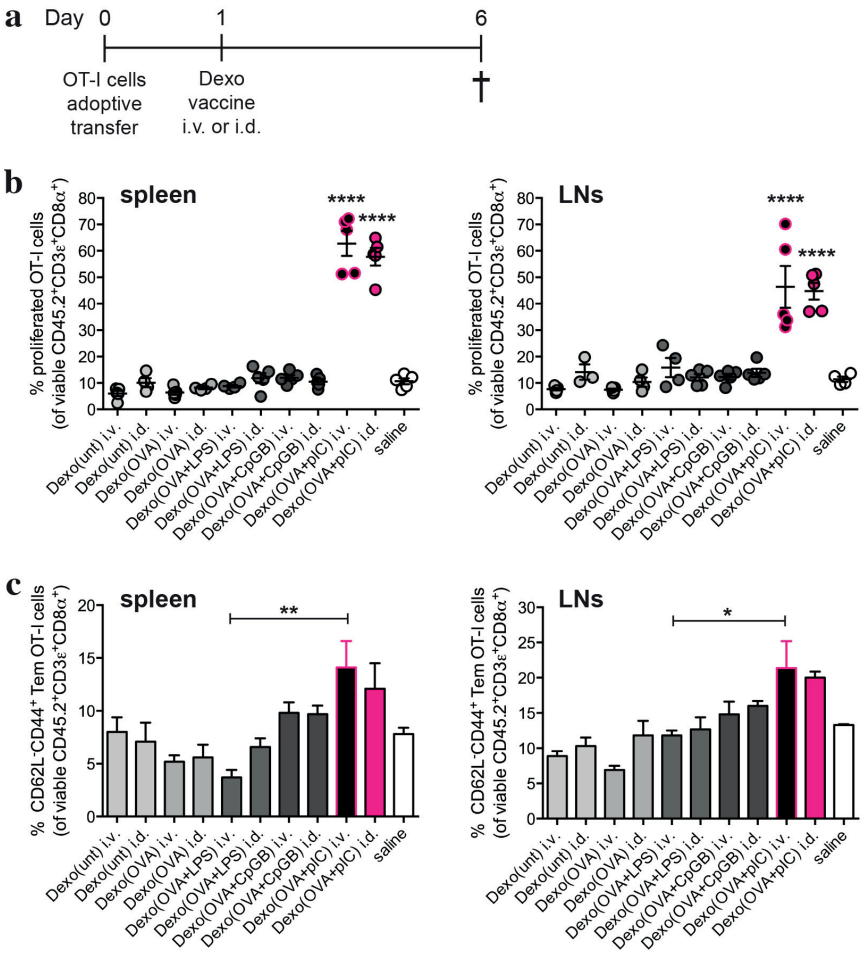

Figure 2.2 Vaccination with exosomes from OVA-loaded and poly(I:C)-activated DCs strongly activates proliferation and acquisition of effector functions of adoptively transferred OT-I OVA-specific CD8$^+$ T cells *in vivo*. (a) CFSE-labeled OT-I CD8$^+$ T cells (CD45.2$^+$) were intravenously transferred into CD45.1$^+$ recipient mice on day 0. Recipient mice were vaccinated on day 1 with 50 μg of the indicated Dexo formulation or saline. On day 6, spleens and brachial, axillary ad inguinal LNs were collected to analyze OT-I cells. (b) Proliferation was measured by flow cytometry as dilution of CFSE dye in adoptively transferred CD45.2$^+$CD3ε$^+$CD8α$^+$ OT-I cells retrieved from the spleen (left) and LNs (right). (c) Acquisition of the CD62L$^-$CD44$^+$ effector memory phenotype of adoptively transferred CD45.2$^+$CD3ε$^+$CD8α$^+$ OT-I cells was measured by flow cytometric analysis of cells harvested from the spleen (left) and LNs (right). Data represent mean ± s.e.m. from 2 independent experiments (n = 10). Statistical analysis was performed by one-way ANOVA and Bonferroni *post-hoc* test correction. In (b) statistics represent comparisons between Dexo(OVA+pIC) i.v. with both Dexo(OVA+LPS) i.v. and Dexo(OVA+CpGB) i.v. groups or between Dexo(OVA+pIC) i.d. with both Dexo(OVA+LPS) i.d. and Dexo(OVA+CpGB) i.d. groups. In (c) statistics represent comparisons between the indicated experimental groups. * $P < 0.05$ ** $P < 0.01$ and **** $P < 0.0001$.

These results prove that in an OT-I adoptive transfer model of vaccination, Dexo(OVA+pIC), i.e. Dexo generated from BMDCs cultured in the presence of OVA and

matured by the TLR-3 agonist poly(I:C), efficiently stimulate antigen-specific $CD8^+$ T cells to expand and to acquire effector functions. The overall immune stimulatory effect of Dexo(OVA+pIC) on OT-I cells was significantly higher than the effect of the Dexo vaccines purified from LPS- or CpG-B-matured BMDCs, demonstrating the higher efficacy of TLR-3 stimulation for the induction of cellular immune responses by Dexo vaccines. Interestingly, comparison of the i.v. and i.d. routes of administration showed that, unlike usual vaccine formulations, Dexo vaccines are equally immunogenic when administered either i.v. or i.d.

2.3.3 Increased induction of OVA-specific endogenous $CD4^+$ and $CD8^+$ T cell immune responses by Dexo(OVA+pIC) vaccination

Although the OT-I adoptive transfer model of vaccination showed a significant increase in the ability of Dexo(OVA+pIC) vaccination to activate OVA-specific $CD8^+$ T cells compared to other Dexo formulations, we wanted to test if the same vaccine was also able to initiate an endogenous OVA-specific Th1 response. Since other groups have previously used i.v. administration of Dexo-based vaccines, and Dexo formulations obtained with LPS-matured DCs have previously been shown to elicit beneficial antigen-specific immune responses [16,21], we sought to compare our Dexo(OVA+pIC) formulation administered either i.v. or i.d. into the four footpads to i.v. administration of either Dexo(unt), Dexo(OVA) or Dexo(OVA+LPS). To do so, the immune system of C57BL/6 recipient mice was first primed on day 0 and then boosted twice on day 14 and 40 with 50 μg of the indicated Dexo vaccine, as shown in Fig. 2.3a.

We monitored the frequency of $OVA_{257–264}$ (SIINFEKL)-specific $CD8^+$ T cells throughout the experimental period by H-2Kb/SIINFEKL pentamer staining and flow cytometric analysis of circulating lymphocytes on day 19 and of splenocytes and brachial, axillary ad inguinal LN cells on day 45. As compared to vaccination with the other Dexo vaccine formulations tested, vaccination with Dexo(OVA+pIC) resulted in significantly increased frequencies of circulating SIINFEKL-specific $CD8^+$ T lymphocytes already 19 days after priming, with up to 0.47% and 0.52% of pentamer positive viable $CD3^+CD8^+$ T cells upon i.v. and i.d. vaccination, respectively (Fig. 2.3b, top left). The difference in the frequencies of SIINFEKL-specific $CD8^+$ T cells between mice administered with Dexo(OVA+pIC) and those administered with the other Dexo vaccines was even more significant at the end of the experimental timeline 45 days after priming. At this time point, in the spleens of the mice vaccinated with i.v. or i.d. Dexo(OVA+pIC) we detected 0.22% and 0.21% of pentamer positive viable $CD3^+CD8^+$ T lymphocytes, respectively, as compared to 0.0062% detected in the spleens of mice vaccinated with i.v. Dexo(OVA+LPS) (Fig. 2.3b, top right). In the LNs, Dexo(OVA+pIC) vaccination induced 0.19% SIINFEKL-specific $CD8^+$ T

lymphocytes when performed either i.v. or i.d., as compared to only 0.082% upon i.v. administration of Dexo(OVA+LPS) (Fig. 2.3b, bottom).

The acquisition of cytotoxic effector functions by OVA-specific $CD8^+$ T lymphocytes in Dexo vaccinated mice was measured after splenocytes and brachial, axillary ad inguinal LN cells were restimulated for 6 hr in the presence of SIINFEKL peptide. Cytotoxic effector functions were evaluated by intracellular staining of IFN-γ and Granzyme-B and flow cytometric analysis of $CD3^+CD8^+$ lymphocytes. In mice vaccinated with i.v. or i.d. Dexo(OVA+pIC), we measured a significantly higher frequency of IFN-γ^+ or Granzyme-B^+ $CD3^+CD8^+$ splenocytes (Fig. 2.3c). 0.031% and 0.026% of IFN-γ^+ $CD3^+CD8^+$ splenocytes were detected in mice vaccinated with Dexo(OVA+pIC) either i.v. or i.d., respectively, as compared to 0.0085% measured in mice receiving i.v. Dexo(OVA+LPS) vaccination (Fig. 2.3c, left). While in the spleens of mice vaccinated with i.v. Dexo(OVA+LPS) we detected 0.038% of Granzyme-B^+ $CD3^+CD8^+$ T cells, in mice vaccinated with i.v. or i.d. Dexo(OVA+pIC) we measured 0.25% and 0.15% of Granzyme-B^+ $CD3^+CD8^+$ splenocytes, respectively (Fig. 2.3c, right). Similar trends were also observed in the LNs of vaccinated mice, with i.v. or i.d. administration of Dexo(OVA+pIC) resulting in a significantly higher frequency of IFN-γ^+ or Granzyme-B^+ $CD3^+CD8^+$ T lymphocytes as compared to the other Dexo formulations tested (Supplementary Fig. 2.2a).

To evaluate acquisition of the Th1 phenotype by OVA-specific $CD4^+$ T lymphocytes, splenocytes and brachial, axillary ad inguinal LN cells from vaccinated mice were restimulated for 6 hr in the presence of OVA, stained for IFN-γ and TNF-α and analyzed by flow cytometry. In mice vaccinated with i.v. or i.d. Dexo(OVA+pIC), we measured a significantly higher frequency of IFN-γ^+ or TNF-α^+ $CD3^+CD4^+$ lymphocytes as compared to mice vaccinated with the other Dexo formulations (Fig. 2.3d). 0.31% and 0.25% of IFN-γ^+ $CD3^+CD4^+$ splenocytes were measured in mice vaccinated with Dexo(OVA+pIC) either i.v. or i.d., respectively, as compared to 0.064% detected in mice receiving i.v. Dexo(OVA+LPS) vaccination (Fig. 2.3d, left). Vaccination with Dexo(OVA+pIC) also significantly raised TNF-α^+ $CD3^+CD4^+$ splenocytes up to 0.083% and 0.11% upon i.v. or i.d. administration, respectively (Fig. 2.3d, right). Similarly to the spleen, the frequencies of IFN-γ^+ and TNF-α^+ $CD3^+CD4^+$ lymphocytes were also significantly higher in the LNs of mice vaccinated with Dexo(OVA+pIC) (Supplementary Fig. 2.2b). Significantly increased expression and release of the Th1 cytokines IFN-γ and TNF-α by the splenocytes of mice vaccinated with i.v. or i.d. administration of Dexo(OVA+pIC) was further confirmed by ELISA (Fig. 2.3e, left, and Supplementary Fig. 2.2c). Secretion of IL-10, instead, was limited, and differences were not significant among the different vaccine treatments tested, thus confirming skewing towards a

Th1 immune response rather than Th2 by vaccination with Dexo(OVA+pIC) (Fig. 2.3e, right).

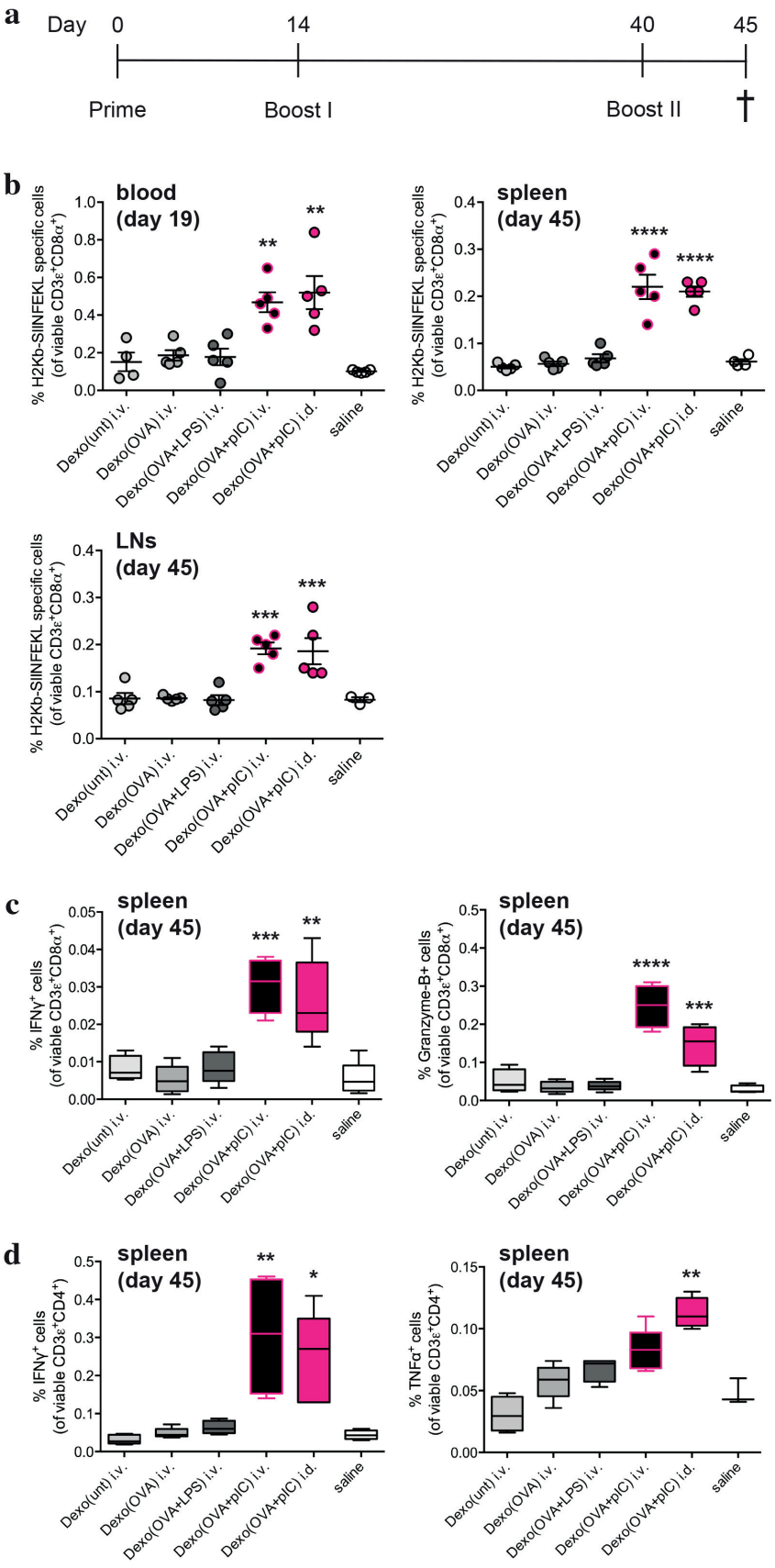

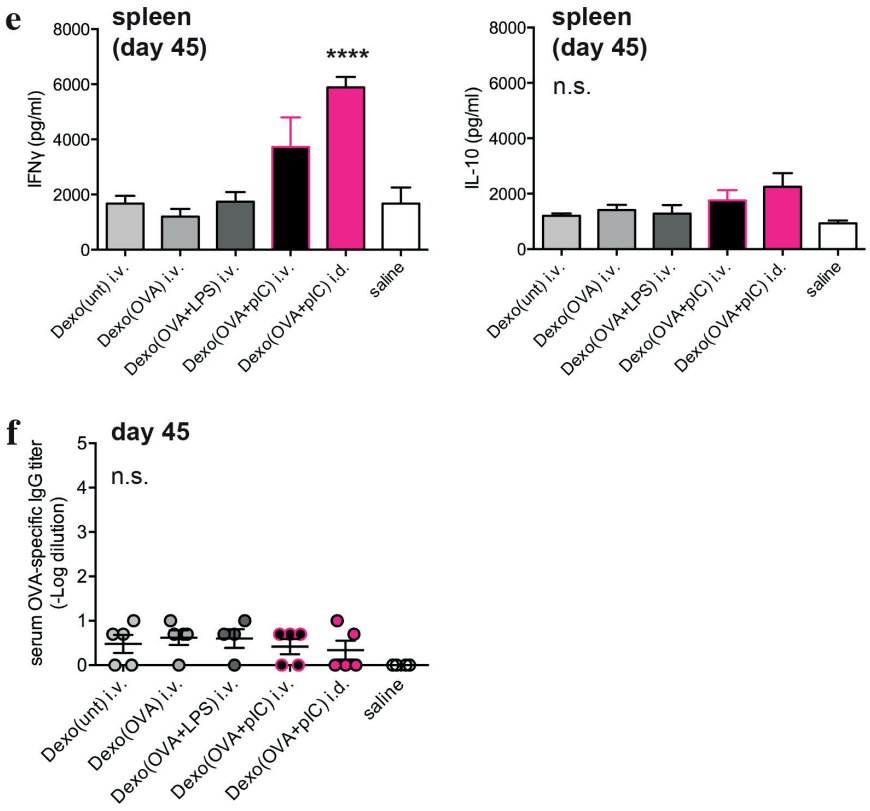

Figure 2.3 Vaccination with exosomes from OVA-loaded and poly(I:C)-activated DCs induces the expansion and acquisition of effector functions of endogenous OVA-specific CD4$^+$ and CD8$^+$ T cells with negligible OVA-specific antibody titers *in vivo*. (a) Wild-type mice were vaccinated i.v. or i.d. with 50 µg of the indicated Dexo formulation or saline on day 0 (prime), 14 (boost I) and 40 (boost II). On day 45, spleens and brachial, axillary ad inguinal LNs were collected to analyze OVA-specific T cell responses, and blood was sampled to measure the titer of OVA-specific IgG antibodies in the serum. (b) Pentamer staining and flow cytometric analysis were used to measure the frequency of SIINFEKL-specific CD8$^+$ T lymphocytes in the blood of vaccinated mice on day 19 (top left) or at the end of the experimental time on day 45 in the spleen (top right) and LNs (bottom) in the population of viable CD3ε$^+$CD8α$^+$ cells. (c) Splenocytes from vaccinated mice were collected on day 45 to measure acquisition of effector functions by SIINFEKL-specific CD8$^+$ T lymphocytes as detected by intracellular staining for IFN-γ (left) and Granzyme-B (right) and flow cytometric analysis. (d) Splenocytes from vaccinated mice were collected on day 45 to measure acquisition of effector functions by OVA-specific CD4$^+$ T lymphocytes as detected by intracellular staining for IFN-γ (left) and TNF-α (right) and flow cytometric analysis. (e) Splenocytes from vaccinated mice were collected on day 45 to measure IFN-γ or IL-10 secreted in the cell supernatant by ELISA upon restimulation in the presence of OVA. (f) Blood from vaccinated mice was collected on day 45 and the titer of OVA-specific IgG antibodies in the serum was measured by ELISA. Data represent mean ± s.e.m. from 2 independent experiments (n = 10). Statistical analysis was performed by one-way ANOVA and Bonferroni *post-hoc* test correction. * $P < 0.05$ ** $P < 0.01$, *** $P < 0.001$, **** $P < 0.0001$ and n.s. = not significant for comparisons of Dexo(OVA+pIC) administered i.v. or i.d. with Dexo(OVA+LPS).

Even though vaccination with Dexo(OVA+pIC) stimulated a greater OVA-specific Th1 immune response as compared to Dexo(unt), Dexo(OVA) and Dexo(OVA+LPS), none of the Dexo formulations tested was able to induce the production of OVA-specific antibodies (Fig. 2.3f), thus confirming the absence of free intact OVA contaminating the Dexo formulations, rather suggesting the presence of OVA or OVA-derived peptides encapsulated inside exosomes or bound to MHC class I and class II molecules on the surface of exosomes, as previously shown by other groups [16,30,44].

These data indicate that poly(I:C)-induced maturation of DCs cultured in the presence of an antigen improves the ability of DC-released Dexo to stimulate antigen-specific cellular rather than humoral immune responses. In particular, vaccination with Dexo(OVA+pIC) stimulates the expansion and activation of endogenous OVA-specific $CD4^+$ and $CD8^+$ T cells, skewing the former towards the pro-inflammatory Th1 phenotype and stimulating the latter to acquire cytotoxic functions more potently than Dexo derived by DC maturation induced by TLR ligands previously used by other groups, most notably LPS [16].

2.3.4 Isolation of DC-derived exosomes containing B16F10 antigens and their use as a therapeutic vaccine in the B16F10 melanoma model

Dexo vaccination had previously entered clinical trials for the treatment of melanoma patients, resulting in poor therapeutic benefit [18]. We therefore sought to test whether our poly(I:C)-based Dexo vaccine could improve the efficacy of Dexo vaccination in a clinically relevant setting of therapeutic vaccination in melanoma-bearing mice, taking advantage of the B16F10 model. Based on the higher immunogenicity of Dexo produced with poly(I:C) as compared to Dexo produced with either LPS or CpG-B as shown in Fig. 2.2 and 2.3, we chose to only utilize poly(I:C) for the production of a Dexo vaccine that could be compared to a Dexo formulation resembling those tested in the clinical trials produced from DCs cultured in the presence of tumor antigens but without adjuvants. To produce DC-derived exosomes carrying native B16F10 antigens instead of the model antigen OVA, we adopted the protocol developed by Chiang et al. to pulse patient-derived DCs with autologous tumor antigens [31,32]. To do so, B16F10 cells were incubated with 60 μM HOCl buffer to induce oxidation-dependent necrosis of the tumor cells, thus allowing the release of melanoma antigens in an immunogenic fashion (Fig. 2.4a). Following the same procedure utilized for the production of our OVA-containing Dexo vaccine formulations, HOCl-oxidized B16F10 cells were cultured together with BMDCs in the presence or not of poly(I:C) to harvest Dexo(B16+pIC) or Dexo(B16), respectively. As an experimental control, we also purified exosomes from DCs matured with poly(I:C) in the absence of oxidized B16F10 cells (Dexo(pIC)).

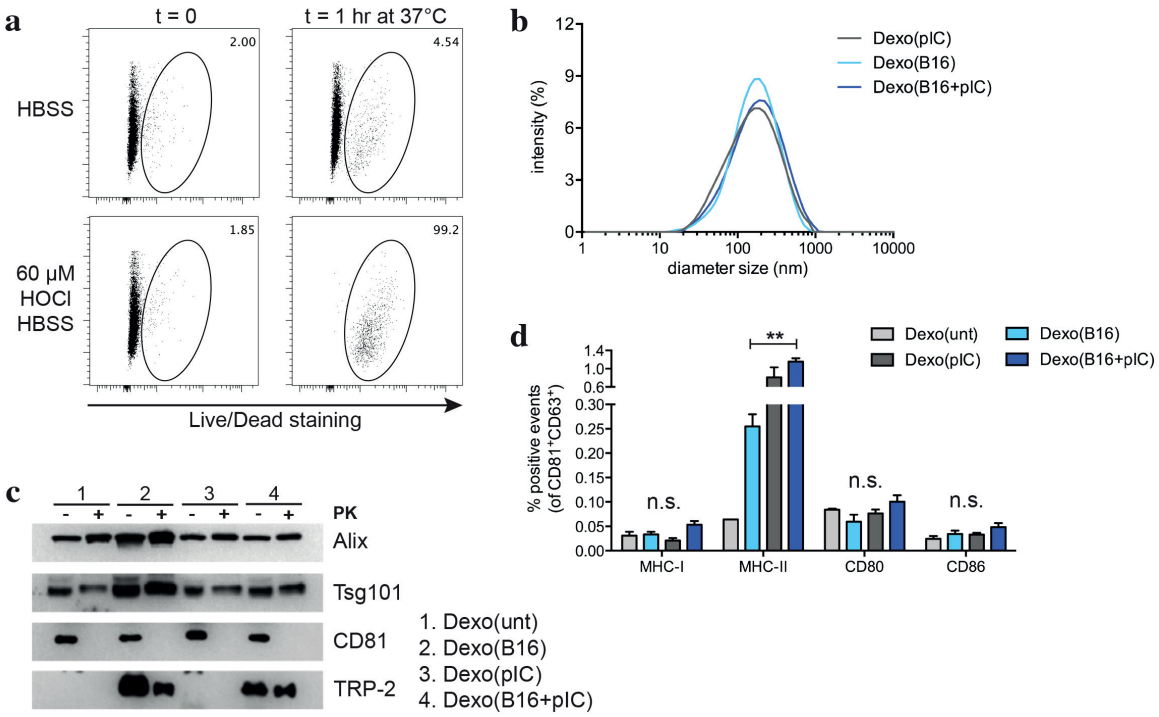

Figure 2.4 HOCl-oxidized B16F10 melanoma cells can be used as a source of tumor antigens for the production of DC exosomes containing melanoma-derived epitopes. (a) B16F10 melanoma cells were resuspended in 60 µM HOCl HBSS buffer and incubated at 37°C for 1 hr to induce oxidation of the tumor cells. After incubation, cells were stained with a viability dye and analyzed by flow cytometry. As controls, viability of B16F10 cells before incubation (t = 0) or B16F10 cells resuspended in HBSS buffer was also analyzed. Numbers indicate the frequency of dead cells gated in the total population of B16F10 cells. (b) Dexo were purified from the supernatant of DCs preincubated with oxidized B16F10 obtained as in (a) with or without poly(I:C) (Dexo(B16+pIC) and Dexo(B16), respectively) or with poly(I:C) only as a control (Dexo(pIC)) following the described protocol for exosomes isolation. After purification, the size of Dexo was measured by DLS analysis. (c) Presence of the exosome-specific markers Alix (100 kDa) and Tsg101 (46 kDa) (intravesicular) and CD81 (26 KDa) (vesicle membrane) and of the full-length melanoma-derived protein TRP-2 (59 kDa) was detected by western blot analysis of Dexo(unt), Dexo(B16), Dexo(pIC) and Dexo(B16+pIC) digested or not with proteinase K to confirm purification of *bona-fide* exosomes and exosomal localization of the antigens. (d) Surface staining for MHC-I, MHC-II, CD80 and CD86 and flow cytometric analysis of Dexo(unt), Dexo(B16), Dexo(pIC) and Dexo(B16+pIC). Percentages represent the frequency of positive events among $CD81^{+}CD63^{+}$ particles. Data in (d) represent mean ± s.e.m. from 2 independent experiments (n = 6). Statistical analysis was performed by one-way ANOVA and Bonferroni *post-hoc* test correction to compare Dexo(B16), Dexo(pIC) and Dexo(B16+pIC). ** $P < 0.01$ and n.s. = not significant.

DLS and western blot analysis of Dexo(B16), Dexo(pIC) and Dexo(B16+pIC) were used to confirm the presence of vesicles with size (30-150 nm in diameter) and markers (Alix,

Tsg101 and CD81) indicative of *bona-fide* exosomes (Fig. 2.4b,c). To prove exosomal packaging of melanoma antigens in Dexo(B16) and Dexo(B16+pIC), we probed Dexo(B16), Dexo(pIC) and Dexo(B16+pIC) samples for the B16F10-derived tyrosinase-related protein 2 (TRP-2). To provide information about the localization of the melanoma-derived TRP-2, Dexo samples were digested with proteinase K (PK) or left untreated before western blot analysis. While detection of the intra-exosomal markers Alix and Tsg101 was not affected by digestion with PK, the exosomal membrane-spanning antigen CD81 could not be revealed after treatment of the exosomes with PK, indicating its export to the extra-vesicular space. Similarly to Alix and Tsg101, TRP-2 was also protected from the enzymatic activity of PK, indicating its intra-exosomal localization, in this case at its expected full-length molecular weight, as contrasted to that observed in Fig. 2.1c with OVA (Fig. 2.4c).

Differences among Dexo(B16), Dexo(pIC) and Dexo(B16+pIC) could be detected by flow cytometry in their surface expression of the antigen-presenting complex MHC-II, which was significantly enriched especially on Dexo(B16+pIC), as a consequence of strong DC maturation upon incubation with oxidized tumor cells in the presence or not of poly(I:C) (Fig. 2.4d).

We proceeded to test whether therapeutic i.d. vaccination with Dexo(B16) or Dexo(B16+pIC) could result in any beneficial outcome in B16F10 tumor-bearing mice. Vaccination with Dexo(pIC) was chosen as a control to test the melanoma specificity of the immune responses raised by Dexo(B16) and Dexo(B16+pIC) vaccination. For this purpose, 10^5 B16F10 cells were inoculated subcutaneously (s.c.) between the scapulae in C57BL/6 mice on day 0 and left to engraft and grow for 4 days. On day 4, 7, 11 and 15, mice were either administered with saline or vaccinated with 50 μg of Dexo(B16), Dexo(pIC) or Dexo(B16+pIC) i.d. in the frontal footpads to improve vaccine efficacy by targeting the immune cells of the tdLNs [33]. Tumor growth was measured until 18 days after inoculation of the B16F10 cells, when the anti-melanoma immune response in the tumor mass, spleen and tdLNs was also analyzed. To determine the survival rate, vaccinated tumor-bearing mice were also kept until death occurred or euthanasia was necessary due to ethical reasons. In the case of mice surviving with no sign of debilitating sickness, experiments were ended 60 days after implantation of the tumor cells (Fig. 2.5a).

Interestingly, all of the Dexo formulations tested were able to significantly reduce the growth of B16F10 tumors as compared to vehicle administration. Most importantly, vaccination with Dexo(B16+pIC) proved the combination of loading with melanoma antigens and stimulation with poly(I:C) for DC-derived exosome production beneficial, resulting in significant reduction of tumor growth not only as compared to saline treatment but also as compared to vaccination with either Dexo(B16) or Dexo(pIC) (Fig. 2.5b, left). The Dexo

vaccines also improved the survival rate of B16F10 tumor-bearing mice and, even though therapeutic vaccination with Dexo(B16+pIC) could not prevent B16F10 tumors from growing, it did slow tumor progression, improving long-term survival of vaccinated mice, with 58% of Dexo(B16+pIC)-vaccinated mice showing no sickness symptoms at the end of the experimental time of 60 days (Fig. 2.5b, right).

To dissect the immunological effects behind the benefits provided by Dexo vaccination, we chose the melanoma-derived protein TRP-2 as a representative antigen to analyze the immune response elicited against B16F10 tumor cells upon Dexo vaccination. The frequency of TRP-$2_{180–188}$ (SVYDFFVWL)-specific $CD3^+CD8^+$ T lymphocytes was measured in the cells from the tdLNs, spleens and tumor masses of vaccinated mice 18 days after tumor cells were inoculated by pentamer staining and flow cytometry. All of the Dexo vaccine formulations tested were able to increase the frequency of TRP2-specific $CD8^+$ T cells as compared to saline treatment, but only vaccination with Dexo(B16+pIC) resulted in significantly increased TRP2-specific $CD8^+$ T lymphocytes as compared to saline and to the other Dexo formulations, not only in the tdLNs (1.32%) and spleens (0.94%) but also in the tumor masses of treated mice (9.7%) (Fig. 2.5c). Of note, the TRP2-specific $CD8^+$ T cells induced by vaccination with Dexo(B16+pIC) also showed increased expression of the effector memory phenotype markers $CD62L^-CD44^+$, with 22.28%, 0.94% and 88.1% of $CD62L^-CD44^+$ TRP2-specific $CD8^+$ T lymphocytes detected in the tdLNs, spleens and tumor masses, respectively (Fig. 2.5d). The acquisition of effector functions by B16F10-specific $CD8^+$ T cells was further confirmed by restimulating *ex vivo* for 6 hr tdLN cells and splenocytes from vaccinated mice with oxidized B16F10 cells (obtained as in Fig. 2.4a) and staining for intracellular IFN-γ and TNF-α for flow cytometric analysis. Cells from mice receiving Dexo(B16+pIC) vaccination responded more strongly to B16F10 antigen-specific restimulation, resulting in 0.062% and 0.176% of IFN-γ^+ $CD3^+CD8^+$ T lymphocytes and 0.0073% and 0.024% of IFN-γ^+TNF-α^+ $CD3^+CD8^+$ T cells in the tdLNs and spleens, respectively (Fig. 2.5e).

Interestingly, tdLN-targeted administration of our Dexo vaccines resulted in favorable recruitment and stimulation of cytotoxic $CD45^+$ cells infiltrating the tumors, especially when Dexo(B16+pIC) vaccine was administered. In the population of tumor-infiltrating $CD8^+$ T lymphocytes, effector memory $CD62L^-CD44^+$ cells were significantly increased (65.1%), while exhausted PD-1^+ cells were significantly reduced (45.95%), in mice vaccinated with Dexo(B16+pIC) (Fig. 2.5f, top). Even though the difference was not statistically significant, also NK cells showed a trend toward increased frequency in the population of hematopoietic cells infiltrating the tumors of Dexo(B16+pIC)-treated mice (15.5%) as compared to mice administered with saline or the other Dexo formulations (Fig.

2.5f, bottom left). NK-T cells, instead, were significantly more represented among CD45$^+$ tumor-infiltrating cells (3.57%) upon Dexo(B16+pIC) vaccination (Fig. 2.5f, bottom right).

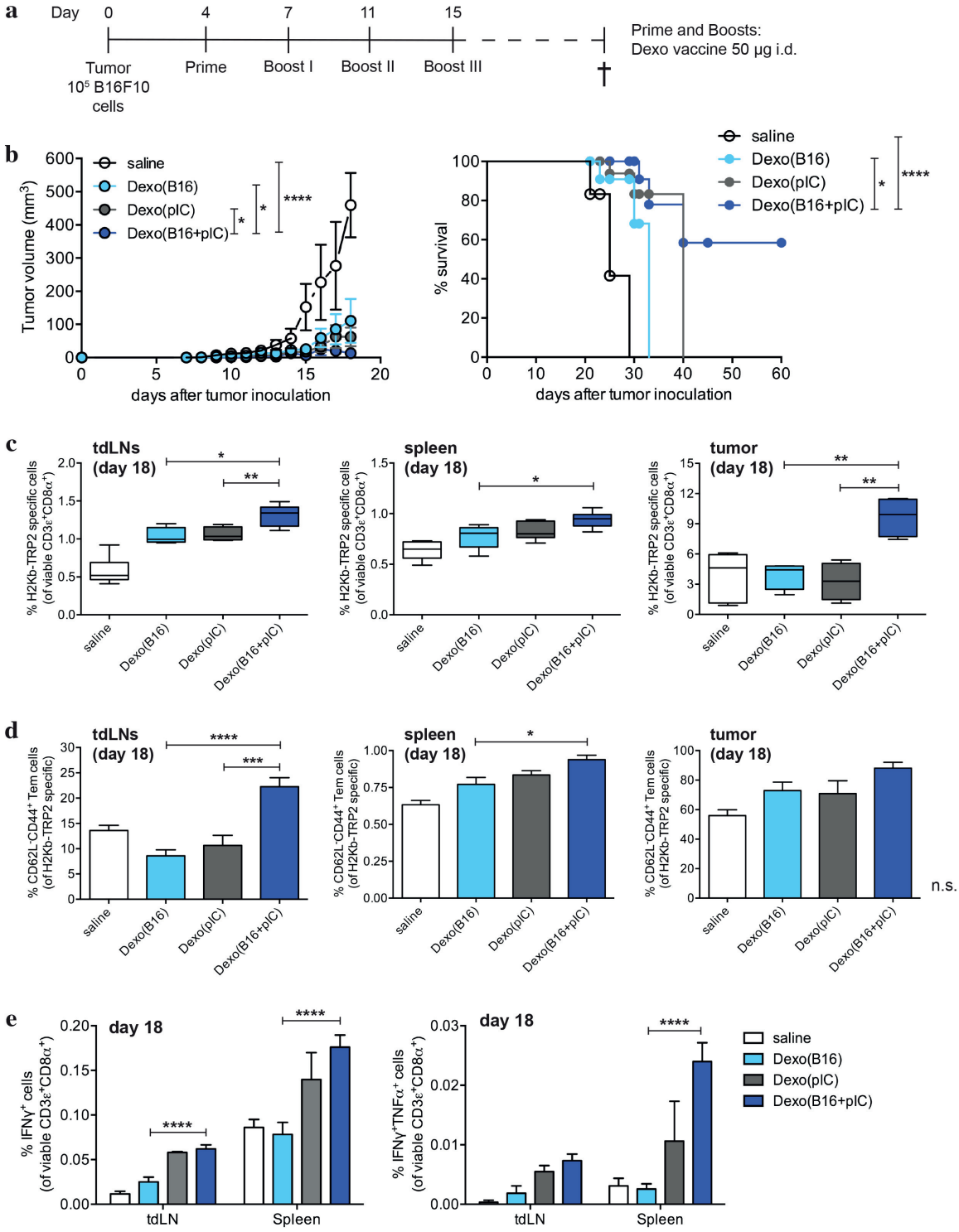

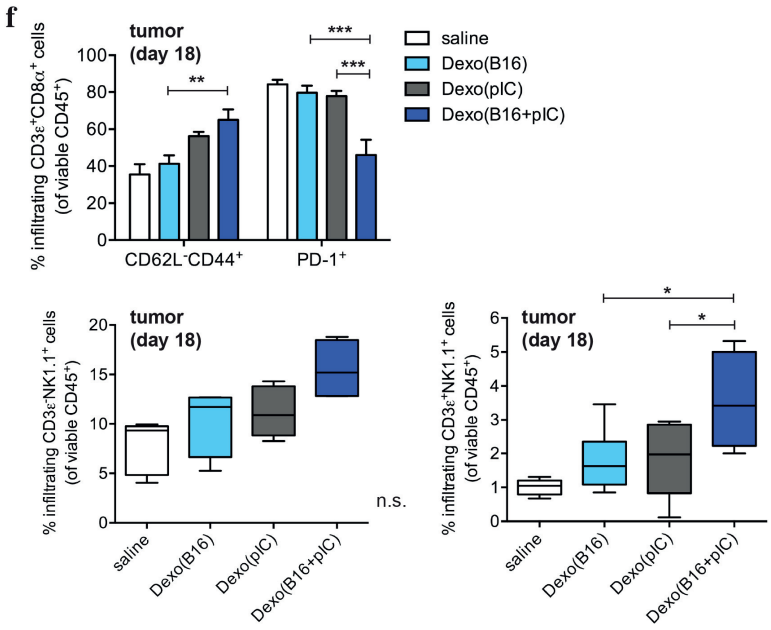

Figure 2.5 Therapeutic vaccination with tumor cell antigen-loaded exosomes from poly(I:C)-activated DCs significantly reduces the growth of B16F10 tumors and improves the survival of tumor-bearing mice by activating melanoma-specific CD8$^+$ T cells and promoting tumor infiltration of cytotoxic cells. (a) B16F10 melanoma cells were inoculated subcutaneously between the scapulae of C57BL/6 mice on day 0. To target the tdLNs, recipient mice were vaccinated i.d. in the frontal footpads with 50 µg of the indicated Dexo formulation or saline on day 4 (prime), 7 (boost I), 11 (boost II) and 15 (boost III). (b) Tumor volumes (left) and survival rate (right) were measured from day 0 to day 18 and from day 0 to day 60 after tumor inoculation, respectively. (c) Frequencies of TRP-$2_{180–188}$ (SVYDFFVWL)-specific CD8$^+$ T lymphocytes in the population of viable CD3ε$^+$CD8α$^+$ cells harvested on day 18 from the tdLNs (left), spleen (middle) and tumor mass (right). (d) Frequencies of CD62L$^-$CD44$^+$ effector memory TRP2-specific CD8$^+$ T lymphocytes harvested on day 18 from the tdLNs (left), spleen (middle) and tumor mass (right). (e) Acquisition of effector functions by B16F10-specific CD8$^+$ T lymphocytes as indicated by intracellular staining of IFN-γ and TNF-α and flow cytometric analysis. (f) Frequencies of tumor-infiltrating CD62L$^-$CD44$^+$ effector memory and exhausted PD-1$^+$ CD8$^+$ T lymphocytes in the population of total viable CD45$^+$CD3ε$^+$CD8α$^+$ cells (top). Frequencies of tumor-infiltrating NK cells (bottom left) and NK-T cells (bottom right) among viable CD45$^+$CD3ε$^-$NK1.1$^+$ or CD45$^+$CD3ε$^+$NK1.1$^+$ cells, respectively. Data represent mean ± s.e.m. from 2 independent experiments (n = 15). Statistical analysis of tumor volumes in (b) was performed by unpaired t test comparing Dexo(B16+pIC) group with either saline, Dexo(B16) or Dexo(pIC) group. * $P < 0.1$; **** $P < 0.0001$. Statistical analysis of survival rates in (b) was performed by Log-rank Mantel-Cox test comparing Dexo(B16+pIC) group with saline, Dexo(B16) and Dexo(pIC) groups. * $P < 0.05$; **** $P < 0.0001$. Statistical analysis of data in (d), (e) and (f) was performed by one-way ANOVA and Bonferroni *post-hoc* test correction. * $P < 0.05$, ** $P < 0.01$, *** $P < 0.001$, **** $P < 0.0001$ and n.s. = not significant for comparisons of Dexo(B16+pIC) with Dexo(B16) and Dexo(pIC).

Confocal microscopy of tumor sections revealed that even though all the Dexo vaccines tested were capable of recruiting $CD45^+$ hematopoietic cells and, especially, $CD3^+$ cells at the tumor site as compared to saline treatment, Dexo(B16+pIC) vaccination induced greater hematopoietic recruitment and, most importantly, infiltration of the tumor mass by lymphocytes (Fig. 2.6, top). Confirming the flow cytometry data described in Fig. 2.5f, the majority of tumor-infiltrating $CD3^+$ cells in the tumors harvested from Dexo(B16+pIC)-vaccinated mice was also $PD\text{-}1^-$ (Fig. 2.6, bottom).

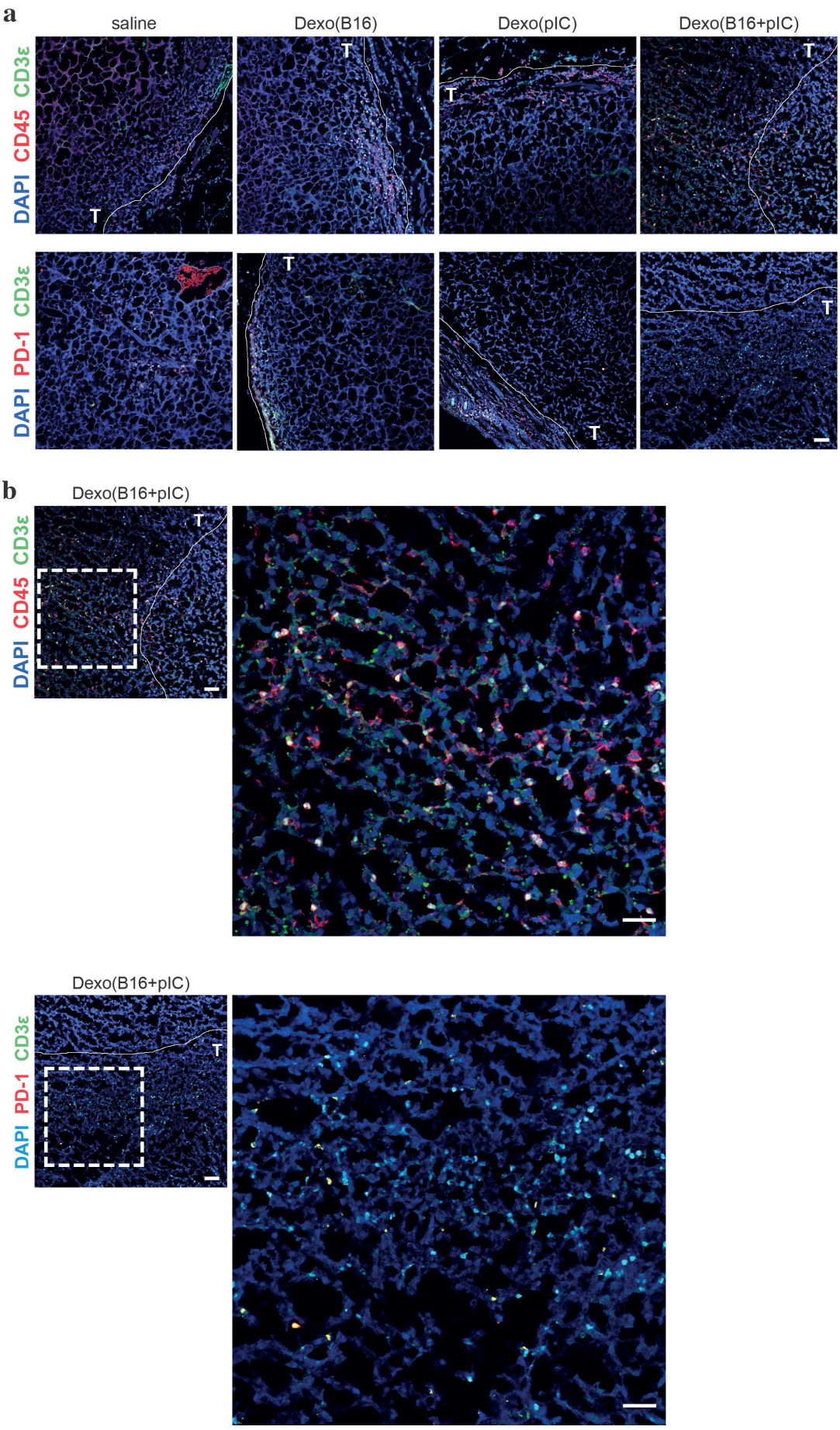
a
saline
Dexo(B16)
Dexo(pIC)
Dexo(B16+pIC)
DAPI CD45 CD3ε
DAPI PD-1 CD3ε
T
b
Dexo(B16+pIC)
DAPI CD45 CD3ε
Dexo(B16+pIC)
DAPI PD-1 CD3ε

Figure 2.6. Vaccination with tumor cell antigen-loaded exosomes from poly(I:C)-activated DCs induces massive recruitment and infiltration of the tumor mass by PD-1$^-$ lymphocytes. (a) Tumor sections from C57BL/6 mice vaccinated as indicated in Fig. 2.5a with the indicated Dexo formulation or saline and euthanized on day 18 were stained for either CD45 and CD3ε (top) or CD45 and PD-1 (bottom) and imaged by confocal microscopy. (b) Higher magnification of the area in the rectangular dashed outline in tumor sections of C57BL/6 mice vaccinated with Dexo(B16+pIC) shown in (a). T = intratumoral area. Representative images from 2 independent experiments are shown (n = 15). Scale bar = 50 μm.

These data indicate that the purification of exosomes containing antigens from a specific tumor cell type, in our case the B16F10 melanoma cells, is feasible. Moreover, tdLN-targeted therapeutic vaccination with exosomes derived from DCs loaded with B16F10 antigens and matured with poly(I:C) shows a beneficial capacity of stimulating B16F10-specific effector CD8$^+$ T cells and recruiting effector T lymphocytes, NK and NK-T cells to the tumor site resulting in smaller tumors and prolonged survival of tumor-bearing mice.

2.4 Discussion

DC-derived exosomes represent an attractive alternative to DC-based vaccines for immunotherapy in cancer patients [5,7,20]. Dexo display immunologically active components derived from DCs but, as vesicles, they constitute a non-living cell-free vaccine tool. Importantly, pre-clinical use of Dexo vaccines in murine tumor models, especially melanoma, has shown the ability of Dexo to stimulate strong antitumoral adaptive immunity, resulting in the suppression of tumor growth [11-17]. On the basis of these promising pre-clinical results, clinical trials were conducted to test therapeutic vaccination with Dexo in patients with late-stage melanoma and non-small cell lung carcinoma. For vaccination in the human subjects, Dexo were produced from autologous DCs and were loaded either directly or indirectly with tumor peptides in the absence of any adjuvants. Even though such clinical trials proved the feasibility of large-scale production of antigen-loaded autologous DC-derived exosomes for use in humans, they failed to prove therapeutic benefits of the vaccination protocol since tumor-specific immunity was elicited only in a limited number of the treated patients [18-20].

Other groups have tried to improve the immunogenicity of Dexo vaccines by developing a formulation that could more effectively induce anti-tumor cytotoxic responses. Use of Dexo rather than tumor cell-derived exosomes and their loading with intact antigens rather than with peptides was shown to induce more potent antitumor immunity related to the activation of a broader repertoire of antigen-specific immune cell clones *in vivo*. Moreover, incubation with TLR ligands, either during exosome production (LPS) or after exosome

purification (Pam_3 or poly(I:C)), resulted in the induction of beneficial pro-inflammatory Th1 responses both *in vitro* and *in vivo* in tumor-bearing animals [16,17,21,25].

The goal of this study was to exploit the intrinsic properties of DCs to take up and process antigens and sense danger signals to mount strong antigen- and adjuvant-tailored immune responses. To do so, we produced exosomes from antigen-loaded DCs that were matured with different TLR ligands, to explore the effects of DC stimulation with different danger signals on the immunogenicity of the exosomes that they secrete. As TLR ligands for DC maturation, we chose TLR agonists that could result in efficient stimulation of Th1 responses both in mice and in humans and that could be easily transferrable to a clinical setting, such as the TLR-3 agonist poly(I:C) and the TLR-9 agonist CpG-B [25,27-29]. Future studies will also explore alternative and possibly more potent TLR agonists for the production of novel Dexo-based vaccine formulations, either as single adjuvant or in combination. Among other candidates, the TLR-4 ligand monophosphoryl lipid A (MPLA) component of LPS is of particular interest as it has shown a promising profile in terms of both safety and immunogenicity in several clinical trials for cancer immunotherapy [39].

Our results show that exosomes purified from the supernatant of DCs loaded with the model antigen OVA and matured with poly(I:C) (Dexo(OVA+pIC)) are significantly more potent activators of antigen-specific Th1 responses than exosomes purified from CpG-B- or LPS-matured DCs, both in an OT-I transfer model of vaccination and in an endogenous model of vaccination. While adoptively transferred OT-I cells responded to Dexo(OVA+pIC) vaccination with vigorous proliferation but only modest acquisition of effector phenotype ($CD62L^-CD44^+$) and functions (IFN-γ expression) (Fig. 2.2), endogenous OVA-specific $CD4^+$ and $CD8^+$ T cells strongly expanded and synthesized Th1 cytokines upon Dexo(OVA+pIC) administration (Fig. 2.3). Interestingly, vaccination with Dexo(OVA+pIC) elicited an anti-OVA cellular response in the absence of detectable OVA-specific antibodies (Fig. 2.3f). The lack of humoral response is consistent with the measurement of no intact OVA antigen being present in the Dexo vaccines we produced, and rather indicates the presence of OVA or OVA-derived peptides encapsulated inside exosomes or bound to MHC class I and class II molecules on the surface of exosomes that could be transferred or presented to APCs and T cells initiating the antigen-specific immune response *in vivo*, as previously published [10,16,30,44].

The efficient stimulation of antigen-specific cellular responses by a poly(I:C)-based Dexo vaccine is highly attractive in the context of therapeutic vaccination for cancer immunotherapy. We thus compared the outcome of a therapeutic vaccination protocol with Dexo produced from B16F10 antigen-loaded DCs with or without poly(I:C)-driven maturation. The B16F10-Dexo vaccines were produced by loading the DCs with a B16F10

cell lysate obtained by oxidation-induced necrosis, rather than with a single melanoma antigen, to stimulate a polyclonal immune response against the tumor cells and provide additional cell-derived danger signals to the DCs other than poly(I:C). In fact, DC pulsing with oxidized tumor cells has been previously shown to enhance the immunogenicity of tumor lysates, resulting in more potent T cell responses in murine models of ovarian cancer and in effective broad anti-tumor immunity and therapeutic beneficial effects in ovarian cancer patients [31,32]. Even though we cannot exclude that a part of the exosomes we purify after co-culturing the DCs with oxidized B16F10 cells is derived from the tumor cells rather than from the DCs, our data show that we are able to purify exosomal vesicles containing antigens from the melanoma cells (like TRP-2), so that they can act as antigen carriers upon vaccination (Fig. 2.4). In contrast to the results with Dexo from OVA-pulsed DCs, we did find full-length TRP-2 in the Dexo from DCs pulsed with oxidized B16F10 cells (Fig. 2.1c and Fig. 2.4c). This may be due to differential efficiency of the antigen processing mechanisms within the DCs between two protein antigens, to differences in the processing mechanisms of free versus cellular antigens, or to presence of exosomes derived from the tumor cells themselves. The intact TRP-2 antigen was not carried over as soluble contaminant, in that it was protected from degradation by extravesicular proteinase K, thus demonstrating its presence within the Dexo particles (Fig. 2.4c). More importantly, significant enrichment of MHC-II molecules could be detected on the surface of Dexo(B16+pIC) particles, indicating not only that treatment of exosome-secreting DCs with oxidized tumor cells and poly(I:C) provides strong maturation signals but also that the secreted Dexo inherit improved antigen-presenting and immune stimulatory capabilities from their cells of origin (Fig. 2.4d).

To maximize the therapeutic effect of Dexo vaccines, we chose to administer Dexo intradermally only at those anatomic sites suitable to target the vaccine to the immune cells of the tdLNs, as it was previously published that targeting the tdLNs provides a more beneficial outcome than targeting the non-tdLNs [33-35]. Indeed, tdLN-targeted vaccination with Dexo(B16+pIC) resulted in reduced tumor growth and prolonged survival of tumor-bearing mice, associated with significantly higher frequencies of melanoma-specific cytotoxic $CD8^+$ T cells and of $CD62L^-CD44^+$ effector memory $CD8^+$ T, NK and NK-T cells and lower frequencies of PD-1^+ exhausted $CD8^+$ T cells infiltrating the tumors as compared to all the other Dexo vaccine formulations we tested (Fig. 2.5 and 2.6). Of note, only vaccination with Dexo(B16+pIC) stimulated massive infiltration of hematopoietic cells, and in particular of PD-1^- lymphocytes, into the tumor mass of treated mice (Fig. 2.6).

Vaccination with Dexo(pIC), i.e. exosomes produced from poly(I:C)-matured DCs in the absence of tumor antigens, was also capable of stimulating a melanoma-specific immune

response resulting in reduced tumor growth and prolonged survival as compared to vaccination with Dexo(B16). This finding is not completely unexpected, as locally administered immune adjuvants in cancer immunotherapy are known to contribute to tumor-associated inflammation leading to the enhancement of protective immunity [40-43]. In our experimental setting of tdLN-targeted vaccination, the simultaneous presence in the tdLNs of Dexo(pIC)- or Dexo(B16+pIC)-delivered danger signals and of tumor-derived antigens (both draining from the tumor site and carried by Dexo) resulted in beneficial anti-cancer immunity, more effectively stimulated by vaccination with Dexo(B16+pIC).

Previous groups showed that the adjuvants used to induce DC maturation during exosome production can bind to the exosome membrane and can thus be co-injected with the Dexo vaccine, directly activating APCs *in vivo* as a by-stander effect [21]. We provide further evidence that small amounts of poly(I:C) are in fact consistently found in poly(I:C)-Dexo vaccines after purification (Supplementary Fig. 2.3a). Upon Dexo vaccination, poly(I:C) molecules could participate in the induction of immune cell activation and tumor growth arrest by direct engagement of TLR-3 molecules expressed by myeloid DCs and T cells and by tumor cells, respectively, even though exposure to nucleases may lead to their rapid degradation *in vivo* [37,38]. Nevertheless, exosomes isolated from antigen-loaded DCs matured with poly(I:C) have more potent stimulatory effects on antigen-specific $CD8^+$ T lymphocytes than equivalent doses of free poly(I:C) and such effects cannot be abrogated by specifically blocking the TLR-3, thus excluding that the immunogenic effect of poly(I:C)-based Dexo depends exclusively on the adjuvant molecules contaminating each Dexo formulation (Supplementary Fig. 2.3b). We instead speculate that the DC-derived molecular components of Dexo, such as MHC complexes, co-stimulatory molecules, adhesion molecules and pro-inflammatory signals, together with antigenic epitopes as well as adjuvant molecule carry-over all concomitantly participate in positively affecting the immunogenic properties of a Dexo vaccine.

In summary, we provide evidence that exosomes produced from antigen-loaded DCs matured with the TLR-3 agonist poly(I:C) are more potent immunogens than exosomes produced with LPS for TLR-4 or CpG-B for TLR-9. We show that the purification of DC-derived exosomes carrying epitopes from melanoma cells is feasible and is able to produce potent antitumoral immunity, leading to tumor growth control in 58% of the animals treated. This approach is potentially transferrable to any type of clinically relevant tumor cell for the development of potent tumor-tailored Dexo vaccines.

2.5 Supplementary figures

Supplementary Fig. 2.1

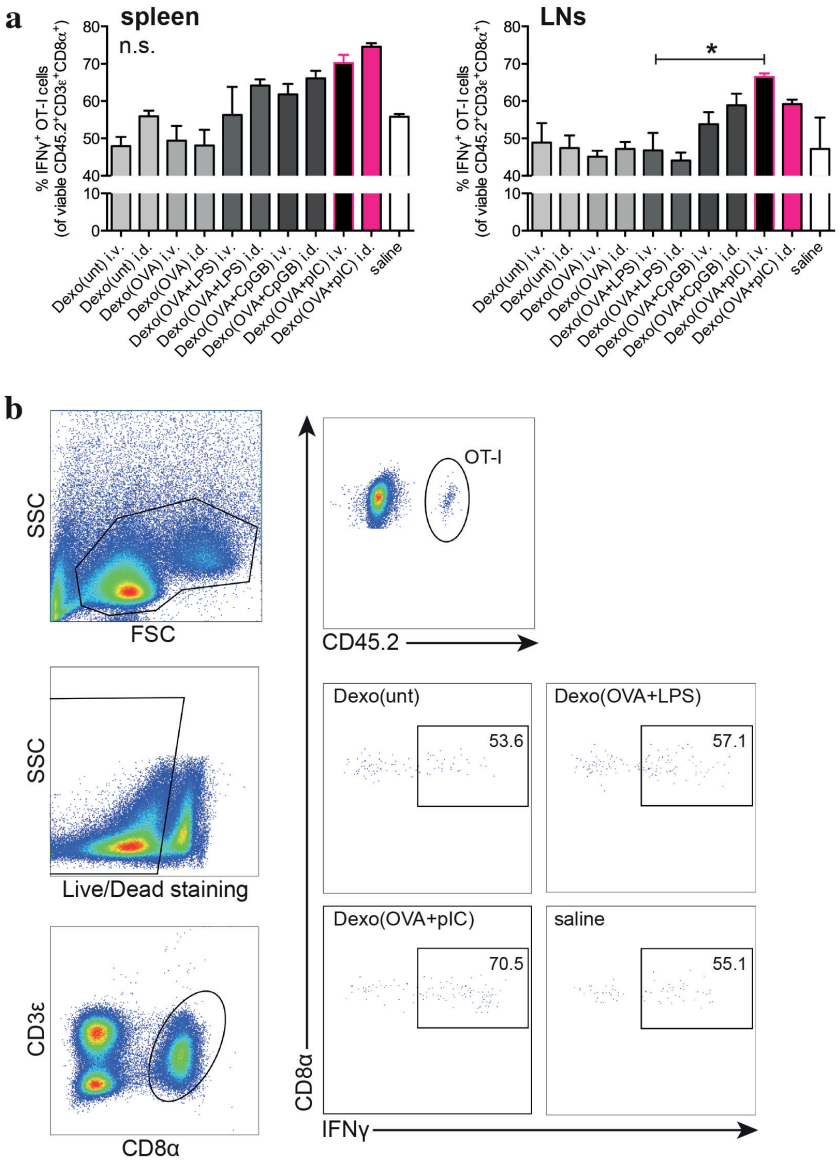

Supplementary figure 2.1 Vaccination with exosomes from OVA-loaded and poly(I:C)-activated DCs strongly activates proliferation and acquisition of effector functions of adoptively transferred OT-I OVA-specific CD8$^+$ T cells *in vivo*. (a) Effector functions of transferred CD45.2$^+$CD3ε$^+$CD8α$^+$ OT-I cells harvested from the spleen (left) or LNs (right) of mice vaccinated as indicated in Fig. 2.1a with the indicated Dexo formulation or saline were evaluated by detecting IFN-γ expression by intracellular staining and flow cytometry. (b) Representative flow cytometric plots of LN cells stained for viability and CD3ε, CD8α, CD45.2 and IFN-γ to identify adoptively transferred IFN-γ$^+$ OT-I cells in mice vaccinated as in Fig. 2.1a with the indicated Dexo formulation administered i.d. or saline. Numbers represent the frequency of IFN-γ$^+$ events in the population of viable CD45.2$^+$CD3ε$^+$CD8α$^+$ OT-I cells. Data represent mean ± s.e.m. from 2 independent experiments (n = 10). Statistical analysis was performed by one-way ANOVA and Bonferroni *post-hoc* test correction between the indicated experimental groups. * $P < 0.05$.

Supplementary Fig. 2.2

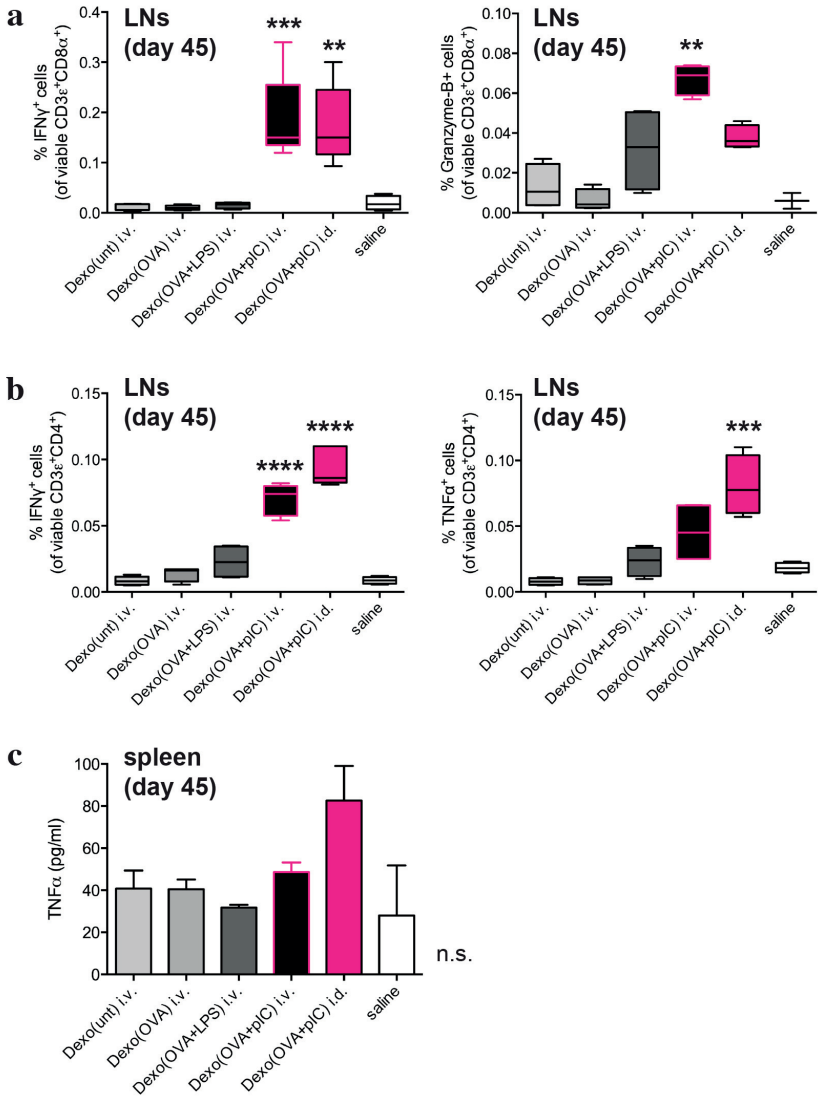

Supplementary figure 2.2 Vaccination with exosomes from OVA-loaded and poly(I:C)-activated DCs induces the expansion and acquisition of effector functions of endogenous OVA-specific CD4$^+$ and CD8$^+$ T cells with negligible OVA-specific antibody titers *in vivo*. (a) LN cells from mice vaccinated as in Fig. 2.3a with the indicated Dexo formulation or saline were collected on day 45 to measure acquisition of effector functions by SIINFEKL-specific CD8$^+$ T lymphocytes as detected by intracellular staining for IFN-γ (left) and Granzyme-B (right) and flow cytometric analysis. (b) LN cells from mice vaccinated as in Fig. 2.3a with the indicated Dexo formulation or saline were collected on day 45 to measure acquisition of effector functions by OVA-specific CD4$^+$ T lymphocytes as detected by intracellular staining for IFN-γ (left) and TNF-α (right) and flow cytometric analysis. (c) Splenocytes from vaccinated mice were collected on day 45 to measure TNF-α secreted in the cell supernatant by ELISA. Data represent mean ± s.e.m. from 2 independent experiments (n = 10). Statistical analysis was performed by one-way ANOVA and Bonferroni *post-hoc* test correction. ** $P <$ 0.01, *** $P < 0.001$, **** $P < 0.0001$ and n.s. = not significant for comparisons of Dexo(OVA+pIC) with Dexo(OVA+LPS).

Supplementary Fig. 2.3

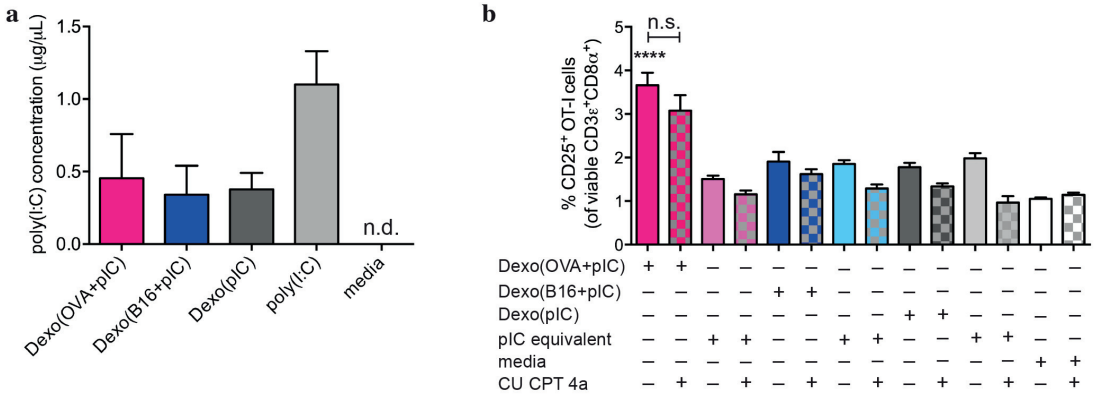

Supplementary figure 2.3 Exosomes purified from poly(I:C)-activated DCs contain poly(I:C) carry-over but show greater antigen-specific immune stimulatory properties than equivalent doses of poly(I:C). (a) To detect and quantify poly(I:C) molecules in Dexo samples, murine TLR-3 reporter HEK-293T cells were treated with exosomes purified from poly(I:C)-activated DCs either loaded with OVA (Dexo(OVA+pIC)) or oxidized B16F10 cells (Dexo(B16+pIC)) or no antigen (Dexo(pIC)). As a control to test the assay quantification, reporter cells were either treated with a known amount of poly(I:C) (1 µg/µL) or left untreated. (b) OVA-specific OT-I cells were co-cultured in the presence of bone-marrow-derived DCs and treated with 25 µg of the indicated Dexo formulation or with a dose of poly(I:C) equivalent to the amount of active poly(I:C) measured in the Dexo formulation as in (a). The TLR-3 specific inhibitor CU CPT 4a was also added in the indicated co-culture conditions to test the involvement of poly(I:C)-triggered TLR-3 activation in the stimulation of OT-I cells by Dexo. Activation of the OT-I cells was measured by flow cytometric analysis of viable $CD25^+CD3\varepsilon^+CD8\alpha^+$ OT-I cells. Data represent mean ± s.e.m. from two independent experiments (n = 6). Statistical analysis was performed by one-way ANOVA and Bonferroni *post-hoc* test correction. **** $P < 0.0001$.

Supplementary Fig. 2.4

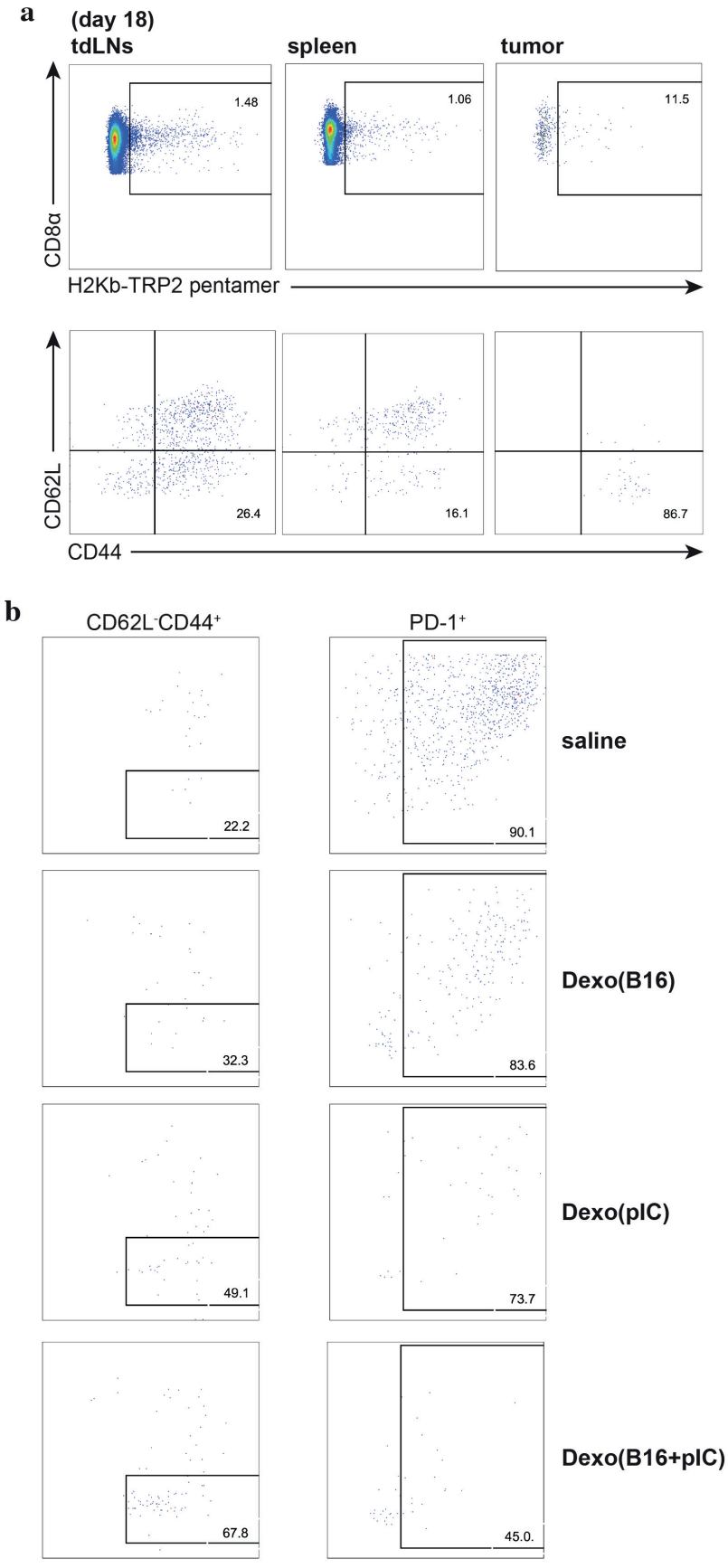

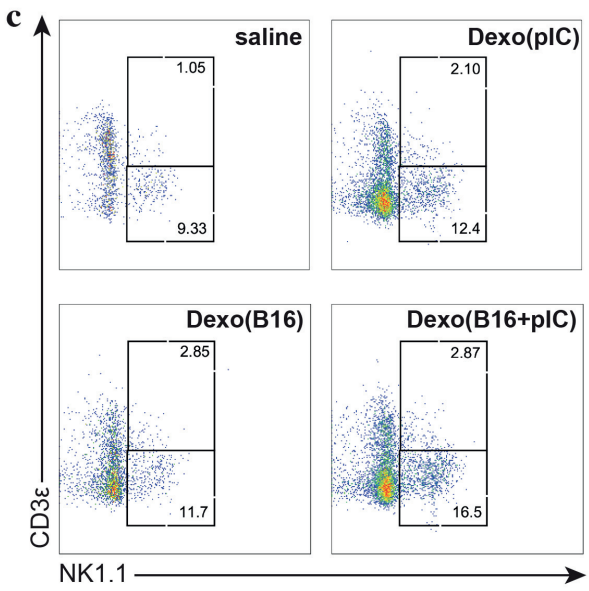

Supplementary figure 2.4 Therapeutic vaccination with tumor cell antigen-loaded exosomes from poly(I:C)-activated DCs significantly reduces the growth of B16F10 tumors and improves the survival of tumor-bearing mice by activating melanoma-specific CD8$^+$ T cells and promoting tumor infiltration of cytotoxic cells. (a) Representative flow cytometry dot plots of TRP-2$_{180–188}$ (SVYDFFVWL)-specific CD8$^+$ T lymphocytes (top) and of CD62L$^-$CD44$^+$ effector memory TRP2-specific CD8$^+$ T lymphocytes (bottom) harvested on day 18 from the tdLNs (left), spleen (middle) and tumor mass (right) of mice vaccinated as in Fig. 2.5a with Dexo(B16+pIC). Numbers indicate the frequency of gated cells among viable CD3ε$^+$CD8α$^+$ cells (b) Representative flow cytometry dot plots of tumor-infiltrating CD62L$^-$CD44$^+$ effector memory (left) and exhausted PD-1$^+$ CD8$^+$ T lymphocytes (right) in mice treated as in Fig. 2.5a with the indicated Dexo formulation or saline. Numbers represent the frequency of gated events among viable CD45$^+$CD3ε$^+$CD8α$^+$ cells. (c) Representative dot plots of tumor-infiltrating NK (CD3ε$^-$NK1.1$^+$) and NK-T (CD3ε$^+$NK1.1$^+$) cells from mice vaccinated as in Fig. 2.5a with the indicated Dexo formulation or saline. Numbers represent the frequency of gated events among viable CD45$^+$ cells. Representative data from 2 independent experiments (n = 15).

Author contributions

M. Damo and J. A. Hubbell designed research; M. Damo performed research described in all the Figures and Supplementary Figures; D. S. Wilson helped performing research described in Figure 2.5 and in Supplementary Figure 2.4; M. Damo analyzed data; D. S. Wilson and E. Simeoni helped analyzing data.

2.6 Materials and methods

2.6.1 Reagents

Chemicals and reagents were purchased from Sigma-Aldrich (Buchs, Switzerland), unless specifically indicated. RPMI 1640 GlutaMAX, IMDM GlutaMAX and DMEM GlutaMAX media, FBS, penicillin/streptomycin, 2-Mercaptoethanol and HBSS buffer were purchased from Life Technologies (Carlsbad, CA). Chemically defined X-VIVO 15 medium was from Lonza (Basel, Switzerland). Abs for western blot were purchased from Sigma-Aldrich or Bio-Rad (Hercules, CA). Live/dead fixable cell viability reagents for flow cytometry were from Life Technologies. PE-labeled H-2Kb/SIINFEKL and H-2Kb/TRP-$2_{180–188}$ (SVYDFFVWL) pentamers were purchased from Proimmune (Oxford, UK). Abs used in flow cytometry were from eBioscience (Vienna, Austria) or BioLegend (Lucerne, Switzerland).

2.6.2 Production of OVA-loaded DC-derived exosomes (Dexo)

Bone-marrow derived DCs (BMDCs) were generated by culturing total bone marrow cells from 8-10 week old female C57BL/6 mice (Harlan Laboratories, Gannat, France) in RPMI 1640 GlutaMAX medium supplemented with 10% FBS, 100 IU/mL penicillin-streptomycin, 50 μM 2-Mercaptoethanol and 20 ng/mL recombinant murine GM-CSF (PeproTech, Rocky Hill, NJ) at 37°C 5% CO_2. On day 3, a volume of complete medium equal to the original culture volume was added to the cells. On day 6, BMDCs were harvested, washed in PBS and cultured for OVA antigen loading. To produce Dexo(unt), BMDCs were cultured in complete medium at 37°C 5% CO_2 for 12 hr. To produce OVA-loaded Dexo, BMDCs were cultured in complete medium supplemented with 300 μg/mL endo-grade chicken OVA (Hyglos, Bernried am Starnberger See, Germany) at 37°C 5% CO_2 for 12 hr. After 12 hr, BMDCs were harvested, washed extensively in PBS to eliminate serum and free OVA and cultured in X-VIVO 15 medium for the production of Dexo(unt) and Dexo(OVA) or X-VIVO 15 medium supplemented with either 50 ng/mL LPS, 8 μg/mL CpG-B 1826 oligonucleotide (5′-TCCATGACGTTCCTGACGTT-3′ from Microsynth, Balgach, Switzerland), or 50 μg/mL poly(I:C) (InvivoGen, San Diego, CA) for the production of Dexo(OVA+LPS), Dexo(OVA+CpGB) or Dexo(OVA+pIC), respectively. On day 8, exosomes were isolated by serial (ultra)centrifugation.

2.6.3 Isolation of Dexo

The supernatant of BMDCs was collected and centrifuged first at 300 × *g* for 5 min at 4°C and then at 2000 × *g* for 10 min at 4°C, passed through 0.22 μm filters (Millipore, Billerica, MA) and subsequently spun at 110,000 × *g* for 90 min at 4°C using a Beckman Coulter (Brea,

CA) ultracentrifuge. Exosome pellets were resuspended in PBS and frozen at -80°C prior to use.

2.6.4 BCA, transmission electron microscopy, dynamic light scattering analysis and flow cytometry of Dexo

Total protein concentration of Dexo samples was measured by BCA assay (Thermo Fisher Scientific, Waltham, MA) following the manufacturer's instructions and it was used to determine the dose of Dexo for *in vitro* and *in vivo* studies. For transmission electron microscopy, 20 μg of Dexo were serially diluted in PBS and samples were transferred onto carbon-coated Formvar grids (SPI Supplies, Structure Probe Inc., West Chester, PA). Dexo were then fixed in 1% glutaraldehyde, stained in uranyl-oxalate pH 7 and imaged with a Tecnai Spirit (FEI, Hillsboro, OR) transmission electron microscope. For dynamic light scattering analysis, exosomes samples were diluted in PBS and analysed with a Zetasizer instrument (Malvern, UK). For flow cytometric analysis, 25 μg of Dexo were adsorbed on magnetic beads coated with anti-CD81 Ab (Life Technologies). After washing, Dexo were stained with Abs specific for the surface markers CD63, H-2Kb (MHC-I), I-A/I-E (MHC-II), CD80 and CD86 in 2% FBS PBS solution. Samples were acquired on an LSR II cytometer (BD Biosciences) and data analyzed with FlowJo software (Tree Star).

2.6.5 Mass spectrometry (LC-MS/MS) and Western blot analysis

20 μg of Dexo were boiled at 70°C for 10 min in Laemmli buffer (Bio-Rad) and loaded onto a 12% polyacrylamide gel (Bio-Rad) for SDS-Page. For LC-MS/MS analysis, after electrophoresis gels were stained with SimplyBlue stain (Life Technologies) and the protein bands of interest were sliced and digested in trypsin solution prior to injection into LC-MS. Data analysis was performed using the Scaffold_4.4.4 software (Proteome Software, Portland, OR). For western blot, after SDS-Page proteins were transferred onto an Immobilon PVDF membrane (Millipore) and the membrane was blocked in 5% skim milk PBS solution O/N at 4°C. Membranes were then incubated with primary Abs specific for Alix, CD81, OVA, TRP-2 or Tsg101 diluted in 5% skim milk PBS for 1 hr at RT, washed in 0.05% Tween-20 PBS and incubated with horseradish peroxidase-conjugated secondary Abs diluted in 5% skim milk PBS for 1 hr at RT. After extensive washing in 0.05% Tween-20 PBS, protein bands were visualized using SuperSignal West Pico Chemiluminescent substrate (Thermo Fisher Scientific) according to manufacturer's instructions. For proteinase K digestion of Dexo samples, 20 μg of Dexo were incubated at 37°C in 50 μg/mL proteinase K (Qiagen, Limburg, The Netherlands) PBS solution for 10 min followed by 15 min at 95°C to deactivate the enzyme. Samples were then prepared as indicated above for SDS-Page and western blot.

2.6.6 Mice

C57BL/6 female mice and CD45.2$^+$ OT-I transgenic female mice (8 to 12 weeks of age) were obtained from Harlan Laboratories, CD45.1$^+$ C57BL/6-Ly5.1 female mice (8 to 12 weeks of age) were purchased from Charles River (Saint-Germain-Nuelles, France). Animals were housed in pathogen-free conditions at the animal facility of the Ecole Polytechnique Fédérale de Lausanne and all experiments were performed in accordance with Swiss law and with approval from the Cantonal Veterinary Office of Canton de Vaud, Switzerland (Authorization number 2935).

2.6.7 Vaccination studies

For the OT-I adoptive transfer model of vaccination, on day 0, CD45.2$^+$ OT-I cells were purified from the spleen and LNs of OT-I transgenic mice by negative selection of CD8α$^+$ T cells using the EasySep mouse CD8α T cell isolation kit (Stemcell Technologies, Grenoble, France) following the manufacturer's instructions. For CFSE labeling, OT-I cells were incubated in 1 μM CFSE (Life Technologies) PBS solution at 5×10^6 cells/mL at RT for 6 min and labeling reaction was quenched by adding an equal volume of 10% FBS PBS. CD45.1$^+$ C57BL/6-Ly5.1 recipient mice were anesthetized with isoflurane and 10^6 OT-I cells/mouse were administered by tail vein injection. On day 1, recipient mice were anesthetized with isoflurane and vaccinated either intravenously by tail vein injection or intradermally into the 4 footpads with a dose of 50 μg of the indicated Dexo formulation. On day 6, recipient mice were euthanized to collect splenocytes and LN cells.

For the endogenous vaccination model, C57BL/6 mice were anesthetized with isoflurane and administered either intravenously into the tail vein or intradermally into the 4 footpads with 50 μg of the indicated Dexo formulation on day 0, 14 and 40. Blood was sampled on day 19 performing a small cut on the tail to collect peripheral lymphocytes and perform pentamer staining. On day 45, mice were euthanized to collect splenocytes, LN cells and blood serum.

2.6.8 Ex vivo *restimulation, surface and intracellular staining and flow cytometry*

Splenocytes were obtained by gently disrupting the spleen through a 70-μm cell strainer (Corning, NY), followed by extensive washing and red blood cell lysis. LNs were first digested for 45 min in RPMI 1640 GlutaMAX medium supplemented with 1 mg/mL Collagenase D (Roche, Basel, Switzerland).

Intracellular IFN-γ of OT-I cells was determined after 2 hr of PMA (50 ng/mL)/ionomycin (1 μg/mL) treatment followed by 2 hr of BFA treatment (5 μg/mL) of the splenocytes and LN cells. For T cell antigen-specific restimulation and intracellular cytokine staining, cells were cultured for 6 hr at 37 °C in the presence of 1 μg/mL SIINFEKL (GenScript, Piscataway, NJ)

or 100 μg/mL OVA grade V protein for $CD8^+$ T cell or $CD4^+$ T cell restimulation, respectively, with the addition of 5 μg/mL BFA for the last 3 hr of culture.

Cells were then processed, counted and stained for viability and immunological markers to be analyzed by flow cytometry. Cells were first stained using Live/Dead fixable cell viability reagents (Life Technologies) according to the manufacturer's instructions and then stained with Abs specific for the surface markers CD45.2, CD3ε, CD4, CD8α, CD62L and CD44. Staining with PE-labeled H-2Kb/SIINFEKL pentamer was performed according to the manufacturer's instructions. For intracellular cytokine staining, cells were fixed in 2% paraformaldehyde solution, washed with 0.5% saponin (Sigma-Aldrich) in 2% FBS PBS solution, and incubated with Abs specific for IFN-γ, Granzyme-B and TNF-α diluted in saponin solution. After washing, cells were resuspended in 2% FBS PBS solution for analysis. Samples were acquired on an LSR II cytometer (BD Biosciences) and data analyzed with FlowJo software (Tree Star). Alternatively, splenocytes were restimulated for 4 days in the presence of 100 μg/mL OVA grade V protein for the measurement of IFN-γ, TNF-α and IL-10 released in the supernatant by ELISA using Ready-SET-go! ELISA kits from eBioscience. OVA-specific antibody ELISAs on serum samples were performed as described previously [36]. All cells were cultured in IMDM GlutaMAX medium supplemented with 10% FBS and 100 IU/mL penicillin-streptomycin.

2.6.9 Culture and oxidation of B16F10 cells

B16F10 (CRL-6475) cells were obtained from the American Type Culture Collection and cultured according to the instructions. Cells were checked for *Mycoplasma* prior to use; no additional authentication was performed. The procedure to obtain oxidation-dependent necrosis of tumor cells was previously published [31]. Briefly, B16F10 cells were resuspended at 10^6 cells/mL in 60 μM HOCl solution, obtained by diluting the stock NaOCl in HBSS buffer, and incubated at 37°C for 1 hr. Cells were extensively washed in HBSS and either analyzed for viability using Live/Dead fixable cell viability reagent followed by flow cytometry or used for Dexo production or *ex vivo* restimulation.

2.6.10 Production of B16F10 antigen-loaded Dexo

BMDCs were differentiated as described above. On day 6, cells were cultured in complete medium together with HOCl-oxidized B16F10 cells (1:1) at 37°C 5% CO_2 for 12 hr. After 12 hr, BMDCs were harvested, washed extensively in PBS and cultured in X-VIVO 15 medium for the production of Dexo(B16) or X-VIVO 15 medium supplemented with 50 μg/mL poly(I:C) for the production of Dexo(B16+pIC). For the production of Dexo(pIC), BMDCs

were only cultured with X-VIVO 15 medium supplemented with 50 μg/mL poly(I:C). On day 8, we proceeded to isolate Dexo by serial (ultra)centrifugation as indicated above.

2.6.11 B16F10 tumor vaccination studies

On day 0, C57BL/6 mice were anesthetized with isoflurane and their back was shaved. 10^5 B16F10 cells resuspended in 100 μL of PBS were inoculated subcutaneously between the scapulae of each mouse. On day 4, 7, 11 and 15 mice were anesthetized with isoflurane and vaccinated intradermally into the 2 frontal footpads with 50 μg of the indicated Dexo formulation. Tumors were measured with a digital caliper until day 18 after tumor inoculation, and volumes (V) were calculated as ellipsoids ($V = \pi/6 \times \text{length} \times \text{width} \times \text{height}$). For survival rate assessment, mice were kept until death occurred or sacrifice was necessary due to sickness or tumor volumes > 1 cm^3, as required by Swiss law. In the case of mice surviving with no sign of debilitating sickness, experiments were ended 60 days after implantation of the tumor cells. For immunological readouts and imaging by confocal microscopy, vaccinated tumor-bearing mice were euthanized on day 18 after tumor inoculation to collect cells from the spleen, tdLNs and tumor mass. Splenocytes and tdLN cells were obtained as described above. Tumors were processed as previously published [33].

For restimulation with oxidized B16F10 cells and intracellular cytokine staining, splenocytes and tdLN cells were cultured for 6 hr at 37 °C in the presence of 10^5 HOCl-oxidized B16F10 cells, with the addition of 5 μg/mL BFA for the last 3 hr of culture. Cells were then processed, counted and stained for viability and immunological markers to be analyzed by flow cytometry. Cells were first stained using Live/Dead fixable cell viability reagents and then stained with Abs specific for the surface markers CD45, CD3ε, CD8α, CD62L, CD44, PD-1 and NK1.1 Staining with PE-labeled H-2Kb/TRP-$2_{180\text{-}188}$ pentamer was performed according to the manufacturer's instructions. For intracellular staining of IFN-γ and TNF-α, cells were processed as indicated above. Samples were acquired on an LSR II cytometer and data analyzed with FlowJo software. For imaging by confocal microscopy, tumors were fixed in 4% paraformaldehyde solution and frozen in OCT (Sakura, Osaka, Japan). 10 μm-thick sections were sliced and stained with primary Abs specific for CD45, CD3ε and PD-1 and fluorescently labeled secondary Abs (Life Technologies). Samples were mounted using ProLong Gold antifade reagent with DAPI (Life Technologies) and imaged with a LSM 700 inverted confocal microscope (Zeiss, Jena, Germany).

2.6.12 TLR-3 reporter assay and OT-I in vitro *activation*

Murine TLR-3 reporter HEK-293T cells were purchased from InvivoGen and cultured as indicated by the manufacturer's instructions. For the reporter assay, 2×10^4 cells were

cultured with serial dilutions of poly(I:C) as standard curve or 10 μg of the indicated Dexo formulation for 24 hr at 37°C 5% CO_2. Engagement of TLR-3 resulting in NF-κB activation was measured by QUANTI-Blue colorimetric assay (InvivoGen) as indicated by the manufacturer's instructions. To measure *in vitro* activation of OT-I cells by Dexo, 10^5 OT-I cells were cultured in IMDM GlutaMAX medium supplemented with 10% FBS and 100 IU/mL penicillin-streptomycin together with 2×10^4 BMDCs in the presence of 25 μg of the indicated Dexo formulation or of a dose of free poly(I:C) equivalent to the amount of active poly(I:C) detected in the correspondent Dexo sample or left untreated for 24 hr at 37°C 5% CO_2. To block poly(I:C)/TLR-3 interactions, the TLR-3 specific inhibitor CU CPT 4a (Bio-Techne, Minneapolis, MN) was added to the culture media at 27 μM concentration, as previously published [45]. After incubation, cells were stained for viability using Live/Dead fixable cell viability reagents and with Abs specific for the surface markers CD3ε, CD8α and CD25. Samples were acquired on an LSR II cytometer and data analyzed with FlowJo software.

2.6.13 Statistics

Statistically significant differences between experimental groups were determined by one-way ANOVA followed by Bonferroni *post-hoc* test correction. $^{*}P < 0.05$, $^{**}P < 0.01$, $^{***}P < 0.001$, $^{****}P < 0.0001$ and n.s. = not significant. For tumor volumes, differences between groups were determined by unpaired t test. $^{*}P < 0.1$; ******** $P < 0.0001$. For survival rate, differences between groups were determined by Log-rank Mantel-Cox test. $^{*}P < 0.05$; $^{****}P < 0.0001$. Statistical analyses were performed using Prism software (v6.0f, GraphPad Software, San Diego, CA).

2.7 References

1. Gajewski, T. F. Cancer immunotherapy. *Mol. Oncol.* **6,** 242-250 (2012).
2. Mellman, I., Coukos, G. & Dranoff, G. Cancer immunotherapy comes of age. *Nature.* **480,** 480-489 (2011).
3. Mac Keon, S., Ruiz, M. A. S., Gazzaniga, S. & Wainstok, R. Dendritic cell-based vaccination in cancer: therapeutic implications emerging from murine models. *Front. Immunol.* **6,** 1-18 (2015).
4. Palucka, K. & Banchereau, J. Cancer immunotherapy via dendritic cells. *Nat. Rev. Cancer.* **12,** 265-277 (2012).
5. Chaput, N. *et al.* Dendritic cell derived-exosomes: biology and clinical implementations. *J. Leukoc. Biol.* **80,** 471-478 (2006).

6. Stoorvogel, W., Kleijmeer, M. J., Geuze, H. J. & Raposo, G. The biogenesis and functions of exosomes. *Traffic.* **3,** 321-330 (2002).
7. Pitt, J. M. *et al.* Dendritic Cell-Derived Exosomes as Immunotherapies in the Fight against Cancer. *J. Immunol.* **193,** 1006-1011 (2014).
8. Théry, C. *et al*. Molecular Characterization of Dendritic Cell-derived Exosomes. *J. Cell. Biol.* **147,** 599-610 (1999).
9. Théry, C., Zitvogel, L. & Amigorena, S. Exosomes: composition, biogenesis and function. *Nat. Rev. Immunol.* **2,** 569-79 (2002).
10. Robbins, P. D. & Morelli, A. E. Regulation of immune responses by extracellular vesicles. *Nat. Rev. Immunol.* **14,** 195-208 (2014).
11. Raposo, G. *et al.* B lymphocytes secrete antigen-presenting vesicles. *J. Exp. Med.* **183,** 1161-72 (1996).
12. Zitvogel, L. *et al.* Eradication of established murine tumors using a novel cell-free vaccine: dendritic cell-derived exosomes. *Nat. Med.* **4,** 594-600 (1998).
13. Théry, C. *et al.* Indirect activation of naïve CD4+ T cells by dendritic cell-derived exosomes. *Nat. Immunol.* **3,** 1156–1162 (2002).
14. Segura, E. *et al.* ICAM-1 on exosomes from mature dendritic cells is critical for efficient naive T-cell priming. *Blood.* **106,** 216–223 (2005).
15. Luketic, L. *et al.* Antigen presentation by exosomes released from peptide-pulsed dendritic cells is not suppressed by the presence of active CTL. *J. Immunol.* **179,** 5024-5032 (2007).
16. Näslund, T. I., Gehrmann, U., Qazi, K. R., Karlsson, M. C. I. & Gabrielsson, S. Dendritic cell-derived exosomes need to activate both T and B cells to induce antitumor immunity. *J. Immunol.* **190,** 2712-2719 (2013).
17. Näslund, T. I., Gehrmann, U. & Gabrielsson, S. Cancer immunotherapy with exosomes requires B-cell activation. *OncoImmunology.* **2,** e24533-2 (2014).
18. Escudier, B. *et al.* Vaccination of metastatic melanoma patients with autologous dendritic cell (DC)-derived exosomes: results of the first phase I clinical trial. *J. Transl. Med.* **3,** 10-13 (2005).
19. Morse, M. A. *et al.* A phase I study of dexosome immunotherapy in patients with advanced non-small lung cancer. *J. Transl. Med.* **3,** 9-8 (2005).
20. Viaud, S. *et al.* Dendritic cell-derived exosomes for cancer immunotherapy: what's next? *Cancer Res.* **70,** 1281-1285 (2010).
21. Sobo-Vujanovic, A., Munich, S. & Vujanovic, N. L. Dendritic-cell exosomes cross-present Toll-like receptor-ligands and activate bystander dendritic cells. *Cell. Immunol.* **289,** 119-127 (2015).

22. Qazi, K. R., Gehrmann, U., Domange Jordo, E., Karlsson, M. C. I. & Gabrielsson, S. Antigen-loaded exosomes alone induce Th1-type memory through a B cell-dependent mechanism. *Blood.* **113,** 2673-2683 (2009).
23. Akira, S. & Takeda, K. Toll-like receptor signalling. *Nat. Rev. Immunol.* **4,** 499-511 (2004).
24. Chu, R. S., Targoni, O. S., Krieg, A. M., Lehman, P. V. & Harding, C. V. CpG oligodeoxynucleotides act as adjuvants that switch on T helper 1 (Th1) immunity . *J. Exp. Med.* **186,** 1623-31 (1997).
25. Adams, M. *et al.* The rationale for combined chemo/immunotherapy using a Toll-like receptor 3 (TLR3) agonist and tumour-derived exosomes in advanced ovarian cancer. *Vaccine.* **23,** 2374-2378 (2005).
26. Applequist, S. E., Wallin, R. P. E. & Ljunggren, H. G. Variable expression of Toll-like receptor in murine innate and adaptive immune cell lines. *Int. Immunol.* **14,** 1065-74 (2002).
27. Dubensky, T. W., Jr & Reed, S. G. Adjuvants for cancer vaccines. *Semin. Immunol.* **22,** 155-161 (2010).
28. Zaks, K. *et al.* Efficient immunization and cross-priming by vaccine adjuvants containing TLR3 or TLR9 agonists complexed to cationic liposomes. *J. Immunol.* **176,** 7335-7345 (2006).
29. Moore, T. C., Kumm, P. M., Brown, D. M. & Petro, T. M. Interferon response factor 3 is crucial to poly-I:C induced NK cell activity and control of B16 melanoma growth. *Cancer Lett.* **346,** 122-128 (2014).
30. Dubrot, J. *et al.* Lymph node stromal cells acquire peptide-MHCII complexes from dendritic cells and induce antigen-specific CD4+ T cell tolerance. *J. Exp. Med.* **211,** 1153-1166 (2014).
31. Chiang, C. L. L., Ledermann, J. A., Rad, A. N., Katz, D. R. & Chain, B. M. Hypochlorous acid enhances immunogenicity and uptake of allogeneic ovarian tumor cells by dendritic cells to cross-prime tumor-specific T cells. *Cancer Immunol. Immunother.* **55,** 1384-1395 (2006).
32. Chiang, C. L. L. *et al.* A dendritic cell vaccine pulsed with autologous hypochlorous acid-oxidized ovarian cancer lysate primes effective broad antitumor immunity: from bench to bedside. *Clin. Cancer Res.* **19,** 4801-4815 (2013).
33. Jeanbart, L. *et al.* Enhancing efficacy of anticancer vaccines by targeted delivery to tumor-draining lymph nodes. *Cancer Immunol. Res.* **2,** 436-447 (2014).
34. Munn, D. H. & Mellor, A. L. The tumor-draining lymph node as an immune-privileged site. *Immunol. Rev.* **213,** 146-58 (2006).

35. Takeuchi, H., Kitajima, M. & Kitagawa, Y. Sentinel lymph node as a target of molecular diagnosis of lymphatic micrometastasis and local immunoresponse to malignant cells. *Cancer Sci.* **99,** 441-450 (2008).

36. Nembrini, C. *et al.* Nanoparticle conjugation of antigen enhances cytotoxic T-cell responses in pulmonary vaccination. *Proc. Natl. Acad. Sci. U. S. A.* **108,** E989-97 (2011).

37. Smits, E. L. *et al*. Proinflammatory response of human leukemic cells to dsRNA transfection linked to activation of dendritic cells. *Leukemia*. **8**, 1691-1699 (2007).

38. Cheng, Y. S. & Xu, F. Anticancer function of polyinosinic-polycytidylic acid. *Cancer Biol. Ther*. **10**, 1219-1223 (2010).

39. Steinhagen, F. *et al*. TLR-based immune adjuvants. *Vaccine*. **29**, 3341-3355 (2011).

40. Bohle, A. & Brandau, S. Immune mechanisms in bacillus Calmette-Guerin immunotherapy for superficial bladder cancer. *J. Urol*. **170**, 964-69 (2003).

41. Sylvester, R. J. *et al*. Bacillus Calmette-Guerin versus chemotherapy for the intravesical treatment of patients with carcinoma in situ of the bladder: a meta-analysis of the published results of randomized clinical trials. *J. Urol*. **174**, 86-92 (2005).

42. van Seters, M. *et al*. Treatment of vulvar intraepithelial neoplasia with topical imiquimod. *N. Engl. J. Med*. **358**, 1465-73 (2008).

43. Dougan, M. & Dranoff, G. Immune therapy for cancer. *Annu. Rev. Immunol*. **27**, 83-117 (2009).

44. André, F. *et al*. Exosomes as potent cell-free peptide-based vaccine. I. Dendritic cell-derived exosomes transfer functional MHC class I peptide complexes to dendritic cells. *J. Immunol*. **172**, 2126-36.

45. Cheng, K., Wang, X. & Yin, H. Small-molecule inhibitors of the TRL3/dsRNA complex. *J. Am. Chem. Soc*. **11**, 3767-7 (2011).

Chapter 3

Hepatocytes efficiently establish cross-tolerance by inducing deletion and anergy of antigen-specific $CD8^+$ T cells via the PD-1/PD-L1 pathway

Adapted from manuscripts in preparation:

Damo, M., Wilson D.S. & Hubbell, J.A. Hepatocytes efficiently establish cross-tolerance by inducing deletion and anergy of antigen-specific $CD8^+$ T cells via the PD-1/PD-L1 pathway.

Wilson, D.S., Damo, M. & Hubbell, J.A. Synthetic glycopolymer-antigen conjugates induce antigen-specific immune tolerance.

3.1 Abstract

Peripheral tolerance participates in the protection of the organism from developing immunity against auto-antigens and harmless exogenous antigens. Resident cells of lymphoid and non-lymphoid organs contribute to the maintenance of peripheral tolerance. The liver, in particular, has been attributed an important role in establishing tolerance towards circulating extracellular antigens, mainly because of the antigen scavenging properties of liver sinusoid endothelial cells. Nonetheless, hepatocytes are the most abundant cell type of the liver, express MHC-I molecules, lack co-stimulatory signals, and have been shown *in vivo* to induce tolerance to expressed antigens. However, the ability of hepatocytes to take up and induce tolerance to extracellular antigens has yet to be elucidated. In our study we describe for the first time *in vitro* that murine primary hepatocytes efficiently scavenge and present extracellular antigens on MHC-I complexes, a process known as cross-presentation. Moreover, we show *in vivo* that hepatocyte-dependent cross-presentation of the model antigen ovalbumin (OVA) induces apoptosis and emperipolesis of OVA-specific $CD8^+$ OT-I cells, resulting in deletional tolerance. Non-deleted hepatocyte-educated OT-I cells, instead, acquire an anergic phenotype, characterized by poor response to vaccination with adjuvanted OVA. We also confirm that the PD-1/PD-L1 pathway is involved in the establishment of hepatocyte-derived cross-tolerance, by observing that the specific blockade of PD-L1 expressed by OVA cross-presenting hepatocytes could rescue OT-I cells from deletion and anergy. Taken together, our findings indicate that hepatocytes can significantly contribute to the tolerogenic capacity of the liver by cross-presenting extracellular antigens to $CD8^+$ T lymphocytes and employing the negative regulatory PD-1/PD-L1 pathway.

3.2 Introduction

Immunological tolerance prevents the development of adaptive responses against endogenous or harmless exogenous antigens. T lymphocytes are selected for antigen specificity and affinity during their development in the thymus through the establishment of central tolerance, which positively selects functional TCRs and negatively selects potentially autoimmune TCRs [1]. Even though unwanted lymphocytic clones might escape the selection processes of central tolerance, self antigens as well as harmless non-self antigens like environmental components, to which the body is exposed, do not elicit immunity in healthy individuals. This lack of response is the result of peripheral tolerance mechanisms, which through clonal deletion, anergy and the activity of T regulatory cells, protect the organism from unwanted immune responses [2,3].

Unlike central tolerance, peripheral tolerance takes place in both lymphoid and non-lymphoid peripheral tissues, such as the liver. Each day naïve T lymphocytes pass through the hepatic circulation system hundreds of times, yet non-self harmless antigens absorbed into the blood that drains from the gut to the liver or newly formed antigens resulting from hepatic metabolic activities fail to induce an immune response [4,5]. The ability of the liver to induce tolerance to circulating extracellular antigens has been mainly attributed to liver sinusoid endothelial cells (LSECs). These MHC-II- and MHC-I-expressing blood vessel-lining cells represent the first cells to interact with peripheral lymphocytes entering hepatic circulation (Fig. 3.1a). In fact, LSECs efficiently scavenge, process and present, in the absence of co-stimulation, soluble antigens found in the bloodstream to circulating lymphocytes, typically resulting in the induction of $CD4^+$ T regulatory cells or anergic $CD8^+$ T lymphocytes [6-11].

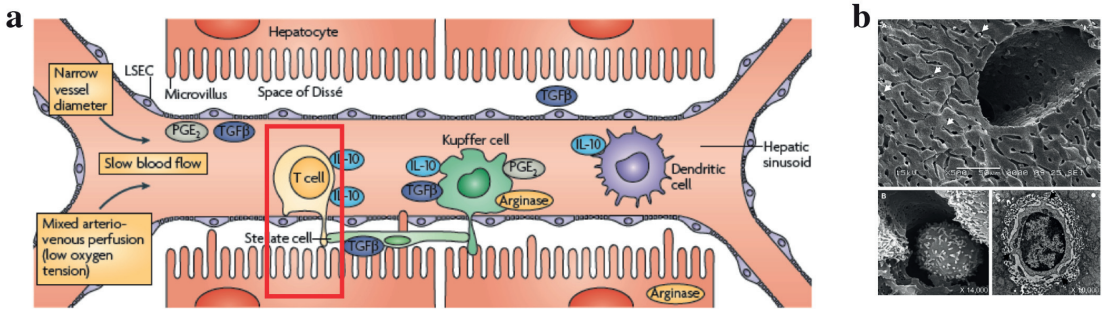

Figure 3.1 Liver microanatomy. (a) Hepatic capillaries or sinusoids allow multiple cell-cell and molecule-cell interactions. In particular, circulating T lymphocytes make direct contact with endothelial cells (LSECs) and hepatocytes (red square). (b) Scanning electron microscopy showing lymphocytes (white arrows) in murine hepatic sinusoids. Lymphocyte dendrites make contact with hepatocytes through sinusoid fenestrations (black arrows) (adapted from Holz, L. E. *et al*., *J. Autoimmun*., 2010 and from Thomson A. W. & Knolle P. A., *Nat. Rev. Immunol*., 2010).

Unlike other organs, where circulating lymphocytes only extravasate and gain access to the parenchyma in case of inflammation, the liver microvasculature has a peculiar fenestrated endothelium devoid of any basal membrane that allows direct physical contact between circulating $CD8^+$ T lymphocytes and the liver MHC-I^+ parenchymal cells, hepatocytes (Fig. 3.1a,b) [12,13]. Hepatocytes are the most abundant cells of the liver, composing 80% of its mass, and they represent the metabolic unit of the organ as they are responsible for the processing of food molecules, drugs, environmental antigens, gut bacterial derivatives and potential toxins flowing through the portal vein into the hepatic capillaries or sinusoids [13]. As most nucleated cells, hepatocytes can present cellular antigens in the context of the MHC-I to $CD8^+$ T lymphocytes. It has been reported that hepatocytes possess poor cross-presentation capacity *in vitro* as compared to other liver cells, especially LSECs [8]. Nonetheless, several publications have shown that direct antigen expression, obtained by either transgenesis or viral vector transduction, and subsequent MHC-I-dependent antigen presentation in hepatocytes can result in peripheral tolerance *in vitro* and *in vivo*. Hepatocyte-induced tolerance is believed to be due to suboptimal activation of antigen-specific $CD8^+$ T lymphocytes because of lack of CD28 co-stimulation causing clonal deletion of the T cells [14-21]. Moreover, recent reports also described the induction of $CD4^+CD25^+FoxP3^+$ Treg cells upon hepatocyte-dependent antigen expression, thus suggesting a possible involvement of other APCs in the tolerogenic mechanisms of this model [22,23].

Hepatocytes outnumber the other cellular components of the liver and possess enzymatic activities necessary for processing of blood-borne molecules and antigens. We thus reasoned that hepatocytes might significantly contribute to the establishment of liver-mediated $CD8^+$ T cell peripheral tolerance by taking up and cross-presenting circulating extracellular antigens on MHC-I complexes. In this project, we describe the *in vitro* and *in vivo* cross-presentation capabilities of murine hepatocytes and report on the immunological consequences of hepatocyte-dependent antigen cross-presentation.

Unlike previous studies, we were able to determine *in vitro* that markers associated with exogenous antigen processing are highly expressed in hepatocytes and localized to subcellular organelles competent for processing of extracellular antigens, resulting in cross-presentation. *In vivo* antigen cross-presentation by hepatocytes led to a tolerization state characterized by clonal deletion of antigen-specific $CD8^+$ T lymphocytes by apoptosis and emperipolesis. In fact, Annexin V staining and strong upregulation of the pro-apoptotic markers Fas ligand (FasL) and TNF-related apoptosis-inducing ligand (TRAIL) on the surface of T cells indicated pro-apoptotic phenotype of hepatocyte-educated $CD8^+$ T cells. Moreover, the detection of antigen-specific T lymphocytes within lysosomal associated membrane protein 1 (LAMP-1)-positive compartments of antigen cross-presenting

hepatocytes suggested emperipolesis by the T cells. Together with FasL and TRAIL, PD-1 was also strongly upregulated by the $CD8^+$ T cells undergoing hepatocyte-dependent cross-tolerance. High expression of PD-1 ligand 1 (PD-L1) could be detected at steady-state conditions on liver parenchymal cells and PD-L1 has been involved in intrahepatic deletion of activated $CD8^+$ T lymphocytes [24]. We therefore hypothesized that PD-1/PD-L1 interactions between antigen-specific $CD8^+$ T cells and antigen cross-presenting hepatocytes, respectively, could be actively involved in the establishment of cross-tolerance. In fact, blocking PD-L1 on the surface of cross-presenting hepatocytes significantly impaired the development of cross-tolerance.

3.3 Results

3.3.1 Primary hepatocytes efficiently use EEA1- and TAP1-positive cytoplasmic compartments for extracellular antigen processing

Presentation of extracellular antigens requires dedicated subcellular compartments in professional APCs, depending on whether antigens will be presented on MHC-I (cross-presentation) or MHC-II complexes. In particular, cross-presentation is the result of antigen uptake mediated by Fc or C-type lectin receptors (such as the mannose receptor), followed by antigen proteolytic degradation by proteasomes associated to early endosome antigen 1 (EEA1)-positive phagosomes (early endosomes), subsequent antigen transportation and loading onto MHC-I molecules through transporters associated with antigen processing (TAP) and translocation of peptide/MHC-I complexes to the cell plasma membrane via the secretory pathway [25-27].

Physiologically hepatocytes are home to the liver metabolic functions involving uptake and processing of molecules found in the extracellular space. We therefore asked whether hepatocytes would employ cross-presentation-competent subcellular compartments to process soluble extracellular antigens. We first sought to characterize primary murine hepatocytes for their expression and distribution of markers associated with cross-presentation-competent phagosomes. Freshly isolated hepatocytes from C57BL/6 mice were stained for mannose receptor 1 (MR), EEA1, TAP1 and H-2Kb and analyzed by confocal microscopy. The expression and distribution of these markers indicate their localization either on the surface of hepatocytes (MR, H-2Kb) or in subcellular compartments (MR, EEA1, TAP1 and H-2Kb) with a similar pattern compared to sorted $CD11c^+CD8\alpha^+$ BMDCs, chosen as positive reference for their professional antigen cross-presenting functions (Fig. 3.2a). As expected, the abundance of MR-, EEA1-, TAP1- and H-2Kb-positive organelles is higher in professional cross-presenting $CD11c^+CD8\alpha^+$ BMDCs (Fig. 3.2a).

To test whether the subcellular compartments described in Fig. 3.2a are used by hepatocytes to process protein antigens found in the extracellular space, we cultured primary hepatocytes in the presence of DQ-Ovalbumin (DQ-OVA) and analyzed the mean fluorescent intensity (MFI) and localization of the fluorescent signal derived from its proteolytic degradation. Hepatocytes actively degrade proteins added to their supernatant, as DQ-OVA becomes fluorescent when cells are incubated at 37°C but not at 4°C (Fig. 3.2b). As expected, the magnitude of antigen processing in BMDCs is much greater than in hepatocytes as indicated by the MFI of DQ-OVA, but the kinetics appear to be similar between the two cell types with DQ-OVA fluorescence peaking within the first 12 hr of culture and slowly decreasing over time until reaching background signal levels after 60 hr in culture without further addition of the antigen (Fig. 3.2b). By confocal microscopy, we could localize the fluorescent signal originating from the degradation of DQ-OVA in the proximity of or inside $EEA1^+$, $TAP1^+$ and $H\text{-}2Kb^+$ compartments (Fig. 3.2c). Interestingly, DQ-OVA fluorescence could also be detected associated to late endosomes, identified as $LAMP\text{-}1^+$ organelles (Fig. 3.2c), even though quantification of co-localizing signals indicated that DQ-OVA degradation is mainly associated to $EEA1^+$ and $TAP1^+$ compartments (2.45 and 2.7 Pearson's co-localization coefficient fold increase over LAMP-1, respectively) (Fig. 3.2d). This observation prompted us to investigate whether hepatocytes contained phagosomes positive for both EEA1 and TAP, which are considered the hallmark of professional cross-presenting cells, as these phagosomes retain all the functions necessary for cross-presentation [25-28]. Interestingly, $EEA1^+TAP1^+$ subcellular compartments were found to be abundantly distributed in the cytoplasm of primary hepatocytes, even though to a lesser extent as compared to sorted $CD11c^+CD8\alpha^+$ BMDCs (Fig. 3.2e). These results are in line with the current models of cross-presentation, according to which cross-presenting cells contain phagosomes (mainly recognized as $EEA1^+$) equipped with the complete molecular machinery necessary to retro-translocate antigens to the cytoplasm for degradation into phagosome-associated proteasomes and to transport digested peptides into endosomal MHC-I-containing compartments, where peptides are loaded onto MHC-I complexes prior to their transportation to the cell membrane [25-28].

To confirm *in vivo* uptake and processing of blood-borne and extracellular antigens by hepatocytes, we injected 100 μg of DQ-OVA intravenously (i.v.) into C57BL/6 mice and euthanized animals after 12 hr to harvest liver and spleen, as they represent the major blood filtration organs. In the liver, DQ-OVA fluorescence was widely distributed in the parenchyma and, unlike previous reports indicating LSECs as the major blood-filtering cells of the liver [9,10], mainly localized in hepatocytes, identified as non-hematopoietic ($CD45^-$) non-endothelial ($CD31^-$) parenchymal cells (Fig. 3.2f, top panels). As expected, DQ-OVA

processing in the spleen was mostly detected in cross-presenting DCs, identified as $CD45^{+}CD11c^{+}CD8\alpha^{+}$ cells (Fig. 3.2f, bottom panels).

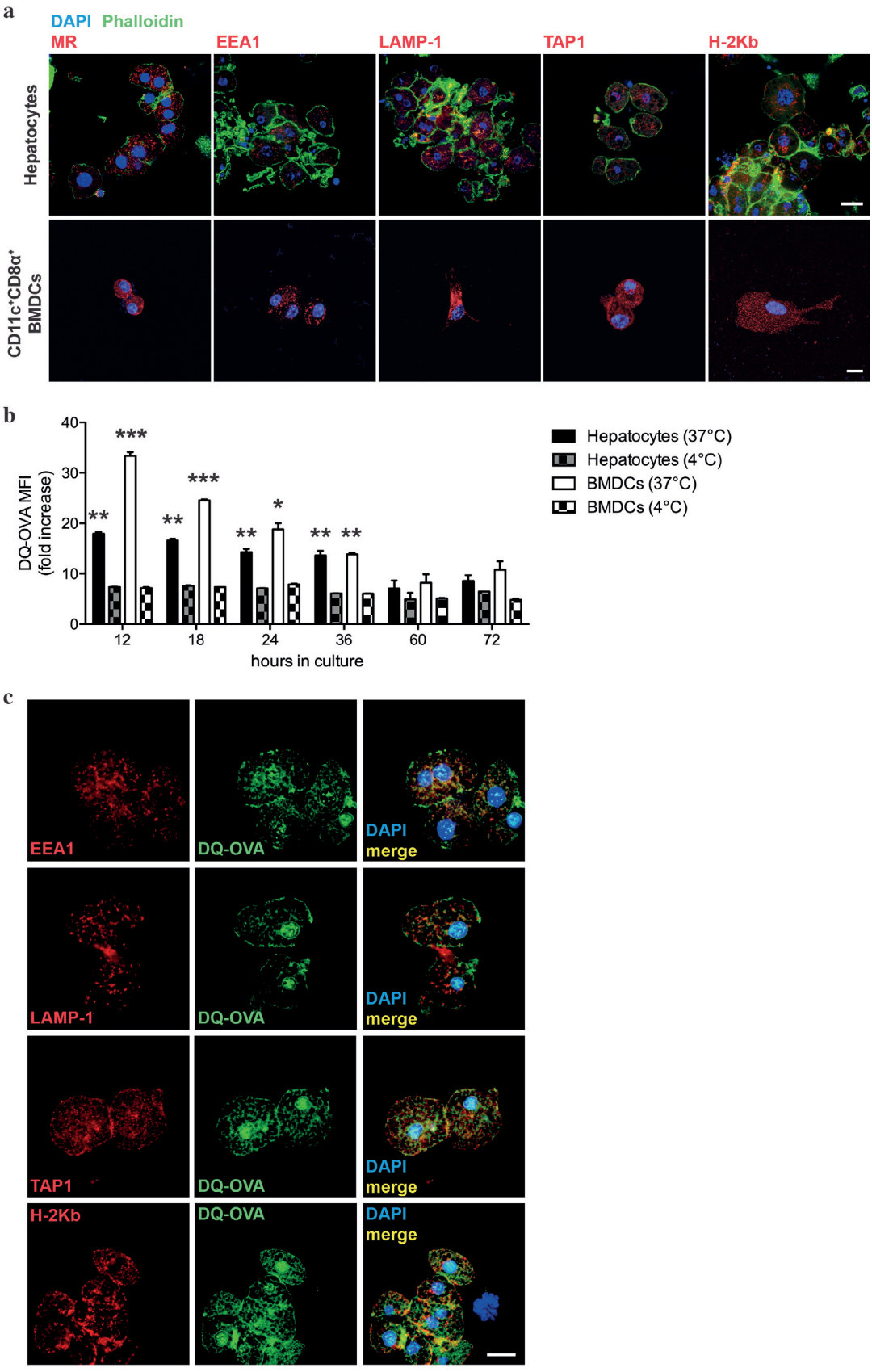

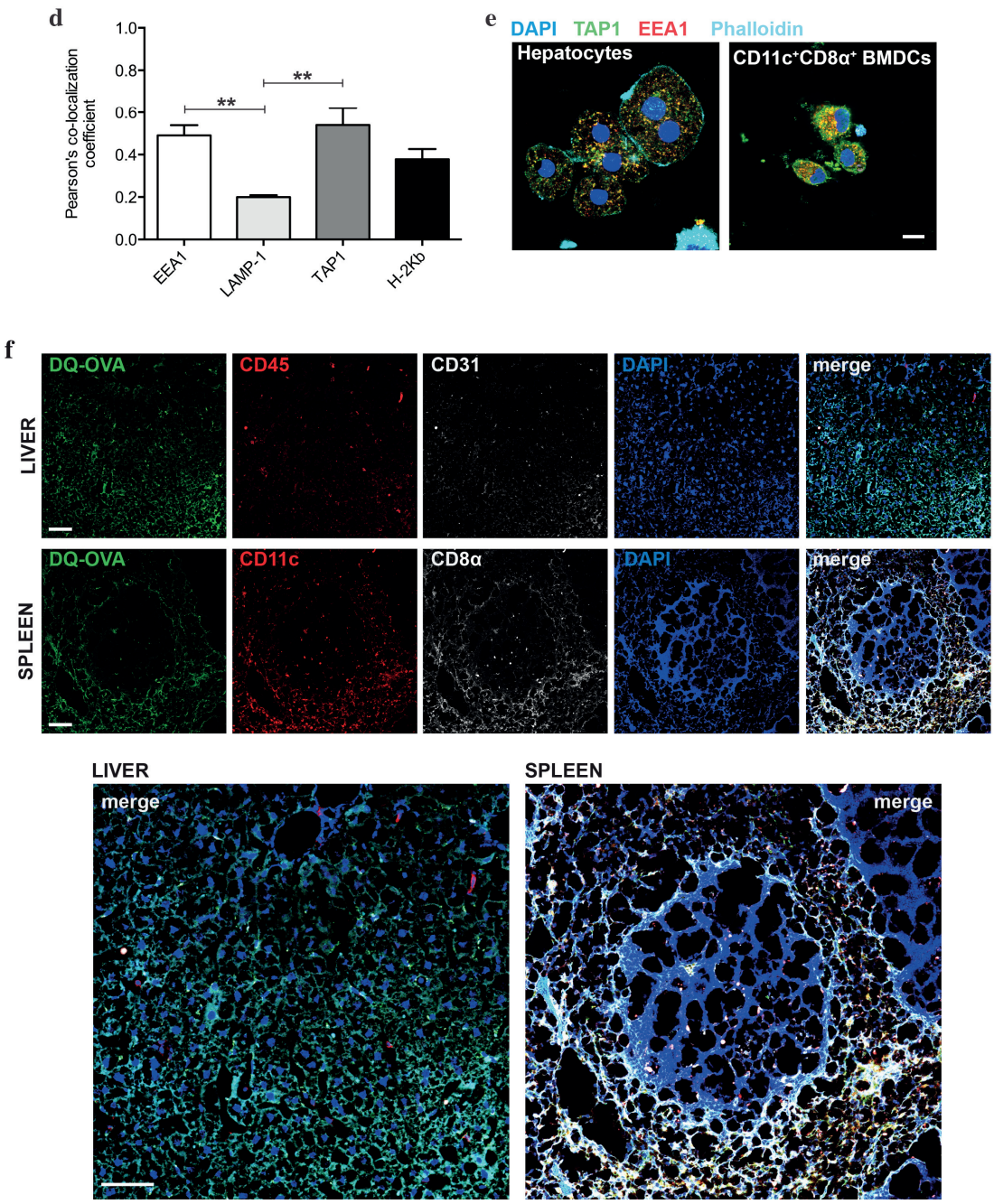

Figure 3.2 Hepatocytes uptake and process extracellular antigens in cross-presentation-competent phagosomes. (a) Confocal microscopy of primary hepatocytes and sorted CD11c^{+}CD8α^{+} BMDCs from C57BL/6 mice stained for MR, EEA1, LAMP-1, TAP1, H-2Kb, DAPI (both hepatocytes and BMDCs) and phalloidin (only hepatocytes). Scale bar = 10 μm. (b) Flow cytometric analysis of primary hepatocytes or BMDCs from C57BL/6 mice cultured in the presence of 20 μg/ml DQ-OVA at either 37°C or 4°C for the indicated amount of time. (c) Confocal microscopy of primary hepatocytes from C57BL/6 mice cultured for 12 hr in the presence of 20 μg/ml DQ-OVA and stained for EEA1, LAMP-1, TAP1, H-2Kb and DAPI. Scale bar = 10 μm. (d) Quantification of signal co-localization of DQ-OVA with either EEA1, LAMP-1, TAP1 or H-2Kb as detected by confocal microscopy in (c). (e) Confocal microscopy of primary hepatocytes and sorted CD11c^{+}CD8α^{+} BMDCs from C57BL/6 mice

stained for EEA1, TAP1, DAPI and phalloidin. Scale bar = 10 μm. (f) Confocal microscopy of liver and spleen sections from C57BL/6 mice euthanized 12 hr after i.v. administration of 100 μg of DQ-OVA. Liver sections were stained for CD45, CD31 and DAPI; spleen sections were stained for CD11c, CD8α and DAPI. Scale bar = 50 μm. $^{*}P < 0.05$, $^{**}P < 0.01$ and $^{***}P < 0.001$ (unpaired t test in (b) and one-way ANOVA and Bonferroni *post-hoc* test correction in (d)). Data in (a,b,c,d) are representative of 3 independent experiments (mean and s.e.m. in (b,d)). Pictures in (f) are representative of 5 different mice.

We thus concluded that murine hepatocytes phenotypically resemble antigen cross-presenting DCs, since actively processed extracellular antigens can be mostly detected in association to $EEA1^{+}$, $TAP1^{+}$ and $H\text{-}2Kb^{+}$ cytoplasmic compartments. Most importantly, hepatocytes contain $EEA1^{+}TAP1^{+}$ phagosomes, which are considered a unique feature of professional cross-presenting cells. Moreover, scavenging and degradation of blood-borne antigens *in vivo* are the main activities of hepatocytes in the liver and of cross-presenting $CD45^{+}CD11c^{+}CD8\alpha^{+}$ DCs in the spleen.

3.3.2 Poly(N-Acetylgalactosamine) covalent modifications increase the efficiency of antigen cross-presentation in primary hepatocytes

Receptor-mediated endocytosis of extracellular antigens is the first step of the cross-presentation pathway. Antigen chemical modifications enhancing receptor binding have been previously exploited to improve either $CD8^{+}$ T cell immunity or tolerance following antigen cross-presentation [29,30]. We therefore decided to test whether an antigen covalently modified with polymeric sugar structures (poly(N-Acetylgalactosamine); D.S.W., M.D., J.A.H., manuscript in preparation), recognized by several cross-presentation-related receptors such as the MR, the fructose receptor and the liver-specific lectin asialoglycoprotein receptor, could improve hepatocyte cross-presentation of the model antigen OVA.

We modified OVA with poly(N-Acetylgalactosamine) (pGal-OVA) and compared its cross-presentation to that of unmodified OVA in hepatocytes or BMDCs incubated with equimolar doses of the two versions of the antigen (Fig. 3.3a). pGal-OVA resulted in a statistically significant 1.2 and 2.1 fold increase of cross-presentation of the OVA-derived $CD8^{+}$ T cell immunodominant epitope SIINFEKL in primary hepatocytes and BMDCs, respectively, as compared to OVA, as indicated by staining for H-2Kb/SIINFEKL complexes and flow cytometric analysis (Fig. 3.3a). Confocal microscopy confirmed improved SIINFEKL cross-presentation by pGal-OVA-treated hepatocytes as compared to OVA-treated hepatocytes (Fig. 3.3b).

We then asked whether cellular processes described in hematopoietic and non-hematopoietic APCs for cross-presentation, such as endosome acidification and proteasomal

degradation [25-28,43], were also employed by hepatocytes for pGal-OVA cross-presentation. We therefore treated primary murine hepatocytes with pGal-OVA alone or with pGal-OVA together with either chloroquine (an inhibitor of endosomal acidification) or MG132 (a proteasome inhibitor) and cultured them *in vitro* with OT-I cells, transgenic $CD8^+$ T cells specific for H-2Kb/SIINFEKL. After 24 hr of co-culture, we analyzed by flow cytometry the expression of CD69 by OT-I cells, as an early indicator of antigen sensing and TCR triggering. Blockade of either endosomal function or proteasomal protein degradation in hepatocytes resulted in statistically significant reduction of the frequency of OT-I cells able to experience antigen presentation by hepatocytes, as indicated by CD69 staining. In fact, after treatment of hepatocytes with pGal-OVA and either chloroquine or MG132, 7.38% and 3.98% of the OT-I cells were $CD69^+$, respectively, as compared to 17% of $CD69^+$ OT-I cells measured when hepatocytes were incubated with pGal-OVA alone (Fig. 3.3c).

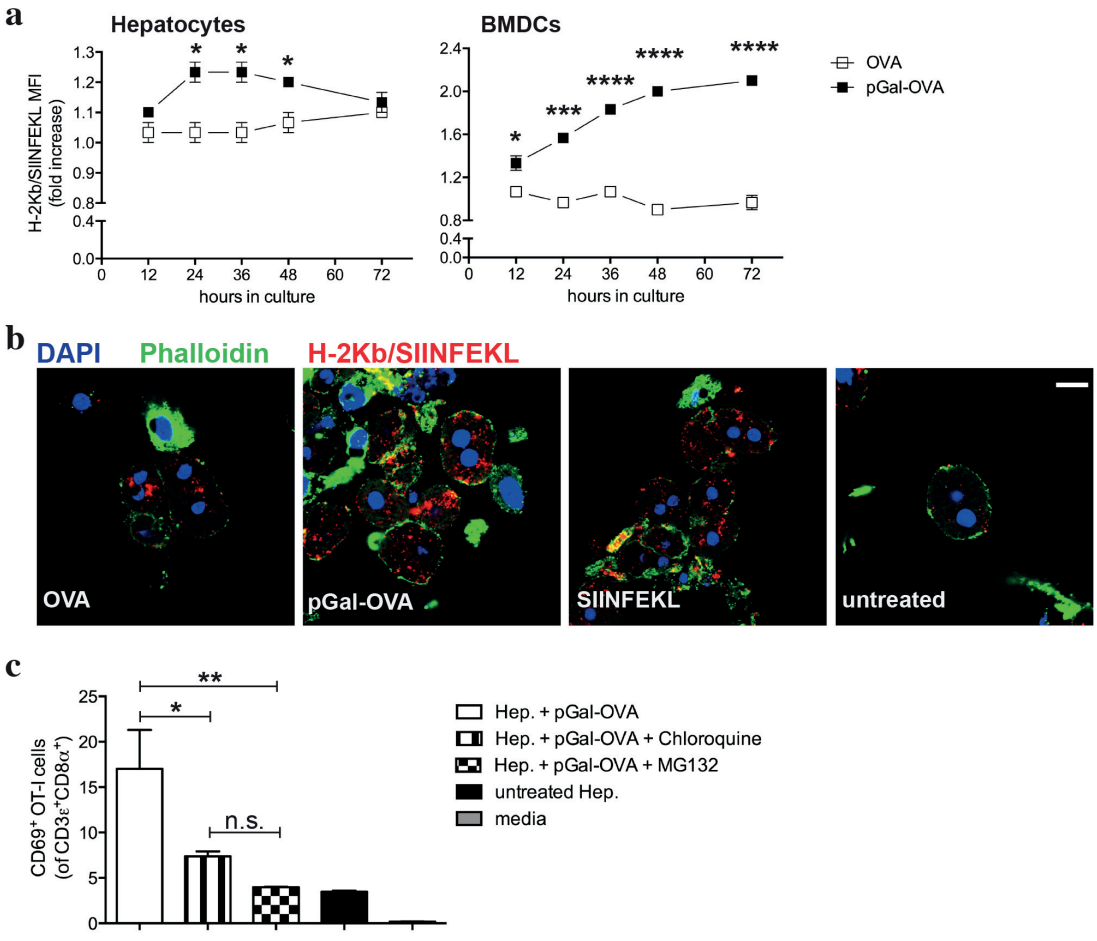

Figure 3.3 Poly(N-Acetylgalactosamine)-modified OVA (pGal-OVA) is processed through the cross-presentation pathway more efficiently than OVA. (a) Flow cytometric analysis of primary hepatocytes (left) and BMDCs (right) from C57BL/6 mice cultured in the presence of 5 μM OVA (open squares) or 5 μM pGal-OVA (black squares) for the indicated amount of time and stained for H-2Kb/SIINFEKL. (b) Confocal microscopy of primary hepatocytes from C57BL/6 mice cultured for 24

hr in the presence of either 5 μM OVA, 5 μM pGal-OVA, 1 nM SIINFEKL or left untreated and stained for H-2Kb/SIINFEKL, phalloidin and DAPI. Scale bar = 10 μm. (c) Flow cytometry of OT-I cells stained for CD69 after 24 hr in culture with primary hepatocytes pre-treated with either pGal-OVA alone, with pGal-OVA and chloroquine or pGal-OVA and MG132 or left untreated. $^{*}P < 0.05$, $^{**}P < 0.01$ $^{****}P < 0.0001$ and n.s. = not significant (one-way ANOVA and Bonferroni *post-hoc* test correction). Data are representative of 3 independent experiments ($n = 3$; mean and s.e.m. in (a,c)).

Our data indicate that pGal-OVA is processed in hepatocytes via the cellular pathway of antigen cross-presentation. Since cross-presentation of pGal-OVA is more efficient than that of OVA, we decided to adopt pGal-OVA as model antigen to characterize the OVA-specific immune response elicited by hepatocyte-dependent cross-presentation *in vivo*.

3.3.3 Cross-presentation of OVA by hepatocytes results in antigen-specific CD8^{+} T cell tolerance by induction of clonal deletion and anergy

Scavenger receptors are expressed by a multitude of cells, especially in the liver and in the spleen, among which DCs, macrophages and LSECs. In order to discriminate the role of hepatocytes in the establishment of cross-tolerance towards extracellular antigens using the pGal-OVA antigen, we developed a model of i.v. adoptive transfer of freshly isolated hepatocytes. When delivered i.v., CFSE-labeled primary hepatocytes appear to selectively home to the spleen and, to a lesser extent, the liver and to survive in those sites for at least 1 month after infusion (Fig. 3.4).

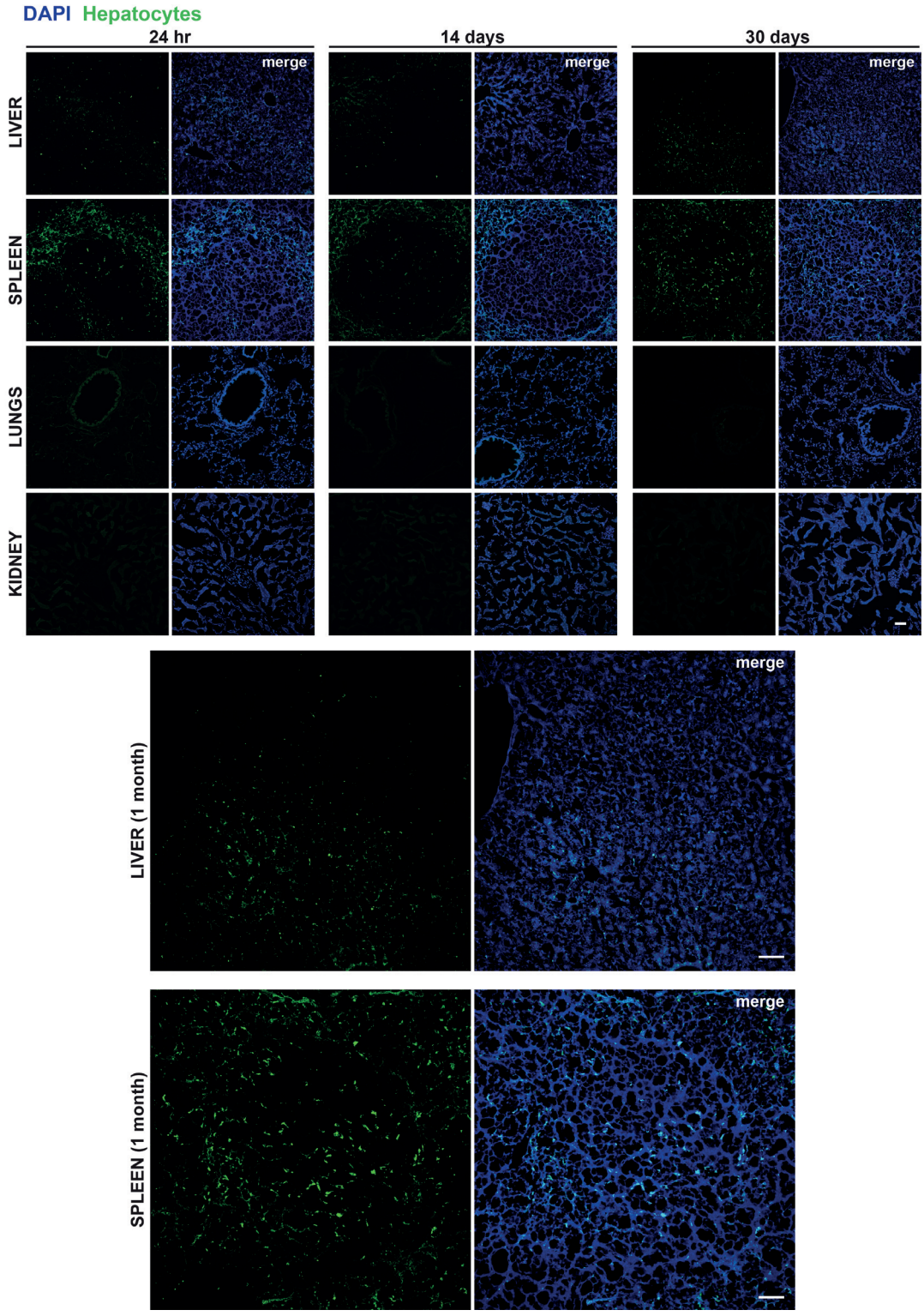

Figure 3.4 Primary hepatocytes survive and home to liver and spleen after i.v. adoptive transfer. Confocal microscopy of liver, spleen, lung and kidney sections stained with DAPI from C57BL/6 mice administered i.v. with CFSE-labeled C57BL/6 hepatocytes and euthanized at either 24 hr, 14 days or 1 month after injection. Scale bar = 50 μm. Data are representative of 5 different mice.

To study the effects of hepatocyte cross-presentation on antigen-specific T cells *in vivo*, we *ex vivo* incubated with pGal-OVA hepatocytes isolated from C57BL/6 mice. After incubation with pGal-OVA and washing, OVA cross-presenting hepatocytes (Fig. 3.5a) were transferred i.v. into recipient $CD45.2^+$ C57BL/6 mice, followed by i.v. administration of CFSE-labeled $CD45.1^+$ OT-I cells 6 hr later. 2 weeks after hepatocyte transfer, recipient mice were vaccinated with an intradermal (i.d.) dose of OVA and LPS (challenge) into the frontal footpads and 4 days after challenge mice were euthanized in order to analyze the phenotype of adoptively transferred OT-I cells retrieved from the spleen and the LNs draining the vaccination site (dLNs) (Fig. 3.5b).

95% to 99.7% of the OT-I cells harvested from mice challenged with OVA/LPS on day 15 responded to vaccination by proliferating, as detected by flow cytometric analysis of CFSE dilution of viable $CD45.1^+CD3^+CD8^+$ cells in the dLNs and spleen of recipient mice (Fig. 3.5c and Supplementary Fig. 3.1a, respectively, top panel). Even though no difference was detectable in the proliferative capacity of OT-I cells harvested from vaccinated mice administered with either vehicle, untreated hepatocytes or OVA cross-presenting hepatocytes on day 0, the frequency of $CD45.1^+$ OT-I cells in the population of total viable $CD3^+CD8^+$ lymphocytes was significantly reduced to 0.4% in the dLNs of mice treated with OVA cross-presenting hepatocytes as compared to mice receiving either vehicle (2.3%) or untreated hepatocytes (2.2%) on day 0 (Fig. 3.5c, bottom panels). Reduced frequencies of $CD45.1^+$ OT-I cells in mice pre-treated with OVA cross-presenting hepatocytes were paralleled by lower OT-I cell counts (Fig. 3.5c, bottom panels). Significantly reduced frequency and cell counts of $CD45.1^+$ OT-I cells were also measured in the population of viable $CD3^+CD8^+$ lymphocytes isolated from the spleen of recipient mice (Supplementary Fig. 3.1a, bottom panels).

The significantly lower frequencies of $CD45.1^+$ OT-I cells among total $CD8^+$ T lymphocytes prompted us to investigate whether non-deleted OT-I cells displayed signature markers of apoptosis or reduced survival. In the dLNs of mice administered with pGal-OVA-treated hepatocytes we could detect significantly higher frequencies of Annexin-V^+ (38.6%), $FasL^+$ (2.6%), $TRAIL^+$ (5.77%) and $KLRG1^{hi}CD127^{low}$ (6.45%) OT-I cells as compared to mice receiving on day 0 either vehicle (20.01%, 0.33%, 1.56% and 0.48%, respectively) or untreated hepatocytes (21.7%, 0.38%, 2.12% and 1.77%, respectively) (Fig. 3.5d). Similarly to the dLNs, the OT-I cells retrieved from the spleen of recipient mice also showed evidence of undergoing apoptosis and reduced survival capacity (Supplementary Fig. 3.1b).

Moreover, administration of pGal-OVA-treated hepatocytes on day 0 also significantly affected the capacity of adoptively transferred OT-I cells to acquire effector functions following vaccination, as indicated by statistically lower frequencies of IFN-γ^+ and

IL-2^+ viable $CD45.1^+CD3^+CD8^+$ OT-I cells in the dLNs (22.2% and 3.5%, respectively), as compared to mice administered on day 0 with either vehicle (61.8% and 10.4% of dLN IFN-γ^+ or IL-2^+ OT-I cells, respectively) or untreated hepatocytes (55.3% and 7.2% of dLN IFN-γ^+ or IL-2^+ OT-I cells, respectively) (Fig. 3.5e). Similar trends were also detected in the spleen of recipient mice (Supplementary Fig. 3.1c). Interestingly, when total dLN cells were restimulated *ex vivo* with SIINFEKL, secreted IFN-γ was significantly reduced to 562.4 pg/mL in the supernatant of the cells harvested from mice receiving pGal-OVA-treated hepatocytes, as compared to 2541.68 pg/mL and 3254.76 pg/mL for mice receiving either vehicle or untreated hepatocytes on day 0, respectively (Fig. 3.5f).

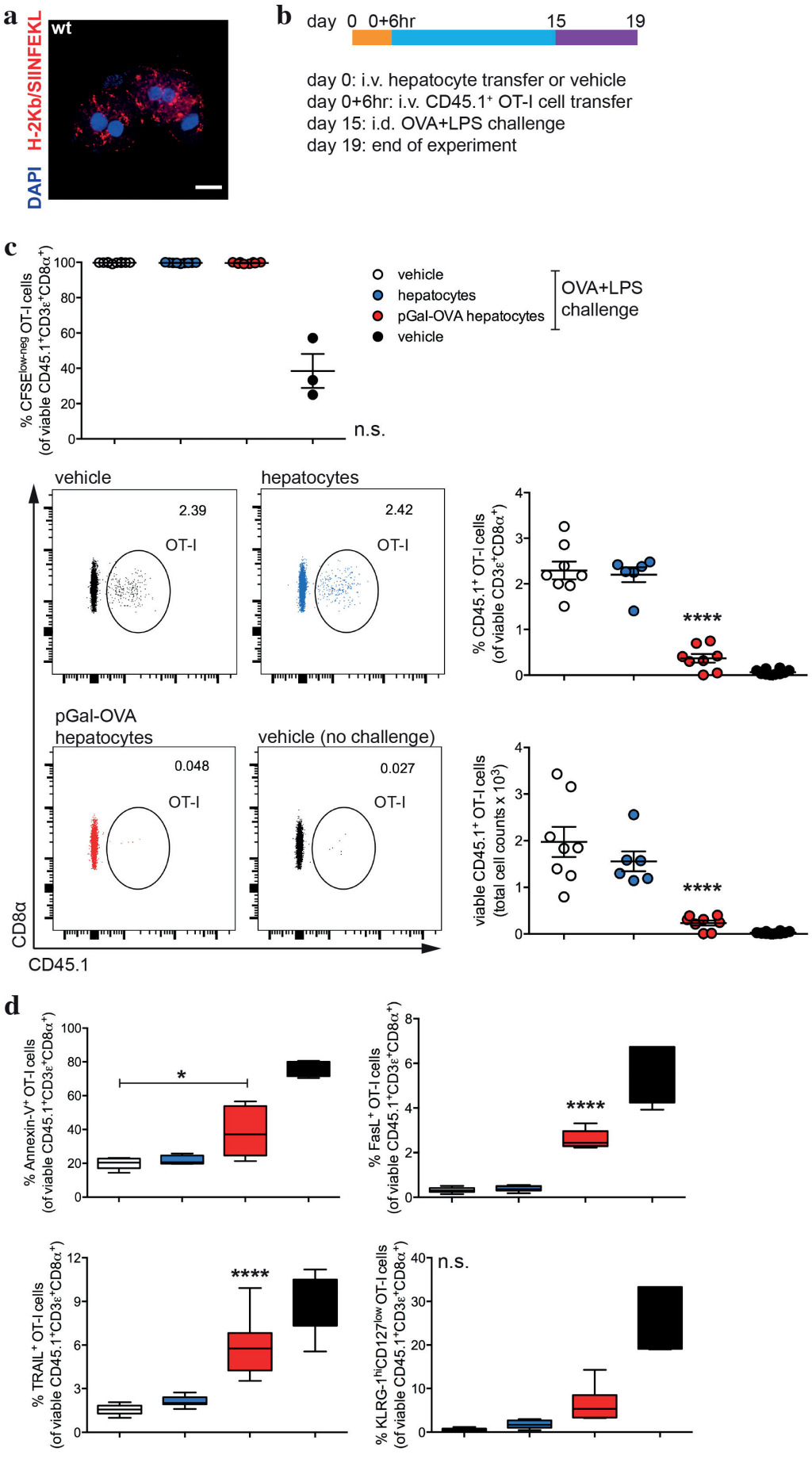
a
wt
DAPI
H-2Kb/SIINFEKL
b
day 0
0+6hr
15
19
day 0: i.v. hepatocyte transfer or vehicle
day 0+6hr: i.v. CD45.1+ OT-I cell transfer
day 15: i.d. OVA+LPS challenge
day 19: end of experiment
c
% CFSE low-neg OT-I cells (of viable CD45.1+CD3ε+CD8α+)
vehicle
hepatocytes
pGal-OVA hepatocytes
vehicle
OVA+LPS challenge
n.s.
vehicle
hepatocytes
2.39
2.42
OT-I
% CD45.1+ OT-I cells (of viable CD3ε+CD8α+)
****
pGal-OVA hepatocytes
vehicle (no challenge)
0.048
0.027
viable CD45.1+ OT-I cells (total cell counts x 10³)
CD8α
CD45.1
d
% Annexin-V+ OT-I cells (of viable CD45.1+CD3ε+CD8α+)
*
% FasL+ OT-I cells (of viable CD45.1+CD3ε+CD8α+)
****
% TRAIL+ OT-I cells (of viable CD45.1+CD3ε+CD8α+)
****
% KLRG-1hiCD127low OT-I cells (of viable CD45.1+CD3ε+CD8α+)
n.s.

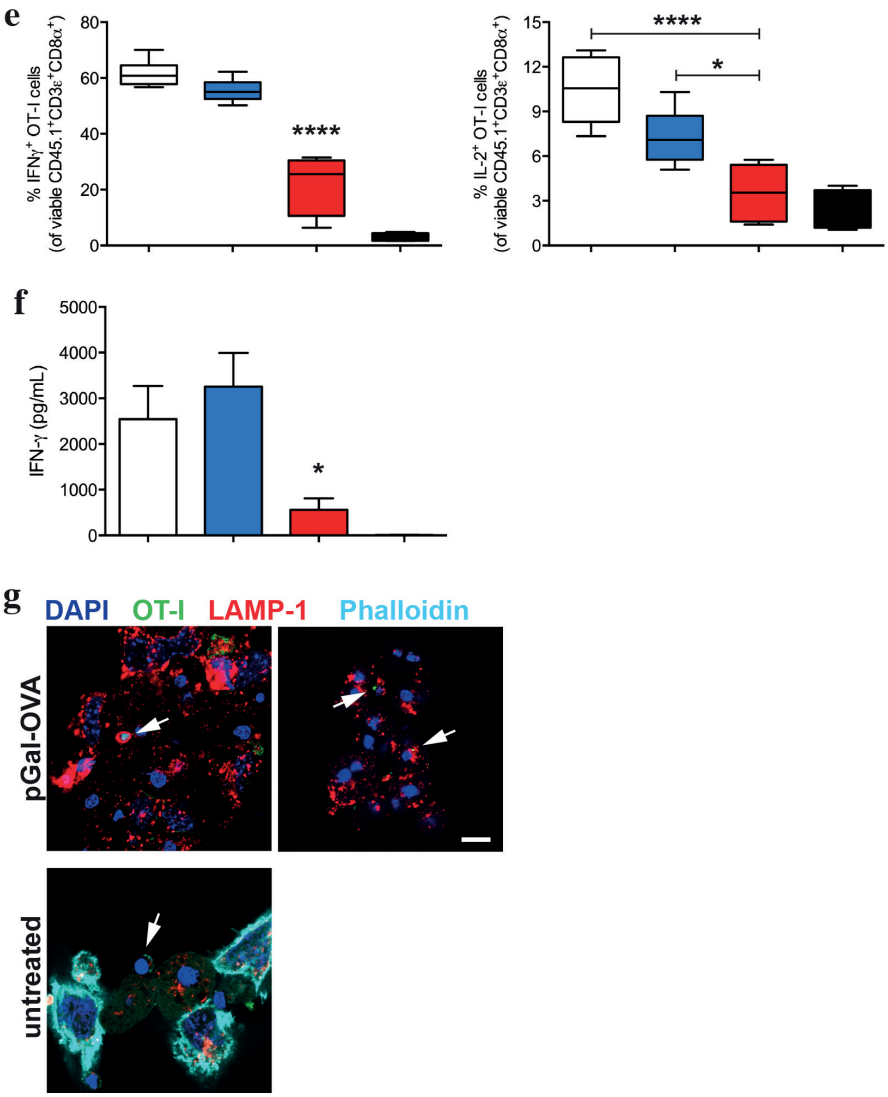

Figure 3.5 OVA cross-presenting hepatocytes induce CD8⁺ T cell tolerance via OT-I cell deletion and anergy. (a) Confocal microscopy of primary hepatocytes from C57BL/6 mice incubated *ex vivo* for 3 hr with 12.5 μM pGal-OVA and stained for H-2Kb/SIINFEKL and DAPI. Scale bar = 10 μm. (b) Adoptive transfer experimental design. (c) Flow cytometric analysis of proliferated ($CFSE^{low\text{-}neg}$) OT-I cells (top) or of the frequency and cell counts of $CD45.1^+$ OT-I cells in the population of total viable $CD3\varepsilon^+CD8\alpha^+$ T cells (bottom) harvested from the dLNs of recipient $CD45.2^+$ C57BL/6 mice treated as indicated in (b). Numbers in the representative dot plots indicate the frequency of $CD45.1^+$ OT-I cells gated in the population of viable $CD3\varepsilon^+CD8\alpha^+$ cells. (d) Flow cytometry of OT-I cells from the dLNs of recipient C57BL/6 mice treated as in (b) stained with either Annexin V, FasL, TRAIL or KLRG-1 and CD127. (e) Flow cytometric analysis of OT-I cells harvested from the dLNs of recipient C57BL/6 mice treated as in (b) stained intracellularly for IFN-γ (left) or IL-2 (right). (f) ELISA quantification of secreted IFN-γ released by total dLN cells harvested from recipient C57BL/6 mice treated as in (b) and restimulated with SIINFEKL. (g) Confocal microscopy of primary hepatocytes incubated with 5 μM pGal-OVA (top) or left untreated (bottom) for 24 hr followed by 24 hr of co-culture with CFSE-labeled OT-I cells. Cells were stained for LAMP-1 and with DAPI and phalloidin (only bottom panel). Arrows

indicate $CFSE^+$ OT-I cells or their debris. Scale bar = 10 μm. $^*P < 0.05$, $^{****}P < 0.0001$ and n.s. = not significant for comparisons of pGal-OVA hepatocyte-treated group with either vehicle (plus challenge)- or hepatocyte-treated group (one-way ANOVA and Bonferroni *post-hoc* test correction). Data are representative of 2 independent experiments ($n = 8$; mean and s.e.m. in (c-f)).

Emperipolesis has been described as a mechanism of T cell clonal deletion by hepatocytes. During emperipolesis, antigen-specific $CD8^+$ T lymphocytes actively invade antigen-presenting hepatocytes after TCR triggering and are subsequently degraded into $LAMP\text{-}1^+$ organelles [19]. OT-I-into-hepatocytes structures reminiscent of emperipolesis could be observed *in vitro* after co-culturing CFSE-labeled OT-I cells with pGal-OVA-treated hepatocytes for 24 hr (Fig. 3.5g). Specifically, OT-I cells or their debris were detected inside LAMP-1-coated compartments of OVA cross-presenting hepatocytes, while OT-I cells only made contact with the surface of untreated hepatocytes (Fig. 3.5g).

Collectively, our results indicate that antigen cross-presenting hepatocytes significantly affect the phenotype of antigen-specific $CD8^+$ T cells inducing T cell deletion, as indicated by the reduced frequency of $CD45.1^+$ OT-I cells among viable $CD8^+$ T lymphocytes both in the dLNs and spleen of mice administered with pGal-OVA-treated hepatocytes. Moreover, non-deleted OT-I cells isolated from the mice receiving pGal-OVA pre-treated hepatocytes showed a phenotype reminiscent of anergic T cells, characterized by reduced responsiveness to vaccination, as indicated by significantly lower percentages of $IFN\text{-}\gamma^+$ or $IL\text{-}2^+$ cells. Hepatocyte-educated OT-I cells showed a molecular signature of $CD8^+$ T cell deletional tolerance, characterized by upregulation of FasL and TRAIL, and of reduced survival and senescence, as indicated by the $KLRG1^{hi}CD127^{low}$ phenotype [55-56]. Moreover, total dLN cells, and not only OT-I cells, displayed impaired responsiveness to OVA vaccination as indicated by significantly reduced secretion of IFN-γ upon restimulation with SIINFEKL. Importantly, emperipolesis could be observed *in vitro* when OT-I cells were cultured together with pGal-OVA-treated hepatocytes. As expected from the lack of MHC-II expression by hepatocytes, no significant immune effect of pGal-OVA-treated hepatocytes could be detected on $CD4^+$ OT-II cells adoptively transferred into recipient mice instead of OT-I cells (data not shown). The lack of $CD4^+$ T cell tolerance upon hepatocyte-dependent antigen presentation indirectly confirms that the $CD8^+$ T cell clonal deletion and anergy here described result from direct interaction between cross-presenting hepatocytes and antigen-specific $CD8^+$ T lymphocytes (cross-tolerance).

3.3.4 PD-1/PD-L1 interactions participate in the establishment of hepatocyte-dependent cross-tolerance

PD-1 is a negative regulator of T cell responses and has been especially associated with enhanced apoptosis and reduced secretion of pro-inflammatory cytokines of activated lymphocytes [31-35]. Of note, expression of its receptor PD-L1 in the liver parenchyma has been involved in hepatic retention and elimination of $CD8^+$ T cells activated in the periphery [24]. Since we observed induction of deletion and anergy of OT-I cells by antigen cross-presenting hepatocytes (Fig. 3.5c-g), we asked whether these effects could be ascribed to the PD-1/PD-L1 pathway.

43.1% of the OT-I cells isolated from the dLNs of mice treated as in Fig. 3.5b and receiving OVA cross-presenting hepatocytes were $PD\text{-}1^+$, significantly more frequent than in the dLNs of mice receiving either vehicle or untreated hepatocytes, where only 14.2% and 12.4% of the OT-I cells were $PD\text{-}1^+$, respectively (Fig. 3.6a, bottom left). Of note, the majority of the $PD\text{-}1^+$ OT-I cells in mice administered with pGal-OVA pre-treated hepatocytes were apoptotic, as shown by the significantly higher frequency of $Annexin\text{-}V^+PD\text{-}1^+$ OT-I cells (70.6%) as compared to what observed in mice receiving either vehicle (45.4%) or untreated hepatocytes (44.8%) on day 0 (Fig. 3.6a, bottom right). Similar results were also observed for the OT-I cells isolated from the spleen of vaccinated mice treated with OVA cross-presenting hepatocytes on day 0 (Supplementary Fig. 3.2a).

PD-1 interacts with at least two receptors, PD-L1 and PD-L2. While expression of PD-L2 is restricted to activated lymphocytes and APCs, PD-L1 is widely expressed in lymphoid and non-lymphoid tissues [31,36-38]. Hepatocytes have previously been reported to express basal levels of PD-L1, which becomes overexpressed upon viral infection or treatment with type I and II interferons, leading to $CD8^+$ T lymphocyte apoptosis [39]. Unlike previous reports, we could detect, at steady state conditions, high expression levels of PD-L1, but not PD-L2, on liver parenchymal cells from wild-type untreated C57BL/6 mice (Fig. 3.6b).

In order to test whether the interaction between PD-L1 expressed by OVA cross-presenting hepatocytes and PD-1 upregulated on the surface of hepatocyte-educated OT-I cells played a role in the establishment of the cross-tolerance effects observed in Fig. 3.5c-g, we compared the tolerogenic effects of pGal-OVA-treated hepatocytes to those of pGal-OVA-treated hepatocytes incubated with a PD-L1 blocking antibody in the same experimental setting shown in Fig. 3.5b. Vaccination with OVA/LPS induced proliferation of the OT-I cells in the dLNs and spleen of recipient mice with no significant differences among the treatment groups, as indicated by flow cytometric analysis of CFSE dilution of viable $CD45.1^+CD3^+CD8^+$ OT-I cells (Fig. 3.6c and Supplementary Fig. 3.2b, top panel). More

importantly, treatment of OVA cross-presenting hepatocytes with a PD-L1 blocking antibody prior to their infusion into recipient CD45.2$^+$ C57BL/6 mice significantly reduced the induction of deletional tolerance by hepatocytes, since the frequency of CD45.1$^+$ OT-I cells in the population of viable CD3$^+$CD8$^+$ lymphocytes was significantly increased in the dLNs of mice receiving on day 0 pGal-OVA- and αPD-L1-treated hepatocytes (0.45%) as compared to those receiving hepatocytes treated with either only pGal-OVA or with pGal-OVA and an isotype control antibody (0.22% and 0.20%, respectively) (Fig. 3.6c, bottom panels). Similar results were also observed for the OT-I cell counts (Fig. 3.6c, bottom panels) and were paralleled by the frequencies and counts of OT-I cells measured in the spleen of recipient mice (Supplementary Fig. 3.2b, bottom panels).

Confirming reduced CD8$^+$ T cell deletion, pre-treatment of OVA cross-presenting hepatocytes with αPD-L1 also significantly reduced the frequency of Annexin-V$^+$, FasL$^+$, TRAIL$^+$ and KLRG1^{hi}CD127^{low} OT-I cells isolated from the dLNs and spleen of recipient mice (Fig. 3.6d and Supplementary Fig. 3.2c, respectively). In addition, blocking the interaction between OT-I-expressed PD-1 and hepatocyte-expressed PD-L1 also significantly contrasted the induction of anergy and improved the acquisition of effector functions by non-deleted OT-I cells, resulting in increased frequencies of IFN-γ$^+$ (47.11%) and IL-2$^+$ (7.53%) OT-I cells isolated from dLNs and spleen of recipient mice after OVA/LPS challenge as compared to mice receiving either pGal-OVA-treated hepatocytes (24.53% and 3.19% of dLN IFN-γ$^+$ and IL-2$^+$ OT-I cells, respectively) or pGal-OVA and isotype control antibody-treated hepatocytes (29.16% and 4.21% of dLN IFN-γ$^+$ and IL-2$^+$ OT-I cells, respectively (Fig. 3.6e and Supplementary Fig. 3.2d). Pretreatment of OVA cross-presenting hepatocytes with αPD-L1 also resulted in a trend for increased secretion of IFN-γ by total dLN cells harvested from recipient mice and restimulated *ex vivo* with SIINFEKL, even though differences among groups were not statistically significant (Fig. 3.6f). Last, when PD-L1 was blocked, emperipolesis of OT-I cells cultured *in vitro* for 24 hr together with pGal-OVA-treated hepatocytes was abrogated (Fig. 3.6g).

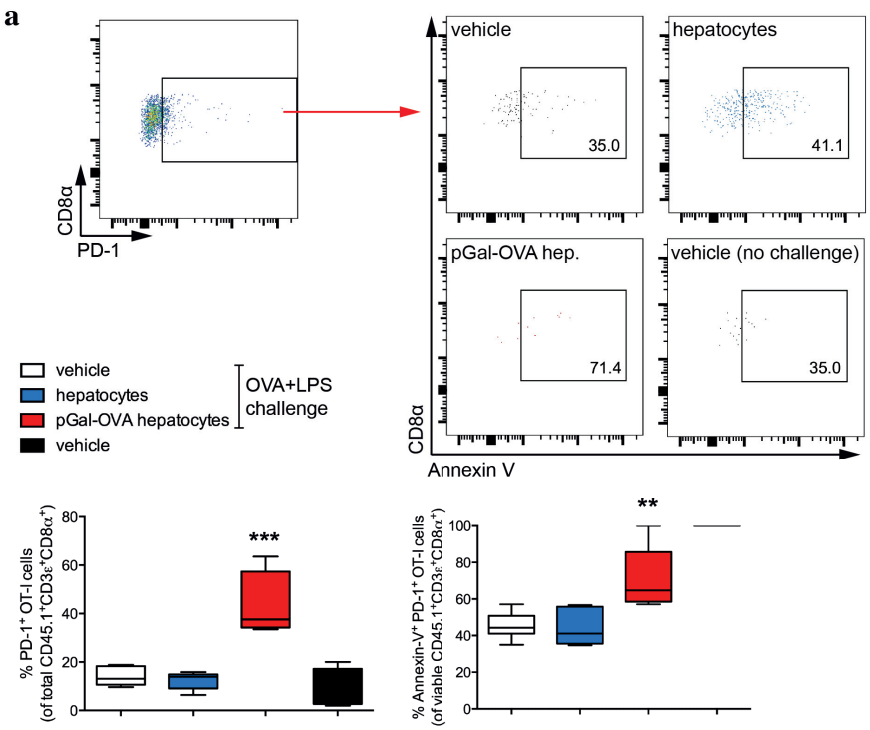
a
CD8α
PD-1
vehicle
hepatocytes
pGal-OVA hep.
vehicle (no challenge)
35.0
41.1
71.4
35.0
CD8α
Annexin V
vehicle
hepatocytes
pGal-OVA hepatocytes
vehicle
OVA+LPS challenge
% PD-1+ OT-I cells (of total CD45.1+CD3ε+CD8α+)
***
% Annexin-V+ PD-1+ OT-I cells (of viable CD45.1+CD3ε+CD8α+)
**

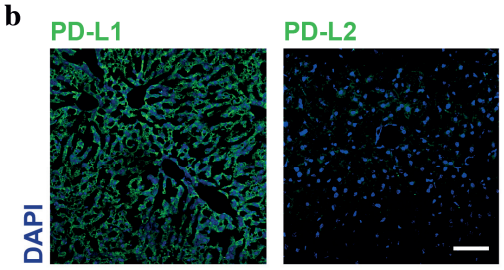
b
PD-L1
PD-L2
DAPI

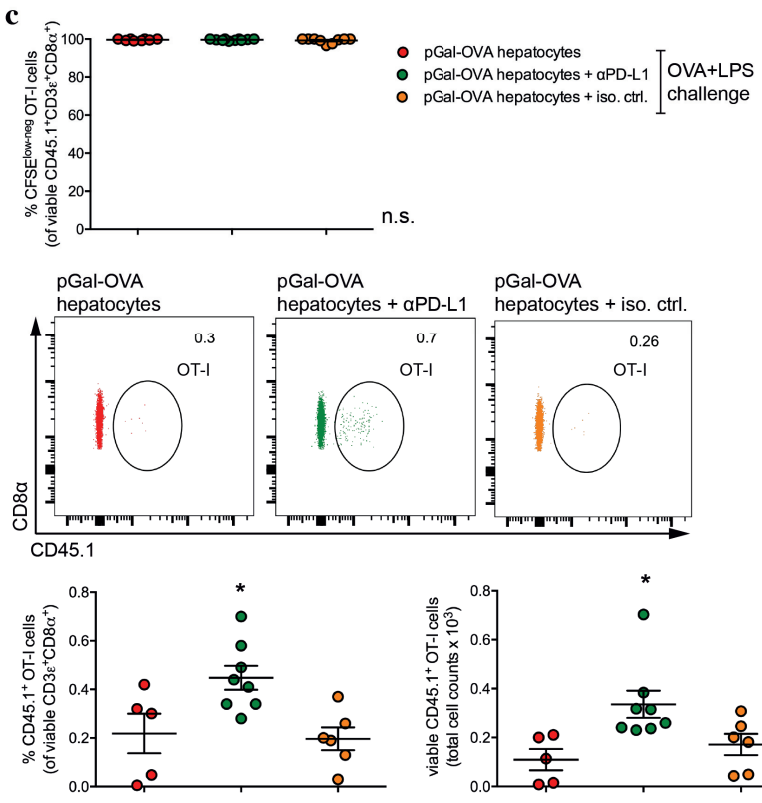
c
% CFSElow-neg OT-I cells (of viable CD45.1+CD3ε+CD8α+)
pGal-OVA hepatocytes
pGal-OVA hepatocytes + αPD-L1
pGal-OVA hepatocytes + iso. ctrl.
OVA+LPS challenge
n.s.
pGal-OVA hepatocytes
pGal-OVA hepatocytes + αPD-L1
pGal-OVA hepatocytes + iso. ctrl.
0.3
0.7
0.26
OT-I
CD8α
CD45.1
% CD45.1+ OT-I cells (of viable CD3ε+CD8α+)
viable CD45.1+ OT-I cells (total cell counts x 10³)
*

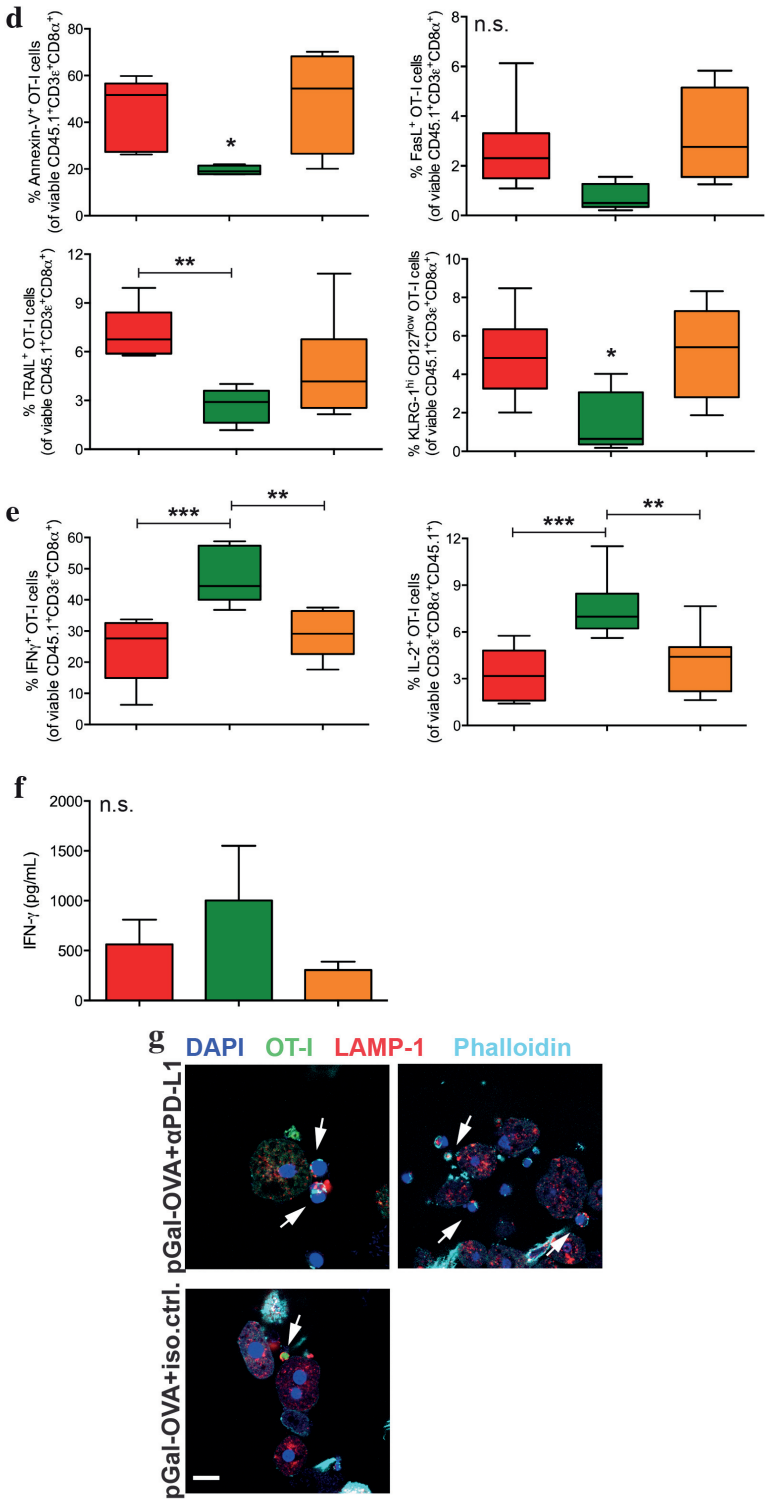

Figure 3.6 PD-1/PD-L1 interactions are involved in hepatocyte-dependent cross-tolerance. (a) Flow cytometry of OT-I cells harvested from the dLNs of recipient C57BL/6 mice treated as in Fig. 3.5b and stained for PD-1 and Annexin V. The frequencies of PD-1$^+$ OT-I cells (bottom left) and of Annexin V$^+$PD-1$^+$ OT-I cells (bottom right) are indicated. Numbers in the representative dot plots (top) indicate the frequency of Annexin V$^+$ OT-I cells in the population of PD-1$^+$ OT-I cells. (b) Confocal microscopy of liver sections from C57BL/6 mice stained for DAPI and either PD-L1 or PD-L2. Scale

bar = 50 μm. (c) Flow cytometry analysis of proliferated ($CFSE^{low\text{-}neg}$) OT-I cells (top) and of the frequency of OT-I cells (gated as $CD45.1^+$) in the population of viable $CD3\varepsilon^+CD8\alpha^+$ T cells and the corresponding cell counts (bottom panels) from the dLNs of recipient $CD45.2^+$ C57BL/6 mice infused with hepatocytes incubated *ex vivo* with pGal-OVA (12.5 μM) or with pGal-OVA (12.5 μM) and 100 μg/ml of either αPD-L1 antibody or isotype control antibody as indicated in Fig. 3.5b. Numbers in the representative dot plots indicate the frequency of $CD45.1^+$ cells in the population of viable $CD3\varepsilon^+CD8\alpha^+$ cells. (d) Flow cytometry of OT-I cells harvested from the dLNs of recipient C57BL/6 mice treated as in (c) and stained with either Annexin V, FasL, TRAIL or KLRG-1 and CD127. (e) Flow cytometric analysis of OT-I cells from the dLNs of recipient C57BL/6 mice treated as in (c) stained intracellularly for IFN-γ (left) or IL-2 (right). (f) ELISA quantification of secreted IFN-γ released by total dLN cells harvested from recipient C57BL/6 mice treated as in (c) and restimulated with SIINFEKL. (g) Confocal microscopy of primary hepatocytes incubated with 5 μM pGal-OVA (top) or left untreated (bottom) for 24 hr followed by 24 hr of co-culture with CFSE-labeled OT-I cells. Cells were stained for LAMP-1 and with DAPI and phalloidin. Arrows indicate $CFSE^+$ OT-I cells or their debris. Scale bar = 10 μm. $^{*}P < 0.05$, $^{**}P < 0.01$, $^{***}P < 0.001$ and n.s. = not significant for comparisons of pGal-OVA hepatocyte-treated group with either vehicle (plus challenge)- or hepatocyte-treated group in (a) or for comparisons of pGal-OVA + αPD-L1 antibody hepatocyte-treated group with either pGal-OVA hepatocyte- or pGal-OVA + iso. ctrl. antibody hepatocyte-treated group in (c-f) (one-way ANOVA and Bonferroni *post-hoc* test correction). Data are representative of 2 independent experiments ($n = 8$; mean and s.e.m. in (a,c-f)).

Taken together, our data show that the interaction between PD-1, highly upregulated on the surface of $CD8^+$ T cells experiencing antigen cross-presentation by hepatocytes, and PD-L1, strongly expressed by hepatocytes, participates to the induction of hepatocyte-dependent cross-tolerance. In particular, PD-1 overexpression is found to correlate with T cell reduced survival and increased apoptosis, as the majority of $PD\text{-}1^+$ OT-I cells also stain positive for Annexin V in mice administered with OVA cross-presenting hepatocytes. Treating OVA cross-presenting hepatocytes with a PD-L1 blocking antibody prior to their infusion, significantly interferes with the establishment of hepatocyte-dependent cross-tolerance, as indicated by increased frequency of $CD45.1^+$ OT-I cells, reduced pro-apoptotic OT-I cells, increased IFN-γ- and IL-2-producing OT-I cells and IFN-γ-secreting total dLN cells and abrogation of emperipolesis.

3.3.5 Cross-tolerance is a direct effect of hepatocyte-dependent antigen presentation and does not require antigen presentation by host APCs

Prolonged survival of hepatocytes after i.v. administration (Fig. 3.4), lack of $CD4^+$ T cell tolerance in the mice administered with pGal-OVA-treated hepatocytes (data not shown), and

impaired tolerance after blocking PD-L1 specifically on OVA cross-presenting hepatocytes (Fig. 3.6) altogether provide indirect evidence that the establishment of tolerance following hepatocyte adoptive transfer is a consequence of hepatocyte cross-presentation. Nevertheless, i.v. administered hepatocytes could be phagocytosed, degraded and their antigens, including OVA-derived epitopes, could be presented by host scavenger cells in the absence of co-stimulation, resulting in tolerance induction.

We confirmed the direct role of hepatocyte-dependent cross-presentation in the establishment of $CD8^+$ T cell tolerance by analysing the development of cross-tolerance after administration of pGal-OVA-treated $TAP1^{-/-}$ hepatocytes into wild-type (wt) recipients as compared to administration of pGal-OVA-treated wt hepatocytes, following the same experimental design indicated in Fig. 3.5b. As expected from their genetic defect, *ex vivo* incubation of $TAP1^{-/-}$ hepatocytes with pGal-OVA resulted in significantly lower cross-presentation of OVA-derived SIINFEKL as compared to wt hepatocytes (Fig. 3.5a and Fig. 3.7a).

Upon vaccination, OT-I cells retrieved from the dLNs and spleen of mice receiving either pGal-OVA-treated wt hepatocytes or pGal-OVA-treated $TAP1^{-/-}$ hepatocytes responded by proliferation (Fig. 3.7b and Supplementary Fig. 3.3a, left panel). Nonetheless, in the dLNs of mice administered on day 0 with OVA cross-presenting $TAP1^{-/-}$ hepatocytes, the frequency of $CD45.1^+$ OT-I cells in the population of viable $CD3^+CD8^+$ lymphocytes was significantly greater than in mice infused with cross-presenting wt hepatocytes (0.60% and 0.25%, respectively) (Fig. 3.7b, right panel). A similar trend was also observed for the counts of OT-I cells (Fig. 3.7b, right panel) and was paralleled by the frequencies and counts of OT-I cells measured in the spleen of recipient mice (Supplementary Fig. 3.3a, right panel). In parallel with increased frequency, the percentage of $FasL^+$, $TRAIL^+$ or $KLRG1^{hi}CD127^{low}$ OT-I cells retrieved from the dLNs or spleen of mice treated with $TAP1^{-/-}$ hepatocytes was also significantly decreased as compared to mice receiving wt hepatocytes (Fig. 3.7c and Supplementary Fig. 3.3b,c). Moreover, non-deleted OT-I cells from the dLNs or spleen of mice treated on day 0 with $TAP1^{-/-}$ hepatocytes responded to OVA/LPS challenge more efficiently, as indicated by the frequency of IFN-γ-expressing OT-I cells detected by flow cytometry (44.2% as compared to 24.5% in the dLNs) (Fig. 3.7d and Supplementary Fig. 3.3d). The percentage of IL-2-producing OT-I cells was also significantly increased in both the spleen and dLNs of mice receiving OVA cross-presenting $TAP1^{-/-}$ hepatocytes as compared to wt hepatocytes (4.94% as compared to 2.76% in the dLNs) (Supplementary Fig. 3.3e). The frequency of $PD\text{-}1^+$ and of $Annexin\text{-}V^+PD\text{-}1^+$ OT-I cells harvested from the dLNs or spleen of mice administered with $TAP1^{-/-}$ hepatocytes pre-treated with pGal-OVA was significantly reduced as compared to mice administered with pGal-OVA-treated wt

hepatocytes (20.46% as compared to 43.1% of PD-1$^+$ OT-I cells and 44.77% as compared to 67.2% of PD-1$^+$Annexin-V$^+$ OT-I cells in the dLNs) (Fig. 3.7e and Supplementary Fig. 3.3f). Last, impaired OVA cross-presentation by TAP$^{-/-}$ hepatocytes also resulted in a general stronger response to vaccination with adjuvanted OVA, as suggested by a trend for increased secretion of IFN-γ by total dLN cells upon *ex vivo* restimulation with SIINFEKL (Fig. 3.7f).

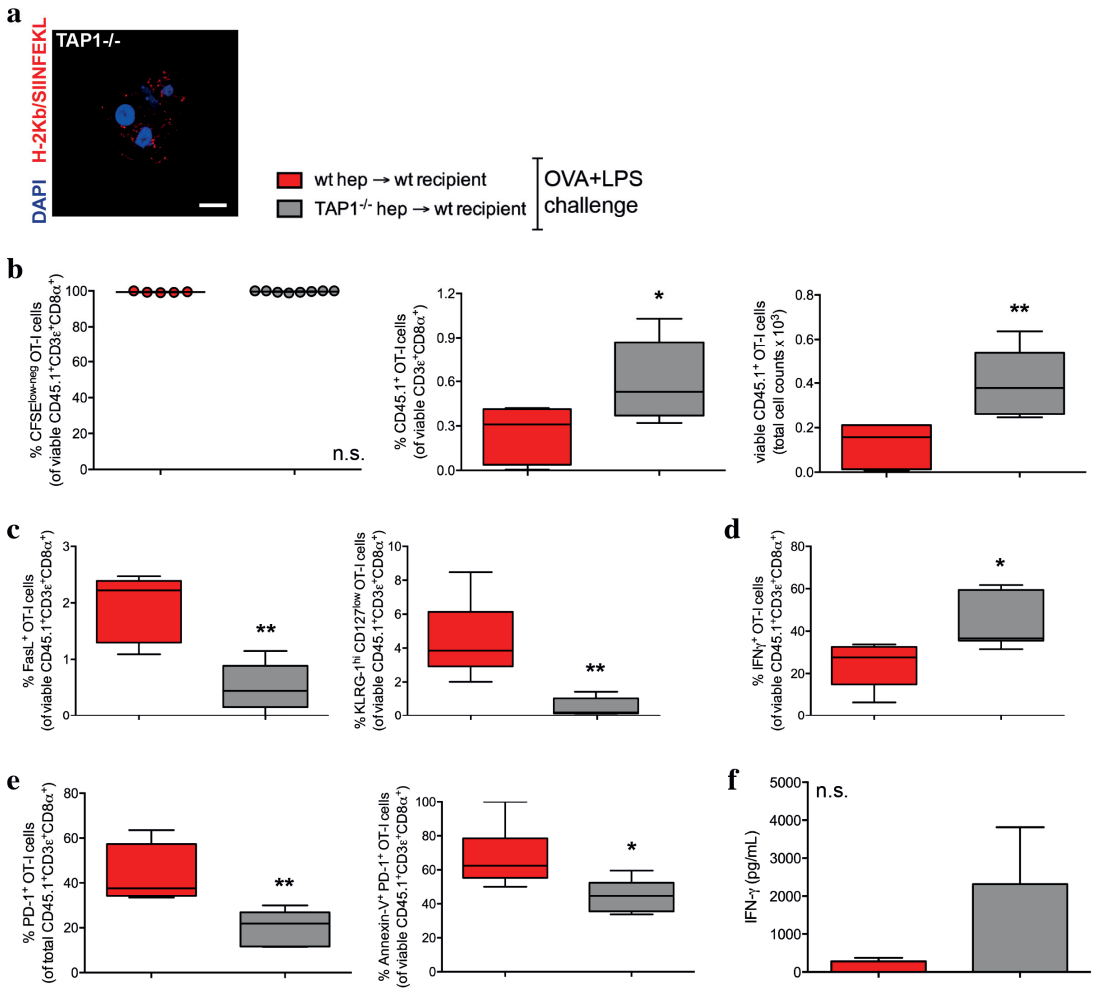

Figure 3.7 CD8$^+$ T cell tolerance is the result of hepatocyte-dependent antigen cross-presentation. (a) Confocal microscopy of primary hepatocytes from TAP1$^{-/-}$ C57BL/6 mice incubated *ex vivo* for 3 hr with 12.5 μM pGal-OVA and stained for H-2Kb/SIINFEKL and DAPI. Scale bar = 10 μm. (b) Flow cytometry analysis of proliferated (CFSE$^{low-neg}$) OT-I cells (left) and of the frequency of OT-I cells (gated as CD45.1$^+$) in the population of viable CD3ε$^+$CD8α$^+$ T cells and the corresponding cell counts (right) from the dLNs of recipient CD45.2$^+$ C57BL/6 mice infused with either wt hepatocytes or TAP1$^{-/-}$ hepatocytes both incubated *ex vivo* with pGal-OVA (12.5 μM). (c) Flow cytometry of OT-I cells from the dLNs of recipient C57BL/6 mice treated as in (b) stained with either FasL (left) or KLRG-1 and CD127 (right). (d) Flow cytometry of OT-I cells from the dLNs of recipient C57BL/6 mice treated as in (b) stained intracellularly for IFN-γ. (e) Flow cytometry of OT-I cells harvested from the dLNs of recipient C57BL/6 mice treated as in (b) stained for PD-1 and Annexin V. The frequencies of PD-1$^+$ OT-I cells (left) and of Annexin V$^+$PD-1$^+$ OT-I cells (right) are indicated. (f) ELISA quantification of

secreted IFN-γ released by total dLN cells harvested from recipient C57BL/6 mice treated as in (b) and restimulated with SIINFEKL. $^{*}P < 0.05$, $^{**}P < 0.01$ (unpaired t test). Data are representative of 2 independent experiments ($n = 8$; mean and s.e.m. in (b-f)).

Collectively, our data confirm that the development of cross-tolerance in mice receiving pGal-OVA-treated hepatocytes depends on the direct interaction between OVA-specific $CD8^+$ T lymphocytes and OVA cross-presenting hepatocytes, and does not require processing of hepatocyte-derived antigens by host APCs. In fact, adoptively transferred hepatocytes survive *in vivo* both in the spleen and liver of recipient mice for at least 1 month after transfer (Fig. 3.4). Therefore, when cross-presentation defective $TAP1^{-/-}$ hepatocytes were treated with pGal-OVA and infused into recipient mice, the induction of $CD8^+$ T cell tolerance was significantly impaired.

3.4 Discussion

The study here described sheds light on the involvement of hepatocytes in the establishment of liver-mediated peripheral cross-tolerance towards soluble extracellular antigens.

Because of its strategic location and microscopic anatomy, the liver has been associated with blood-filtering and immune tolerogenic functions. In fact, the liver is placed between the blood vessel system collecting gut-derived blood and the systemic circulation, and is thus constantly exposed to foreign components, such as food antigens, environmental molecules and bacterial components absorbed from the intestinal lumen into the bloodstream. In healthy individuals, these foreign components entering the body do not elicit immunity [5,13,40]. The hepatic structure is characterized by a complex network of enlarged capillaries, the sinusoids, which are lined by a fenestrated endothelium composed by LSECs and paralleled by plates of hepatocytes [40]. The immunological properties of the liver have been mainly attributed to the ability of LSECs and hepatocytes to interact with circulating lymphocytes, even though both LSECs and hepatocytes are non-hematopoietic cells [13]. LSECs have been so far considered the major cell population responsible for the immunomodulatory functions of the liver, as they are in direct contact with circulating lymphocytes, show efficient antigen scavenging capacity, express both MHC-I and MHC-II, and have low non-inducible levels of co-stimulatory molecules [6-11]. On the other hand, hepatocytes only express MHC-I complexes and have been attributed poor antigen scavenging capacity *in vitro*, but efficient $CD8^+$ T cell deletion ability *in vivo* upon direct antigen expression and MHC-I presentation in the absence of co-stimulation [14-23].

The liver is home to vital metabolic and detoxifying reactions, mostly occurring in hepatocytes, and such reactions require uptake and processing of circulating molecules. We thus reasoned that hepatocytes could express and utilize the molecular machinery of antigen cross-presentation. Cross-presentation of extracellular antigens on the MHC-I has been mainly attributed to specialized subsets of hematopoietic cells, in particular lymphoid organ resident $CD8\alpha^+$ DCs [41]. Nonetheless, in recent years it has been discovered that subsets of non-hematopoietic cells are also capable of cross-presentation, among which stromal cells in the LNs and LSECs in the liver [8,9,42,43]. Cross-presentation requires a dedicated pathway by which extracellular antigens are taken up by endocytotic receptors into phagosomes, degraded by proteasomal digestion, translocated to endoplasmic structures where peptides are loaded onto MHC-I molecules and then subsequently transferred to the cell membrane [25,26,28].

Unlike previous reports, we were able to show that murine primary hepatocytes express high levels of the mannose scavenging receptor 1 (MR) found in other cross-presenting cells and contain abundant cellular compartments positive for markers associated with MHC-I presentation of extracellular antigens, in particular EEA1 and TAP1. Interestingly, hepatocytes were found to contain $EEA1^+TAP1^+$ phagosomes, which are a peculiar characteristic or professional cross-presenting $CD11c^+CD8\alpha^+$ cells [25]. We also show both *in vitro* and *in vivo* that hepatocytes actively process extracellular antigens, such as DQ-OVA, especially in association with $EEA1^+$ and $TAP1^+$ compartments. As expected, the efficiency of antigen processing was reduced as compared to $CD11c^+CD8\alpha^+$ DCs cells, probably due the higher concentration of cross-presentation-competent phagosomes, mostly $EEA1^+TAP1^+$ compartments, in this DC subset as compared to hepatocytes.

To study the molecular mechanisms and the immunological outcomes of antigen cross-presentation by hepatocytes, we decided to utilize a version of the model antigen OVA chemically modified with poly(N-Acetylgalactosamine) (pGal-OVA), which is recognized by several scavenger receptors. Since receptor-mediated uptake of an antigen is the initial step of the cross-presentation pathway, improved uptake of pGal-OVA also led to enhanced cross-presentation of the OVA-derived immunodominant epitope SIINFEKL by hepatocytes. Presentation of SIINFEKL to antigen-specific OT-I cells by pGal-OVA-treated hepatocytes was significantly reduced when endosomal or proteasomal function was blocked using specific drug inhibitors. Reduction of the antigen presentation capacity of hepatocytes upon treatment with chloroquine or MG132 provides direct evidence that the cellular machinery of the antigen cross-presentation pathway is active in hepatocytes and, most importantly, further confirms that extracellular antigens enter this pathway after receptor-mediated endocytosis into hepatocytes.

Scavenger receptors are widely expressed by a variety of cell types in direct contact with the blood, including Kupffer cells and LSECs in the liver and macrophages and DCs in the spleen [27]. In order to specifically characterize the effects of hepatocyte-dependent antigen cross-presentation, we adopted an *ex vivo* system where murine hepatocytes are first isolated from the liver of donor mice and incubated with the pGal-OVA antigen, then subsequently washed and infused i.v. into recipient mice. Surprisingly, adoptively transferred hepatocytes mainly home to the spleen and only to a lesser extent to the liver, while hepatocytes do not seed in other blood-filtering organs, including lungs and kidneys. Upon i.v. infusion, hepatocytes survive for at least 1 month in host animals, indicating that *ex vivo* manipulation of hepatocytes does not affect their viability.

When the phenotype of H-2Kb/SIINFEKL-specific OT-I cells was analyzed after an immunogenic challenge with OVA and LPS in mice receiving hepatocyte transfer, we observed reduced frequencies of the OT-I cells that had previously experienced cognate antigen presentation by OVA cross-presenting hepatocytes, suggesting an antigen-specific process of T cell deletion. Deletion of the OT-I cells could be attributed to T cell apoptosis, as the remaining non-deleted hepatocyte-educated OT-I cells showed a pro-apoptotic phenotype, indicated by staining with Annexin V and positivity for FasL and TRAIL, and reduced survival capacity, suggested by the increased frequency of OT-I cells displaying the $KLRG1^{hi}CD127^{low}$ phenotypic signature of senescent cells [55-56]. Not only the non-deleted hepatocyte-educated OT-I cells showed reduced survival, but they also responded poorly to vaccination, producing low levels of the pro-inflammatory cytokines IFN-γ and IL-2. Unresponsiveness to vaccination indicated acquisition of anergic phenotype by the OT-I cells, further indicating the establishment of tolerance. Future investigations will elucidate whether hepatocyte-dependent anergy represents a terminally differentiated state leading to T cell deletion or whether such state can be reversed upon antigen re-encounter under pro-inflammatory conditions, similarly to LSEC-mediated $CD8^+$ T cell tolerance [11]. Of note, the significant reduction of IFN-γ secretion by total dLN cells harvested from mice receiving OVA cross-presenting hepatocytes as compared to the other treatment groups suggests establishment of hepatocyte-dependent cross-tolerance not only of adoptively transferred OT-I cells but also of endogenous OVA-specific $CD8^+$ T lymphocytes.

Previous publications have shown that the development of peripheral $CD4^+$ and $CD8^+$ T cell tolerance upon intravenous infusion of antigen-coupled cells depends on the apoptotic phenotype of the transferred cells causing them to be phagocytosed and their antigens to be presented by host APCs in non-inflammatory conditions [44]. The prolonged *in vivo* survival of adoptively transferred hepatocytes indirectly rules out uptake of OVA cross-presenting hepatocytes by host APCs in our experimental system. In order to provide a direct

confirmation that the tolerogenic effects in our experiments were the result of hepatocyte cross-presentation, we adoptively transferred pGal-OVA-treated TAP1$^{-/-}$ hepatocytes into wt recipient mice together with OT-I cells. Impaired antigen cross-presentation by TAP1$^{-/-}$ hepatocytes resulted in significantly reduced OT-I cell tolerance, confirming the direct role of hepatocyte cross-presentation in tolerogenesis. Moreover, hepatocyte-dependent antigen presentation did not lead to CD4^{+} T cell tolerance in our experimental setting (data not shown), further confirming that the tolerance effect here described is the result of antigen presentation on MHC-I molecules by hepatocytes. Opposite to our findings, recent reports described the induction of antigen-specific CD4^{+}CD25^{+}FoxP3^{+} Treg cells upon hepatocyte-specific antigen expression, suggesting that in the case of an antigen directly expressed by hepatocytes, tolerance could result from antigen spreading and MHC-II presentation by other host APCs [22,23].

The liver displays an unusual enrichment of CD8^{+} T lymphocytes in its parenchyma as compared to other organs and the majority of these cells have an activated phenotype. This peculiarity has gained the liver the name of T cell graveyard, where activated CD8^{+} T lymphocytes accumulate and die by apoptosis, especially during the contraction phase of an immune response [5,45,46]. Hepatic expression of PD-L1 has been involved in the retention and deletion of activated CD8^{+} T cells, in line with the negative effects of PD-1 on T cell functions [24]. PD-1 is upregulated on activated T cells and is therefore considered one of the most important signals involved in the resolution phase of an immune response and associated with T cell exhaustion [31-35]. PD-1 has also been implied in the prevention of autoimmunity and maintenance of immune homeostasis since PD-1-deficient mice develop spontaneous autoimmune manifestations during their lifetime [47,48]. In our experiments, we observed increased frequencies of PD-1^{+} and of apoptotic Annexin-V^{+}PD-1^{+} OT-I cells in those mice administered with pGal-OVA-treated hepatocytes, as compared to the other treatment groups. As we also show that the liver parenchyma expresses PD-L1 in steady-state conditions, we hypothesized that the direct interaction between antigen-experienced PD-1-expressing OT-I cells and antigen cross-presenting PD-L1^{+} hepatocytes is one of the factors responsible for the induction of OT-I tolerance. When pGal-OVA-treated hepatocytes were incubated with a PD-L1 blocking antibody prior to their infusion into recipient mice, OT-I cells could be significantly, but not completely, rescued from deletion and development of anergy. Our data provide evidence that the PD-1/PD-L1 pathway is involved in the induction of hepatocyte-dependent cross-tolerance, even though other interactions could be involved as well. For example, hepatocytes might express ligands of PD-1 different from PD-L1 and, most importantly, hepatocyte-educated T cells might bind to PD-L1 molecules expressed on

other cells, since PD-L1 is widely expressed in both hematopoietic and non-hematopoietic tissues [37].

Interestingly, PD-1 is also overexpressed by hepatitis B virus (HBV)- and hepatitis C virus (HCV)-specific T cells in infected individuals and has been associated with impaired anti-viral immunity [49-52]. HBV and HCV are hepatotropic viruses developing chronic infection in 10% and 80% of adult infected patients, respectively. The peculiar tolerogenic properties of the liver environment have been indicated as the leading cause of HBV or HCV persistent infection, which results from the inability of the immune system to eliminate infected hepatocytes [11,53]. Presentation of viral antigens by infected hepatocytes is the result of both cross-presentation and direct antigen expression followed by presentation on the MHC-I. Nonetheless, it is tempting to speculate that suboptimal priming of virus-specific $CD8^+$ T cells by infected antigen-presenting hepatocytes could induce T cell tolerance via the PD-1/PD-L1 pathway similarly to what we observed in our experiments. Therefore, specific abrogation of PD-L1 expression in hepatocytes or blockade of its activity may provide a novel targeted therapeutic strategy for patients affected by chronic hepatitis in alternative to unspecific inhibition of PD-1/PD-L1 interactions [49].

Emperipolesis has also been observed in liver sections from patients infected with HBV and HCV and has been previously reported to be a mechanism by which $CD8^+$ T cells invade hepatocytes after TCR engagement and are destroyed in $LAMP\text{-}1^+$ organelles [19]. We were able to detect OT-I-into-hepatocytes structures forming when pGal-OVA-treated hepatocytes were co-cultured *in vitro* with OT-I cells, suggesting that emperipolesis is an additional mechanism of hepatocyte-dependent cross-tolerance. Emperipolesis is an active process of cell invasion and elimination, as it has been shown that it does not require apoptosis or phagocytosis of the T cells to occur [19]. Our data suggest that PD-1/PD-L1 interactions participate in hepatocyte emperipolesis, since blocking PD-L1 specifically on OVA cross-presenting hepatocytes could prevent OT-I invasion of hepatocytes *in vitro*.

In summary, we show here for the first time both *in vitro* and *in vivo* that hepatocytes are efficient non-hematopoietic cross-presenting cells. Hepatocyte-dependent cross-presentation was found to induce antigen-specific $CD8^+$ T cell tolerance, mainly by clonal deletion and anergy of the T cells in a PD-1/PD-L1-dependent fashion. Our data also suggest that hepatocyte-dependent tolerogenesis via the PD-1/PD-L1 pathway could be at the origin of hepatic viral chronic infections. Because of their anatomic location, their abundancy and their intense metabolic activities, we propose that hepatocytes are key players in the establishment and maintenance of liver-mediated peripheral tolerance towards both endogenous and exogenous extracellular antigens reaching the liver through the bloodstream.

Moreover, our data support hepatocytes as ideal candidates for targeted tolerogenic immunotherapies.

3.5 Supplementary figures

Supplementary Fig. 3.1

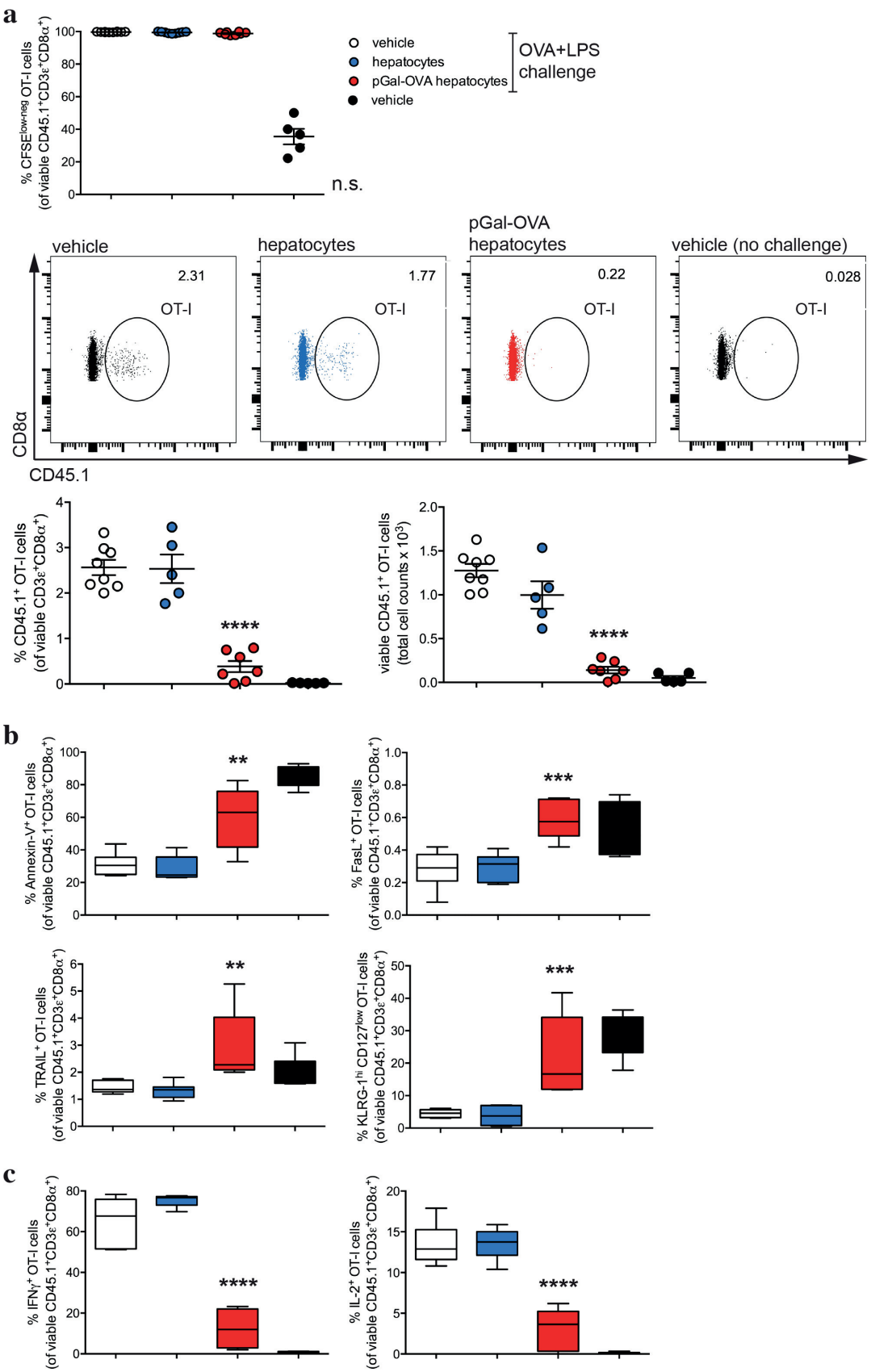

Supplementary figure 3.1 OVA cross-presenting hepatocytes induce CD8$^+$ T cell tolerance via OT-I cell deletion and anergy. (a) Flow cytometric analysis of proliferated (CFSE$^{low\text{-}neg}$) OT-I cells (top) or of the frequency of CD45.1$^+$ OT-I cells in the population of total viable CD3ε$^+$CD8α$^+$ T cells and cell counts (bottom) from the spleen of recipient CD45.2$^+$ C57BL/6 mice treated as indicated in Fig. 3.5b. Numbers in the representative dot plots indicate the frequency of CD45.1$^+$ OT-I cells in the population of viable CD3ε$^+$CD8α$^+$ cells. (b) Flow cytometry of OT-I cells from the spleen of recipient C57BL/6 mice treated as indicated in (a) stained with either Annexin V, FasL, TRAIL or KLRG-1 and CD127. (c) Flow cytometric analysis of OT-I cells harvested from the dLNs of recipient C57BL/6 mice treated as indicated in (a) stained intracellularly for IFN-γ (left) or IL-2 (right). $^{**}P < 0.01$, $^{***}P < 0.001$, $^{****}P < 0.0001$ for comparisons of pGal-OVA hepatocyte-treated group with either vehicle (plus challenge)- or hepatocyte-treated group (one-way ANOVA and Bonferroni *post-hoc* test correction). Data are representative of 2 independent experiments ($n = 8$; mean and s.e.m. in (a-c)).

Supplementary Fig. 3.2

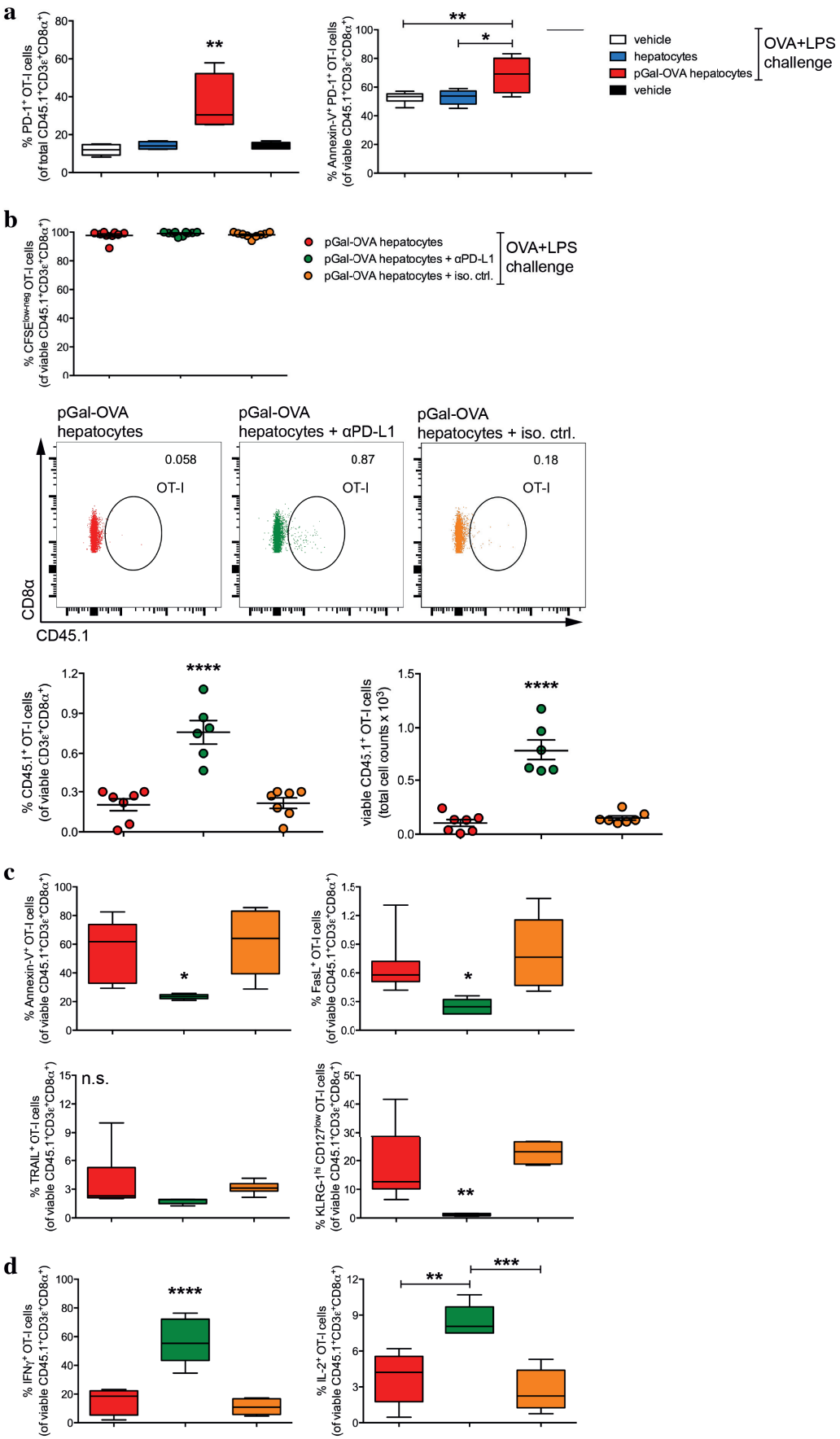

Supplementary figure 3.2 PD-1/PD-L1 interactions are involved in hepatocyte-dependent cross-tolerance. (a) Flow cytometry of OT-I cells harvested from the spleen of recipient C57BL/6 mice treated as in Fig. 3.5b and stained for PD-1 and Annexin V. The frequencies of PD-1^+ OT-I cells (left) and of Annexin-V^+PD-1^+ OT-I cells (right) are indicated. (b) Flow cytometry analysis of proliferated ($CFSE^{low\text{-}neg}$) OT-I cells (top) and of the frequency of OT-I cells (gated as CD45.1^+) in the population of viable CD3ε^+CD8α^+ T cells and of the corresponding cell counts (bottom) from the spleen of recipient CD45.2^+ C57BL/6 mice infused with hepatocytes incubated *ex vivo* with pGal-OVA (12.5 μM) or with pGal-OVA (12.5 μM) and 100 μg/ml of either αPD-L1 antibody or isotype control antibody as indicated in Fig. 3.5b. Numbers in the representative dot plots indicate the frequency of CD45.1^+ cells in the population of viable CD3ε^+CD8α^+ cells. (c) Flow cytometry of OT-I cells from the spleen of recipient C57BL/6 mice treated as indicated in (a,b) and stained with either Annexin V, FasL, TRAIL or KLRG-1 and CD127. (d) Flow cytometric analysis of OT-I cells from the spleen of recipient C57BL/6 mice treated as in (a,b) stained intracellularly for IFN-γ (left) or IL-2 (right). $^{*}P < 0.05$, $^{**}P < 0.01$, $^{***}P < 0.001$, $^{****}P < 0.0001$ and n.s. = not significant for comparisons of pGal-OVA hepatocyte-treated group with either vehicle (plus challenge)- or hepatocyte-treated group in (a) or for comparisons of pGal-OVA + αPD-L1 antibody hepatocyte-treated group with either pGal-OVA hepatocyte- or pGal-OVA + iso. ctrl. antibody hepatocyte-treated group in (b-d) (one-way ANOVA and Bonferroni *post-hoc* test correction). Data are representative of 2 independent experiments ($n = 8$; mean and s.e.m. in (a-d)).

Supplementary Fig. 3.3

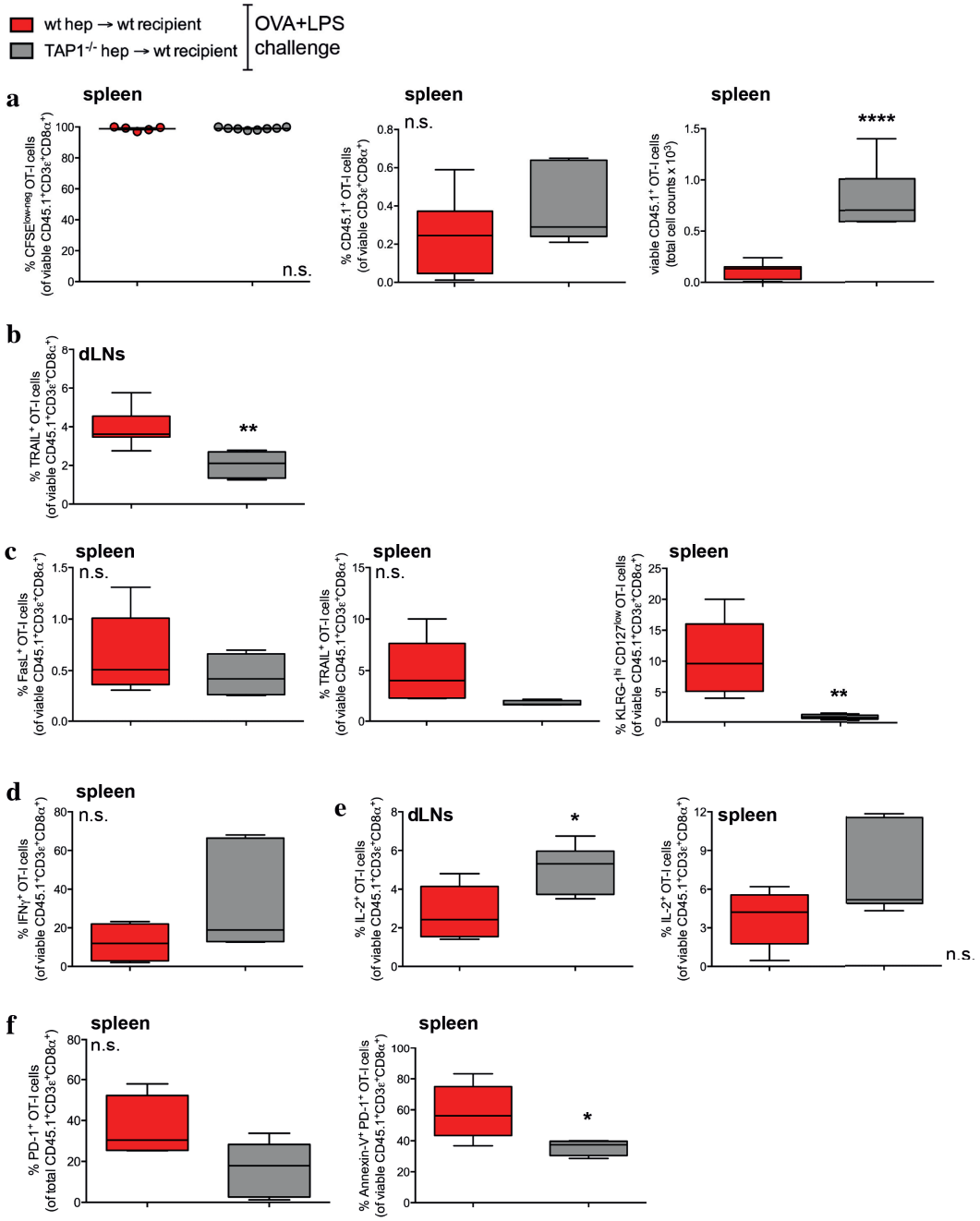

Supplementary figure 3.3 CD8$^+$ T cell tolerance is the result of hepatocyte-dependent antigen cross-presentation. (a) Flow cytometry analysis of proliferated (CFSE$^{low\text{-}neg}$) OT-I cells (left) and of the frequency of OT-I cells (gated as CD45.1$^+$) in the population of viable CD3ε$^+$CD8α$^+$ T cells and the corresponding cell counts (right) from the spleen of recipient CD45.2$^+$ C57BL/6 mice infused with either wt hepatocytes or TAP1$^{-/-}$ hepatocytes both incubated *ex vivo* with pGal-OVA (12.5 μM). (b) Flow cytometry of OT-I cells from the dLNs of recipient C57BL/6 mice treated as indicated in (a) stained with TRAIL. (c) Flow cytometry of OT-I cells from the spleen of recipient C57BL/6 mice treated as in (a) stained for either FasL, TRAIL or KLRG-1 and CD127. (d) Flow cytometry of OT-I cells harvested from the spleen of recipient C57BL/6 mice treated as in (a) stained intracellularly for

IFN-γ. (e) Flow cytometry of OT-I cells harvested from the dLNs (right) or spleen (left) of recipient C57BL/6 mice treated as in (a) stained intracellularly for IL-2. (f) Flow cytometry of OT-I cells harvested from the spleen of recipient C57BL/6 mice treated as in (a) stained for PD-1 and Annexin V. The frequencies of PD-1$^+$ OT-I cells (left) and of Annexin-V$^+$PD-1$^+$ OT-I cells (right) are indicated. $^*P < 0.05$, $^{**}P < 0.01$ and n.s. = not significant (unpaired t test). Data are representative of 2 independent experiments ($n = 8$; mean and s.e.m. in (a-f)).

Supplementary Fig. 3.4

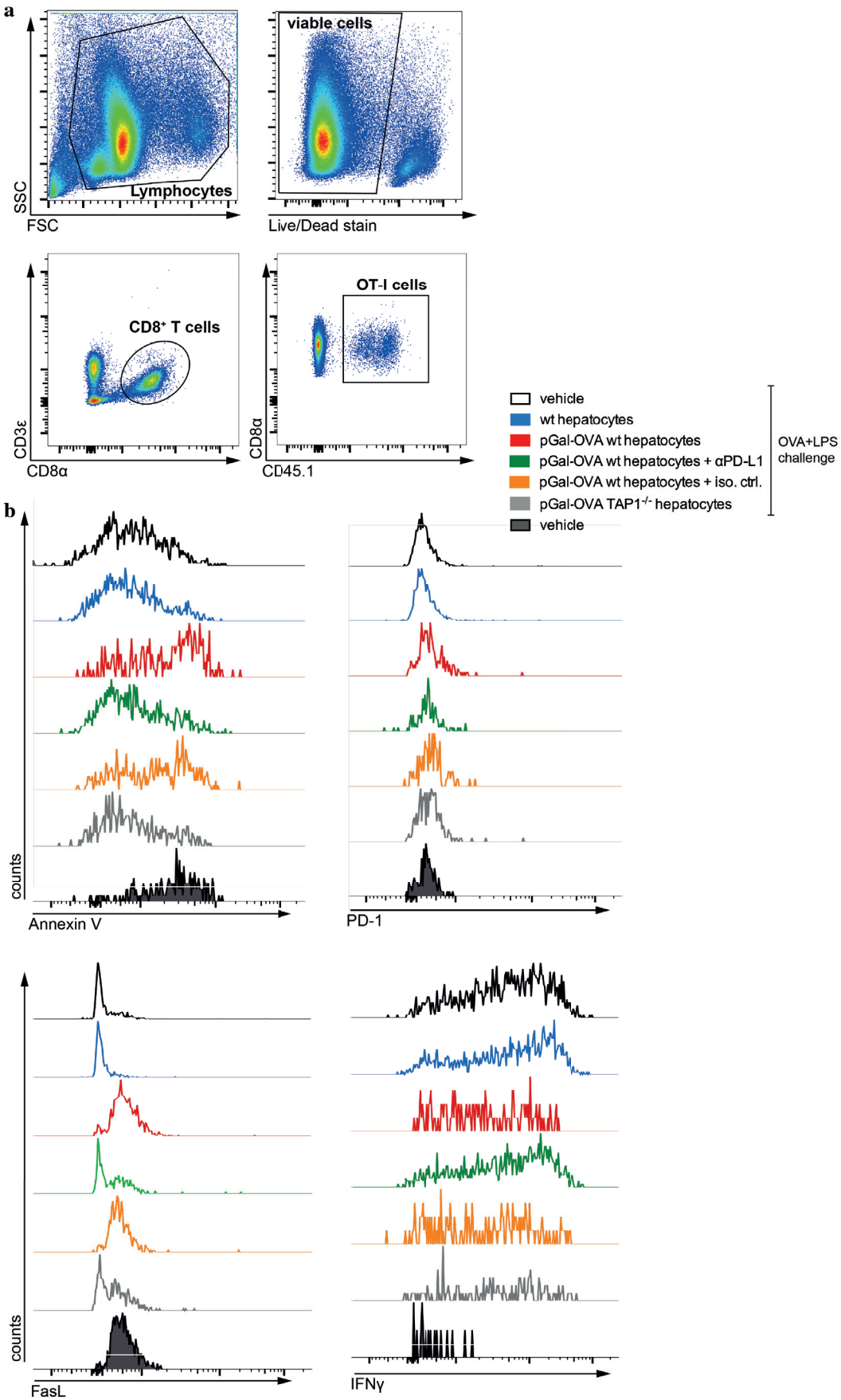

Supplementary figure 3.4 Flow cytometry gating strategy and representative raw data. (a) Gating strategy utilized to identify CD45.1$^+$ OT-I cells in CD45.2$^+$ C57BL/6 mice in Fig. 3.5, 3.6 and 3.7 and in Supplementary Fig. 3.1, 3.2 and 3.3. Briefly, lymphocytes were gated according to SSC and FSC from total spleen or dLN cells, followed by identification of viable cells, CD3ε$^+$CD8α$^+$ T cells and CD45.1$^+$ OT-I cells. (b) Representative histograms of CD45.1$^+$ OT-I cell counts positive for either Annexin V (top left), PD-1 (top right), FasL (bottom) or IFN-γ (bottom right) purified from the spleen of CD45.2$^+$ C57BL/6 mice receiving either one of the treatments indicated in the legend following the experimental schedule described in Fig. 3.5b.

Author contributions

M. Damo and J. A. Hubbell designed research; D. S. Wilson designed and synthesized poly(N-Acetylgalactosamine); M. Damo performed research described in all the Figures and Supplementary Figures; D. S. Wilson helped performing research described in Figure 3.5a-e and 3.6c-f and in Supplementary Figure 3.1a-c and 3.2b-d; M. Damo analyzed data.

3.6 Materials and methods

3.6.1 Mice

C57BL/6 mice were obtained from Harlan Laboratories (Gannat, France), TAP1$^{-/-}$ mice (B6.129S2-*Tap1*^{tm1Arp}/J) were purchased from The Jackson Laboratory (Farmington, CT) and CD45.1$^+$ OT-I mice were generated by crossing C57BL/6-Tg(TcraTcrb)1100Mjb (OT-I) mice (The Jackson Laboratories) with CD45.1$^+$ C57BL/6-Ly5.1 mice (Charles River, Saint-Germain-Nuelles, France). 8-12 week old female mice were used in all animal experiments. Animals were housed in pathogen-free conditions at the animal facility of the Ecole Polytechnique Fédérale de Lausanne and all experiments were performed in accordance with Swiss law and with approval from the Cantonal Veterinary Office of Canton de Vaud, Switzerland.

3.6.2 Cell isolation and antigen loading

Hepatocytes were isolated from the liver of wt C57BL/6 or TAP1$^{-/-}$ mice as previously described [54] and cultured on a feeder layer of 3T3 NIH fibroblasts in DMEM medium supplemented with 10% FBS and 100 IU/mL penicillin-streptomycin at 37°C 5% CO_2. BMDCs were generated by culturing total bone marrow cells from C57BL/6 mice in RPMI 1640 medium supplemented with 10% FBS, 100 IU/mL penicillin-streptomycin, 50 μM 2-Mercaptoethanol and 20 ng/mL recombinant murine GM-CSF (PreproTech) at 37°C 5% CO_2 for 6 days. To isolate CD11c$^+$CD8α$^+$ BMDCs, BMDCs were stained with Abs specific for

CD11c (BioLegend) and CD8α (Life Technologies) and sorted with a FACSAria cell sorter (BD Biosciences). CD45.1$^+$ OT-I cells were purified from the spleen and LNs of CD45.1$^+$ OT-I mice by negative selection of CD8α$^+$ T cells using the EasySep mouse CD8α T cell isolation kit (Stemcell Technologies) and labeled with CFSE (Life Technologies) following manufacturer's instructions. For *in vitro* analysis of OVA processing, hepatocytes and BMDCs were cultured in complete DMEM or complete RPMI 1640, respectively, supplemented with 20 μg/ml DQ-OVA (Life Technologies). For *in vitro* analysis of SIINFEKL cross-presentation, hepatocytes and BMDCs were cultured in 5 μM OVA-, 5 μM pGal-OVA- or 1nM SIINFEKL-supplemented complete medium. For *ex vivo* loading with pGal-OVA prior to administration into mice, hepatocytes were isolated from donor mice and incubated for 3 hr at 37°C 5% CO_2 with 12.5 μM pGal-OVA-supplemented complete DMEM (without feeder layer).

3.6.3 In vitro *co-culture of hepatocytes and OT-I cells*

Freshly isolated C57BL/6 hepatocytes were cultured in 5 μM pGal-OVA-supplemented complete DMEM for 24 hr prior to washing and co-culture with 10^5 OT-I cells for 24 hr. For drug inhibitors, chloroquine was used at 100 μM and MG132 at 10 μM and were added 1 hr after addition of the antigen. After co-culture, OT-I cells were harvested and stained with Abs specific for the markers CD3ε (eBioscience), CD8α (Life Technologies), and CD69 (BioLegend). Samples were acquired on an LSR II cytometer (BD Biosciences) and data analyzed with FlowJo software (Tree Star).

3.6.4 In vitro *emperipolesis*

Freshly isolated C57BL/6 hepatocytes were cultured in 5 μM pGal-OVA-supplemented complete DMEM for 24 hr. After washing with PBS, 10^6 CFSE-labeled OT-I cells in complete DMEM were added to the culture for 24 hr. For PD-L1 blockade, 100 μg/ml αPD-L1 blocking Ab (BioxCell, clone 10F.9G2) or rat IgG isotype control Ab (Abcam) were added to the hepatocytes for 30 min prior to washing and addition of OT-I cells. At the end of the experimental time, samples were extensively washed in PBS and prepared for confocal microscopy.

3.6.5 Confocal microscopy and flow cytometry of primary hepatocytes and BMDCs

For confocal microscopy, primary hepatocytes were adhered onto 3T3 NIH fibroblast-coated glass coverslips and BMDCs were adhered onto poly-L-lysine-coated glass coverslips. At the end of the experimental procedures, cells were fixed in 4% paraformaldehyde solution, permeabilized in 3% BSA 0.1% saponin PBS and stained with primary Abs specific for MR

(AbD Serotec), EEA1 (BioConcept), LAMP-1 (Abcam), TAP1 (Santa Cruz Biotechnology), H-2Kb (BioLegend) or H-2Kb/SIINFEKL (eBioscience) followed by fluorescently labeled secondary Abs (Life Technologies) and fluorochrome-conjugated phalloidin (Life Technologies). Samples were mounted using ProLong Gold antifade reagent with DAPI (Life Technologies), imaged with a LSM 700 inverted confocal microscope (Zeiss) and data were analyzed with ImageJ software. For flow cytometry, at the end of the experimental procedures, hepatocytes or BMDCs were washed in 2% FBS PBS and acquired on an LSR II cytometer (BD Biosciences) and data analyzed with FlowJo software (Tree Star).

3.6.6 Hepatocyte adoptive transfer for biodistribution and tolerance studies

For hepatocyte biodistribution studies, wt C57BL/6 mice were administered i.v. by tail vein injection with 10^6 CFSE-labeled C57BL/6 hepatocytes in 100 μL DMEM. Mice were euthanized after 24 hr, 14 d and 1 month to collect liver, spleen, lungs and kidneys for confocal microscopy. For tolerance studies, on day 0 recipient wt C57BL/6 mice were administered i.v. by tail vein injection with either 10^6 pGal-OVA-treated or untreated hepatocytes in 100 μL DMEM or with 100 μL DMEM (vehicle) followed by i.v. injection of $3*10^5$ CFSE-labeled CD45.1$^+$ OT-I cells 6 hr later. For PD-L1 blockade, 100 μg/ml αPD-L1 blocking Ab (BioxCell, clone 10F.9G2) or rat IgG isotype control Ab (Abcam) were added to the hepatocytes for 30 min prior to washing and administration into mice. On day 15, recipient mice were either vaccinated i.d. with 10 μg endo-grade chicken OVA (Hyglos) + 50 ng ultra-pure LPS (InvivoGen) in 50 μL saline divided into the two frontal footpads or left untreated. On day 19, recipient mice were euthanized to collect spleen and brachial and axillary LNs (dLNs). Spleen and dLN single-cell suspensions were either cultured for 6 hr at 37 °C in the presence of 1 μg/mL SIINFEKL (GenScript) with the addition of 5 μg/mL BFA for the last 3 hr of culture for antigen-specific restimulation and intracellular cytokine staining or directly stained for flow cytometry. For flow cytometry analysis, cells were first stained using Live/Dead fixable cell viability reagents (Life Technologies) followed by surface staining with Abs specific for the markers CD45.1 (eBioscience), CD3ε (eBioscience), CD8α (Life Technologies), FasL (BioLegend), TRAIL (BioLegend), KLRG-1 (BioLegend), CD127 (eBioscience) and PD-1 (BioLegend). Staining with biotinylated Annexin V and fluorescently labeled streptavidin (Life Technologies) was performed according to the manufacturer's instructions. For intracellular cytokine staining, cells were fixed in 2% paraformaldehyde solution, permeabilized in 0.5% saponin 2% FBS PBS solution, and incubated with Abs specific for IFN-γ (BioLegend) and IL-2 (eBioscience). Samples were acquired on an LSR II cytometer (BD Biosciences) and data analyzed with FlowJo software (Tree Star). dLN cells

were restimulated for 4 days in the presence of 1 μg/mL SIINFEKL for the measurement of IFN-γ by ELISA using the specific Ready-SET-go! ELISA kit from eBioscience.

3.6.7 Confocal microscopy of tissue sections

Liver, spleen, lungs and kidneys were harvested after perfusion of euthanized animals with HBSS (Life Technologies). Organs were fixed in 4% paraformaldehyde solution and frozen in OCT (Sakura). 10 μm-thick sections were sliced and stained with primary Abs specific for PD-L1 or PD-L2 (eBioscience) and fluorescently labeled secondary Abs (Life Technologies) or left unstained. Samples were mounted using ProLong Gold antifade reagent with DAPI (Life Technologies), imaged with a LSM 700 inverted confocal microscope (Zeiss) and analyzed with ImageJ software.

3.6.8 Statistics

Statistically significant differences between experimental groups were determined by one-way ANOVA followed by Bonferroni *post-hoc* test correction or by unpaired t test. $^{*}P < 0.05$, $^{**}P < 0.01$, $^{***}P < 0.001$, $^{****}P < 0.0001$ and n.s. = not significant. Statistical analyses were performed using Prism software (v6.0f, GraphPad Software).

3.7 References

1. Klein, L., Kyewski, B., Allen, P. M. & Hogquist, K. A. Positive and negative selection of the T cell repertoire: what thymocytes see (and don't see). *Nat. Rev. Immunol*. **14,** 377–391 (2014).
2. Redmond, W. L. & Sherman, L. A. Peripheral tolerance of CD8 T lymphocytes. *Immunity*. **22,** 275–284 (2005).
3. Kyewski, B. & Derbinski, J. Self-representation in the thymus: an extended view. *Nat. Rev. Immunol*. **4,** 688–698 (2004).
4. Crispe, I. N. *et al.* Cellular and molecular mechanisms of liver tolerance. *Immunol. Rev*. **213,** 101–18 (2006).
5. Crispe, I. N. Hepatic T cells and liver tolerance. *Nat. Rev. Immunol*. **3,** 51–62 (2003).
6. Diehl, L. *et al*. Tolerogenic maturation of liver sinusoidal endothelial cells promotes B7-homolog 1-dependent CD8+ T cell tolerance. *Hepatology*. **47,** 296–305 (2007).
7. Schildberg, F. A., Hegenbarth, S. I., Schumak, B., Limmer, A. & Knolle, P. A. Liver sinusoidal endothelial cells veto CD8 T cell activation by antigen-presenting dendritic cells. *Eur. J. Immunol*. **38,** 957–967 (2008).

8. Ebrahimkhani, M. R., Mohar, I. & Crispe, I. N. Cross-presentation of antigen by diverse subsets of murine liver cells. *Hepatology*. **54,** 1379–1387 (2011).
9. Limmer, A. *et al*. Cross-presentation of oral antigens by liver sinusoidal endothelial cells leads to CD8 T cell tolerance. *Eur. J. Immunol*. **35,** 2970–2981 (2005).
10. Schurich, A. et al. Distinct kinetics and dynamics of cross-presentation in liver sinusoidal endothelial cells compared to dendritic cells. *Hepatology*. **50,** 909–919 (2009).
11. Böttcher, J. P. *et al*. Liver-primed memory T cells generated under noninflammatory conditions provide anti-infectious immunity. *Cell Rep*. **3,** 779–795 (2013).
12. Holz, L. E., Warren, A., Le Couteur, D. G., Bowen, D. G. & Bertolino, P. CD8+ T cell tolerance following antigen recognition on hepatocytes. *J. Autoimmun*. **34,** 15–22 (2010).
13. Thomson, A. W. & Knolle, P. A. Antigen-presenting cell function in the tolerogenic liver environment. *Nat. Rev. Immunol*. **10,** 753–766 (2010).
14. Bertolino, P. *et al.* Death by neglect as a deletional mechanism of peripheral tolerance. *Int. Immunol.* **8,** 1225–38 (1999).
15. Bertolino, P., Bowen, D. G., McCaughan, G. W. & Fazekas de St Groth, B. Antigen-specific primary activation of CD8+ T cells within the liver. *J. Immunol*. **9,** 5430–8 (2001).
16. Bowen, D. G. *et al*. The site of primary T cell activation is a determinant of the balance between intrahepatic tolerance and immunity. *J. Clin. Invest.* **114,** 701–712 (2004).
17. Brown, B. D. *et al*. A microRNA-regulated lentiviral vector mediates stable correction of hemophilia B mice. *Blood*. **13,** 4144–52 (2007).
18. Morimoto, J., Tan, X., Teague, R. M., Ohlen, C. & Greenberg, P. D. Induction of tolerance in CD8+ T cells to a transgenic autoantigen expressed in the liver does not require cross-presentation. *J. Immunol*. **178,** 6849–6860 (2007).
19. Benseler, V. *et al*. Hepatocyte entry leads to degradation of autoreactive CD8 T cells. *Proc. Natl. Acad. Sci. U. S. A*. **40,** 16735–40 (2011).
20. Tay, S. S. *et al*. Antigen expression level threshold tunes the fate of CD8 T cells during primary hepatic immune responses. *Proc. Natl. Acad. Sci. U. S. A.* **111,** E2540–E2549 (2014).
21. Tay, S. S. *et al*. Intrahepatic activation of naive CD4+ T cells by liver-resident phagocytic cells. *J. Immunol.* **193,** 2087–2095 (2014).

22. Annoni, A. *et al*. In vivo delivery of a microRNA-regulated transgene induces antigen-specific regulatory T cells and promotes immunologic tolerance. *Blood*. **25,** 5152–61 (2009).
23. Akbarpour, M. *et al.* Insulin B chain 9–23 gene transfer to hepatocytes protects from type 1 diabetes by inducing Ag-specific FoxP3. *Sci. Transl. Med.* **7,** 289–289ra81 (2015).
24. Dong, H. *et al*. B7-H1 determines accumulation and deletion of intrahepatic CD8(+) T lymphocytes. *Immunity*. **3,** 327–36 (2004).
25. Guermonprez, P. *et al*. ER–phagosome fusion defines an MHC class I cross-presentation compartment in dendritic cells. *Nature*. **425,** 397–402 (2003).
26. Houde, M. *et al*. Phagosomes are competent organelles for antigen cross-presentation. *Nature*. **425,** 402–406 (2003).
27. Burgdorf, S., Kautz, A., Böhnert, V., Knolle, P. A. & Kurts, C. Distinct pathways of antigen uptake and intracellular routing in CD4 and CD8 T cell activation. *Science*. **316,** 612–616 (2007).
28. Burgdorf, S., Schölz, C., Kautz, A., Tampé, R. & Kurts, C. Spatial and mechanistic separation of cross-presentation and endogenous antigen presentation. *Nat. Immunol*. **9,** 558–566 (2008).
29. Carambia, A. *et al*. TGF-β-dependent induction of CD4+CD25+Foxp3+ Tregs by liver sinusoidal endothelial cells. *J. Hepatol*. **61,** 594–599 (2014).
30. Rauen, J. *et al*. Enhanced cross-presentation and improved CD8+ T cell responses after mannosylation of synthetic long peptides in mice. *PLoS ONE*. **9,** e103755–9 (2014).
31. Freeman, G. J. *et al*. Engagement of the PD-1 immunoinhibitory receptor by a novel B7 family member leads to negative regulation of lymphocyte activation. *J. Exp. Med.* **7,** 1027–1034 (2000).
32. Ansari, M. J. I. *et al.* The Programmed Death-1 (PD-1) pathway regulates autoimmune diabetes in nonobese diabetic (NOD) mice. *J. Exp. Med*. **198,** 63–69 (2003).
33. Bennett, F. *et al*. Program Death-1 engagement upon TCR activation has distinct effects on costimulation and cytokine-driven proliferation: attenuation of ICOS, IL-4, and IL-21, but not CD28, IL-7, and IL-15 responses. *J. Immunol*. **170,** 711–718 (2003).
34. Sandner, S. E. *et al*. Role of the Programmed Death-1 pathway in regulation of alloimmune responses in vivo. *J. Immunol*. **174,** 3408–3415 (2005).

35. Fife, B. T. & Bluestone, J. A. Control of peripheral T-cell tolerance and autoimmunity via the CTLA-4 and PD-1 pathways. *Immunol. Rev*. **224,** 166–182 (2008).

36. Latchman, Y. *et al*. PD-L2 is a second ligand for PD-1 and inhibits T cell activation. *Nat. Immunol.* **3,** 261–268 (2001).

37. Yamazaki, T. *et al.* Expression of Programmed Death 1 ligands by murine T cells and APC. *J. Immunol*. **169,** 5538–5545 (2002).

38. Loke, P. & Allison, J. P. PD-L1 and PD-L2 are differentially regulated by Th1 and Th2 cells. *Proc. Natl. Acad. Sci. U. S. A*. **9,** 5336–5341 (2003).

39. Mühlbauer, M. *et al*. PD-L1 is induced in hepatocytes by viral infection and by interferon-α and -γ and mediates T cell apoptosis. *J. Hepatol*. **45,** 520–528 (2006).

40. Crispe, I. N. The liver as a lymphoid organ. *Annu. Rev. Immunol.* **27,** 147–163 (2009).

41. den Haan, J. M., Lehar, S. M. & Bevan, M. J. CD8(+) but not CD8(-) dendritic cells cross-prime cytotoxic T cells in vivo. *J. Exp. Med.* **12,** 1685–1696 (2000).

42. Lund, A. W. *et al.* VEGF-C promotes immune tolerance in B16 melanomas and cross-presentation of tumor antigen by lymph node lymphatics. *Cell Rep*. **1,** 191–199 (2012).

43. Hirosue, S. *et al*. Steady-state antigen scavenging, cross-presentation, and CD8+ T cell priming: a new role for lymphatic endothelial cells. *J. Immunol*. **192,** 5002–5011 (2014).

44. Getts, D. R. *et al.* Tolerance induced by apoptotic antigen-coupled leukocytes is induced by PD-L1+ and IL-10-producing splenic macrophages and maintained by T regulatory cells. *J. Immunol*. **187,** 2405–2417 (2011).

45. Crispe, I. N., Dao, T., Klugewitz, K., Mehal, W. Z. & Metz, D. P. The liver as a site of T-cell apoptosis: graveyard, or killing field? *Immunol. Rev.* **174,** 47–62 (2000).

46. Bertolino, P., Bowen, D. G. & Benseler, V. T cells in the liver: there is life beyond the graveyard. *Hepatology*. **6,** 1580–1582 (2007).

47. Nishimura, H., Nose, M., Hiai, H., Minato, N. & Honjo, T. Development of lupus-like autoimmune diseases by disruption of the PD-1 gene encoding an ITIM motif-carrying immunoreceptor. *Immunity*. **2,** 141–151 (1999).

48. Wang, J. *et al*. Establishment of NOD-Pdcd1-/- mice as an efficient animal model of type I diabetes. *Proc. Natl. Acad. Sci. U. S. A*. **33,** 11823–11828 (2005).

49. Barber, D. L. *et al*. Restoring function in exhausted CD8 T cells during chronic viral infection. *Nature*. **439,** 682–687 (2005).

50. Radziewicz, H. *et al*. Liver-infiltrating lymphocytes in chronic human hepatitis C virus infection display an exhausted phenotype with high levels of PD-1 and low levels of CD127 expression. *J. Virol.* **81,** 2545–2553 (2007).
51. Urbani, S. *et al*. PD-1 expression in acute hepatitis C virus (HCV) infection is associated with HCV-specific CD8 exhaustion. *J. Virol*. **80,** 11398–11403 (2006).
52. Boni, C. *et al*. Characterization of hepatitis B virus (HBV)-specific T-cell dysfunction in chronic HBV infection. *J. Virol*. **81,** 4215–4225 (2007).
53. Crispe, I. N. Immune tolerance in liver disease. *Hepatology*. **60,** 2109–2117 (2014).
54. Liu, W. *et al*. Sample preparation method for isolation of single-cell types from mouse liver for proteomic studies. *Proteomics*. **11,** 3556–3564 (2011).
55. Henson, S. M. & Akbar, A. N. KLRG1-more than a marker for T cell senescence. *Age*. 31, 285–291 (2009).
56. Guocai, L. *et al*. Dynamic analysis of CD127 expression on memory CD8 T cells from patients with chronic hepatitis B during telbivudine treatment. *Virol. J.* **7,** 207 (2010).

Chapter 4

Characterization of peripheral tissue-specific antigen expression in liver cell populations in wild-type and autoimmunity-prone mice

4.1 Abstract

Expression of tissue-specific antigens in the thymus allows negative selection of possible auto-reactive thymocytes before they reach peripheral organs as naïve T lymphocytes. Tissue-specific antigens have also been found expressed in $CD45^+$ and $CD45^-$ cells of the LNs contributing to the maintenance of a self tolerant TCR repertoire. Because of immunological similarities between LN stromal cells and hepatic non-hematopoietic cells, especially LSECs and hepatocytes, we asked whether promiscuous gene expression of otherwise tissue-restricted antigens could also occur in hepatic cells as additional mechanism of peripheral tolerogenesis. We analyzed the expression of *AIRE* and *Deaf1*, the two best known transcriptional regulators of promiscuous gene expression, in isolated hepatocytes and LSECs from adult C57BL/6 mice and found that *Deaf1*, but not *AIRE*, is expressed in hepatocytes both at the RNA and at the protein level. LSECs resulted negative for both *AIRE* and *Deaf1*. Some of the genes coding for peripheral tissue-specific antigens associated to Deaf1-dependent regulation in LNs, such as *Ins1*, *Ins2*, *Afp* and *Tyr*, were also found expressed at the RNA level in hepatocytes. When we compared hepatocytes from 6 week-old diabetes-prone NOD female mice to age-matched diabetes-resistant NOD male mice, we could observe a trend for reduced relative expression of *Deaf1* and *Ins1* and, most importantly, significantly reduced expression of *Ins2*. We describe here for the first time that hepatocytes, which are non-hematopoietic cells of a non-lymphoid organ, are capable of promiscuous gene expression. Our data also suggest a possible alteration of promiscuous gene expression in the hepatocytes of diabetes-prone NOD female mice as a possible factor contributing to autoimmunity.

4.2 Introduction

Until recently, promiscuous gene expression of PTAs was considered the hallmark of central tolerance. In fact, antigens normally expressed in a specific tissue or at a specific time in the organism are also expressed in mTECs and are presented on MHC complexes by both mTECs and DCs in the thymus (Fig. 1.4). Presentation of PTAs in the thymus allows to survey the specificity and affinity of the TCR of developing thymocytes and is crucial for the negative selection of those T cell precursors recognizing self peptide/MHC complexes with strong affinity [1-5].

The PTA library expressed in the thymus does not represent all the possible tissue-specific antigens of the organism. Moreover, since the discrimination between auto-reactive and allo-reactive T cells is based on the affinity of the TCR for its cognate peptide/MHC complex, T cell clones expressing a low-affinity TCR specific for a self peptide/MHC complex can still escape negative selection, complete their maturation into naïve T cells and reach the periphery. Once in the periphery, peripheral tolerance mechanisms are responsible for avoiding their activation [6].

Recently, promiscuous gene expression has been reported in LN $CD45^+$ hematopoietic cells and $CD45^-$ stromal cells, typically distinguished according to their staining for podoplanin (gp38) and the endothelial cell marker CD31 into double-negative cells (DNs, $CD45^-gp38^-CD31^-$), lymphatic endothelial cells (LECs, $CD45^-gp38^+CD31^+$), fibroblastic reticular cells (FRCs, $CD45^-gp38^+CD31^-$) and blood endothelial cells (BECs, $CD45^-gp38^-CD31^+$) (Fig. 4.1a). Different subsets of PTAs have been found expressed in $CD45^+$ cells and in stromal LN cells (Fig. 4.1b). Presentation on MHC molecules has been characterized for some of these antigens and has been associated with induction of deletional tolerance of antigen-specific $CD8^+$ T lymphocytes [7-12].

An extensive characterization of the molecular mechanisms regulating promiscuous gene expression in LN cells is still missing. Preliminary reports seem to suggest that the transcription factor AIRE is only expressed in DNs and in rare extra-thymic AIRE-expressing LN stromal cells of unknown lineage. On the other hand, the transcription factor Deaf1, recently associated with promiscuous gene expression and regulation of immunity and autoimmunity [13], could be instrumental in the regulation of promiscuous gene expression in the periphery as it is broadly expressed in all of the four LN stromal cell populations and in LN $CD45^+$ cells (Fig. 4.1b) [9,12].

a

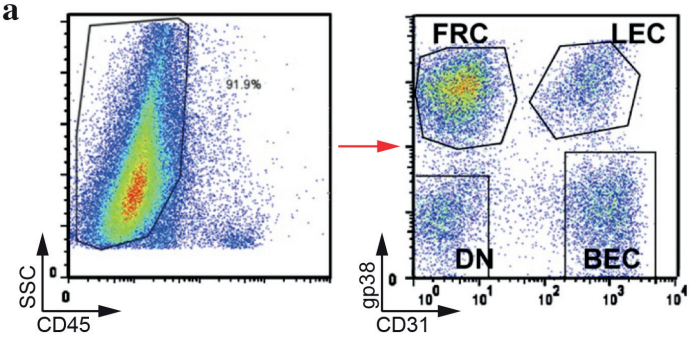

b

	Ins2	*Gad67*	*Ambp*	*Ppy*	*Tyr*	*A33*	*Mart1*	*AIRE*	*Deaf1*
DNs	+	+	+++	+				+	+
FRCs	+	+	+					-	+
LECs				++	+++	++		-	+
BECs								-	+
CD45⁺		++++						+	+

Figure 4.1 Promiscuous gene expression in LN cell populations. (a) Flow cytometric separation of LN CD45$^-$ stromal cells according to staining of gp38 (podoplanin) and CD31. (b) Gene expression analysis of PTA-coding genes (the main murine insulin-coding gene *Ins2*, the neuro-specific *Gad67*, the hepatocyte-specific α-1 microglobulin/bikunin precursor or *Ambp*, pancreatic polypeptide or *Ppy*, the melanocyte-specific genes tyrosinase or *Tyr* and *Mart1*, and the colon epithelium-expressed *A33*) and promiscuous gene expression transcriptional regulators (*AIRE* and *Deaf1*) in CD45$^+$ and CD45$^-$ stromal cells of the LNs (adapted from Lee, J. W. *et al*., *Nat. Immunol*., 2007; Gardner, J. M. *et al*., *Science*, 2008; Yip, L. et al., *Nat. Immunol*., 2009; Cohen, J. N. *et al*., *J. Exp. Med*., 2010; Fletcher, A. L. *et al*., *J. Exp. Med*., 2010; Yip, L. *et al*., *J. Mol. Cell Biol*., 2013).

Similarly to LN stromal cells, non-hematopoietic CD45$^-$ cells composing the liver, especially LSECs and hepatocytes, have also been reported to have antigen-presenting functions and to participate in the establishment of CD4$^+$ and CD8$^+$ T cell peripheral tolerance [14-16]. Moreover, LSECs present several phenotypic and functional similarities to LN LECs. For example, both cell types are in direct contact with circulating fluids (blood and lymph, respectively) and therefore with T cells and they both show efficient extracellular-antigen scavenging and MHC presentation capacity. Antigen presentation by both LSECs and LECs has been associated to the induction of antigen-specific tolerance rather than immunity because of lack of co-stimulation [14-18]. Due to the peculiar fenestrated endothelium of the liver (Fig. 3.1a,b), hepatocytes are also in direct physical contact with circulating lymphocytes and show antigen scavenging ability, leading to cross-presentation of extracellular antigens on MHC-I molecules without co-stimulation and tolerance of antigen-specific CD8$^+$ T lymphocytes (Chapter 3 and Damo M. *et al*., manuscript in preparation) [19].

Because of these characteristics, we asked whether also liver cells could utilize promiscuous gene expression and presentation of PTAs as mechanisms of peripheral

tolerance, similarly to LN stromal cells. We therefore purified hepatocytes and LSECs from adult C57BL/6 livers in order to extract total mRNA and quantify the expression of *AIRE*, *Deaf1* and some of the best characterized PTA-coding genes. We found that while transcription of *AIRE* could not be detected in either primary hepatocytes or LSECs, expression of *Deaf1* could be measured in hepatocytes. Deaf1 expression at the protein level was confirmed by confocal microscopy in hepatocytes. Expression of some PTA-coding genes hypothesized to be dependent on Deaf1 transcriptional regulation in LNs [12], specifically *Ins1* (insulin 1), *Ins2* (insulin 2), the fetal liver-specific version of albumin *Afp* (α-Fetoprotein), the melanocyte-specific *Tyr* (tyrosinase) and the neuronal and pancreatic β-cell-specific *GAD1* or *GAD67* (glutamic acid decarboxylase 1), was also confirmed in hepatocytes at the mRNA level. As a preliminary validation of the role of hepatocyte-dependent promiscuous gene expression in the protection from autoimmunity, we analyzed the gene expression profile of *Deaf1* variants (both the variant coding for the functional native or wild-type Deaf1 and the variant coding for an inhibitory dominant-negative form of Deaf1), *Ins1*, *Ins2* and *GAD67* in hepatocytes harvested from 6 week-old female nonobese diabetic (NOD) mice and compared it to that of age-matched male NOD mice. A trend for reduced relative expression levels of native *Deaf1, Ins1* and *GAD67*, significantly reduced expression of *Ins2* and significantly increased expression of dominant-negative *Deaf1* could be observed in diabetes-prone NOD females as compared to diabetes-resistant NOD males.

4.3 Results

4.3.1 Deaf1 *and* Deaf1*-dependent PTA-coding genes are expressed in murine hepatocytes*

Hepatocytes and LSECs are the two most abundant cellular components of the liver and the major determinants of its immune tolerogenic properties (Fig. 4.2a) [21]. In order to investigate whether hepatocytes and LSECs are capable of promiscuous gene expression, we set up a cell purification protocol to harvest either hepatocytes or LSECs from adult C57BL/6 liver cell suspensions by serial centrifugation or fluorescence-activated cell sorting (FACS), respectively. Hepatocytes are the biggest cells in the liver, with an average cell diameter of ≈ 15 μm and could therefore be isolated by low-speed serial centrifugations, as previously reported by other groups [15,22]. Flow cytometric analysis of the cells after the isolation procedure indicated the presence of an homogeneous cell population, confirmed as *bona-fide* hepatocytes due to their lack of CD45 expression together with positivity for H-2Kb and the non-conventional MHC-I molecule CD1d [32] (Fig. 4.2b). Purification of LSECs was instead performed by FACS of non-parenchymal cells (NPCs) stained for CD45, CD31 and CD146.

LSECs were identified as the $CD45^{-}CD31^{+}CD146^{+}$ fraction of hepatic NPCs, as previously reported [15] (Fig. 4.2c).

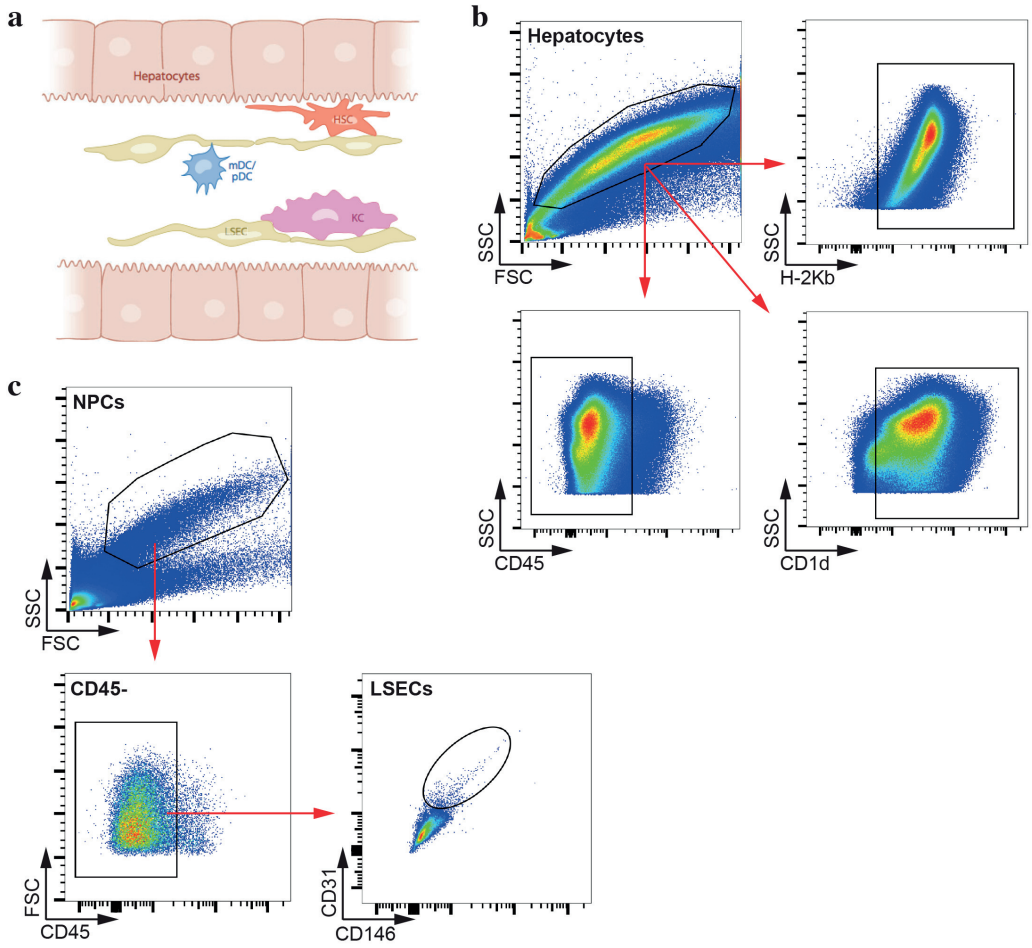

Figure 4.2 Isolation of hepatocytes and LSECs from total murine liver cell suspensions. (a) Schematic representation of liver cells and their distribution in the liver parenchyma (adapted from Crispe, I. N., *Annu. Rev. Immunol.*, 2009). (b) Flow cytometric analysis of murine hepatocytes after centrifugation-based separation. Negativity for CD45 together with positivity for H-2Kb and the non-conventional MHC-I molecule CD1d confirm the identity of *bona-fide* hepatocytes. (c) Flow cytometric sorting strategy of LSECs ($CD45^{-}CD31^{+}CD146^{+}$) from liver NPCs. Data in (b,c) are representative of 2 independent experiments ($n = 8$).

We next asked whether *AIRE* and *Deaf1*, the two master regulators of promiscuous gene expression, could be detected in isolated hepatocytes and LSECs. Quantitative PCR (qPCR) analysis showed that while *AIRE* expression is not detectable in either hepatocytes or LSECs, *Deaf1* is expressed in hepatocytes but not in LSECs (Fig. 4.3a). Total thymic tissue was used as positive control and, interestingly, we could measure higher relative expression of *Deaf1* in hepatocytes as compared to thymic cells, with 3.5E-03 and 0.5E-03 gene expression fold change over *β-Actin*, respectively (Fig. 4.3b). Expression of *Deaf1* was

confirmed at the protein level in both the cytoplasm and nucleus of purified hepatocytes by confocal microscopy (Fig. 4.3c).

Detection of Deaf1 in hepatocytes prompted us to investigate whether PTAs could also be expressed in the same cell type. We therefore analyzed by qPCR the expression of some of the most characterized PTA-coding genes, whose expression has been linked to Deaf1-dependent regulation in previous reports [12]. In particular, we could detect higher relative expression of the two murine insulin genes, *Ins1* (0.6E-04 fold change) and *Ins2* (0.41E-04 fold change), as well as of *Tyr* (0.12E-04 fold change), of the fetal version of albumin *Afp* (0.75E-04 fold change) and of the neuronal and β-cell-expressed *GAD67* (0.68E-04) in hepatocytes as compared to thymic cells (0.0015E-04, 0.13E-04, 0.0026E-04, 0.21E-04 and 0.4E-05 fold change, respectively) (Fig. 4.3a,d). Expression of the PTA genes analyzed in our study could not be detected in LSECs (Fig. 4.3a).

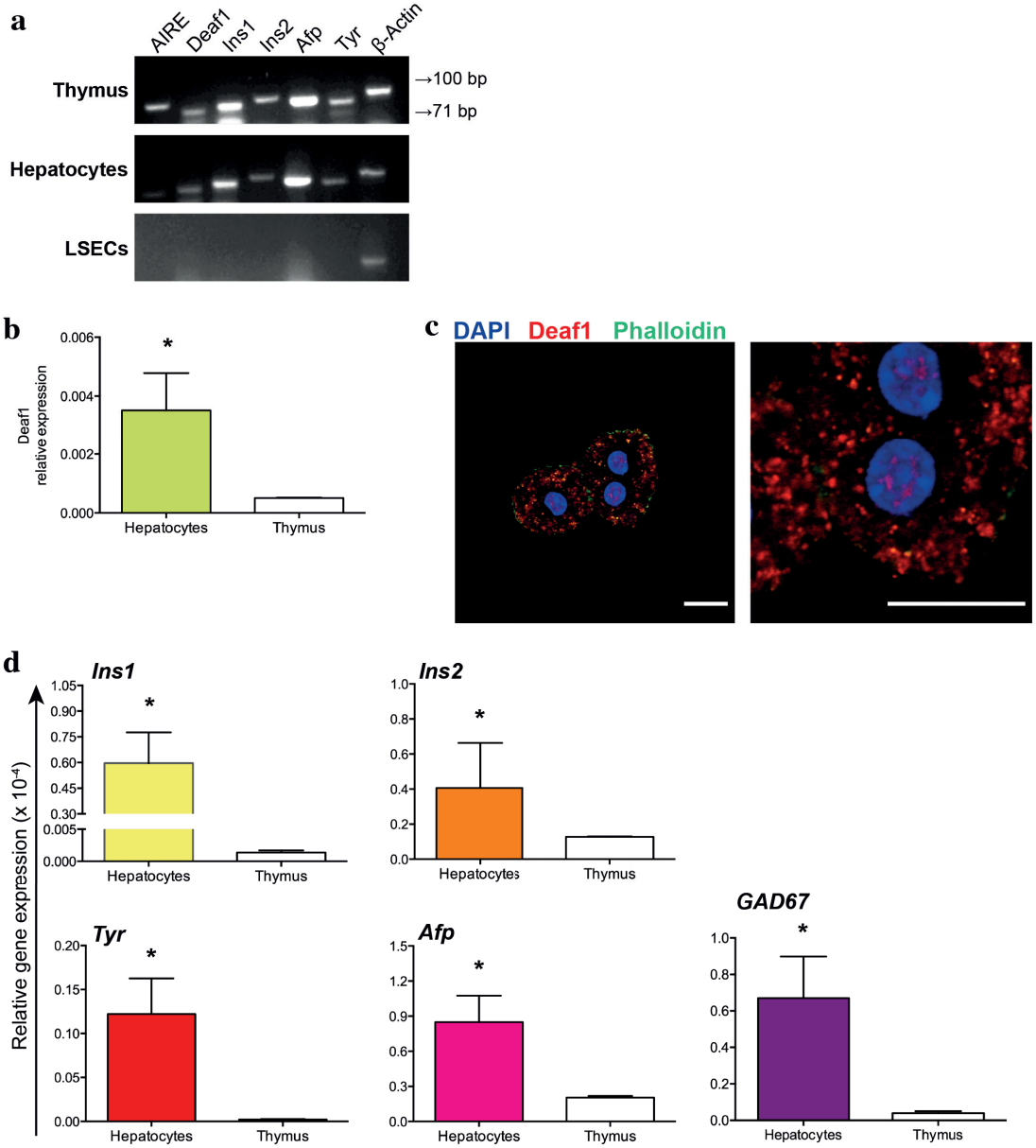

Figure 4.3 Characterization of promiscuous gene expression in adult C57BL/6 hepatocytes and LSECs. (a) Electrophoretic separation of the amplicons obtained by qPCR of the indicated genes from total thymus, hepatocytes or LSECs of adult C57BL/6 mice. Expected amplicon length in base pairs (bp): *AIRE* = 89 bp; *Deaf1* = 71 bp; *Ins1* = 80 bp; *Ins2* = 99 bp; *Afp* = 96 bp; *Tyr* = 88 bp; *β-Actin* = 86 bp. (b) Gene expression analysis by qPCR of *Deaf1* in isolated hepatocytes and thymic tissue from adult C57BL/6. Values indicate gene expression fold change relative to *β-Actin*. (c) Confocal microscopy of C57BL/6 hepatocytes stained for Deaf1 and with DAPI and phalloidin. Scale bar = 10 μm. (d) Gene expression analysis by qPCR of *Ins1*, *Ins2*, *Tyr*, *Afp* and *GAD67* in isolated hepatocytes and thymic tissue from adult C57BL/6. Values indicate gene expression fold change relative to *β-Actin*. $^{*}P < 0.05$ (unpaired t test). Data are representative of 2 independent experiments ($n = 8$; mean and s.e.m. in (b,d)).

Our findings indicate that hepatocytes, but not LSECs, significantly express both at the RNA and at the protein level the transcription factor Deaf1. Deaf1 is detected not only in the cytoplasm but also in the nuclei of hepatocytes, suggesting active transcriptional regulation. *AIRE* expression could not be measured in either hepatocytes or LSECs. Nonetheless, Deaf1 has been indicated as AIRE-independent transcriptional regulator of PTA-coding genes such as *Ins1*, *Ins2*, *Tyr*, *Afp* and *GAD67*, which were all found expressed at the RNA level in hepatocytes but not in LSECs.

4.3.2 Expression analysis of Deaf1 *and PTA genes in pre-diabetic female NOD mice versus male NOD mice*

Dysregulation of promiscuous gene expression has been indicated as one of the genetic susceptibility factors of autoimmune diseases such as type 1 diabetes (T1D) [23]. In particular, reduced expression and functionality of *Deaf1,* also associated with up-regulation of a dominant-negative form of *Deaf1* inhibiting the transcriptional regulatory activity of native *Deaf1*, and decreased expression of islet-specific PTAs have been described in the pancreatic LN of NOD mice [9,12]. We hypothesized that defective PTA expression could also occur in hepatocytes, contributing to the development of T1D.

To test our hypothesis, we analyzed the expression of native and dominant-negative *Deaf1* variants, *Ins1*, *Ins2* and *GAD67* in hepatocytes isolated from the liver of pre-diabetic (6 weeks of age) female NOD mice and compared it to that of hepatocytes from age-matched male NOD mice. It is known, in fact, that the incidence of diabetes in NOD mice is significantly different between the two sexes, with 70% of females developing diabetes at around 12-13 weeks of age versus only 20% of males. Overt diabetes, indicated by fasting hyperglycemia, is preceded by leukocyte infiltration of pancreatic islets (insulitis) appearing at around 5-7 weeks of age in female NOD mice and only later in life in males [24]. As

appearance of insulitis marks the initial phase of immune aggression against pancreatic islets, we decided to investigate whether any difference in promiscuous gene expression could be detected in NOD hepatocytes from diabetes-prone females and diabetes-resistant males at the age of insulitis onset.

qPCR analysis showed a non-significant trend for reduced native *Deaf1* relative expression in pre-diabetic female NOD mice as compared to male mice, as indicated by 7.8E-03 and 1.05E-02 gene expression fold change over *β-Actin*, respectively (Fig. 4.4a, left). Interestingly, the gene expression level of the inhibitory dominant-negative *Deaf1* splice variant was significantly higher in pre-diabetic female NOD hepatocytes as compared to male NOD hepatocytes, with 1.05E-03 and 4.03E-04 fold change, respectively (Fig. 4.4a, right). Most importantly, non statistically significant reduction of *Ins1* and *GAD67* relative expression (0.75E-03 and 1.31E-04 fold change, respectively) together with a statistically significant 171-fold reduction of *Ins2* relative expression (0.0033E-03 fold change) could also be measured in females as compared to males (0.56E-03, 6.25E-04 and 1.87 fold change, respectively) (Fig. 4.4b).

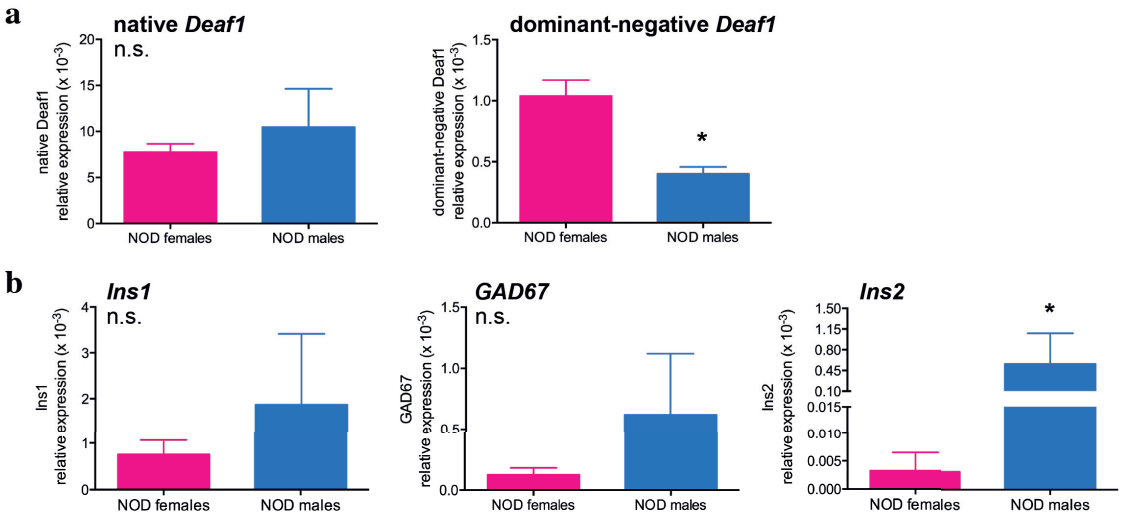

Figure 4.4 Comparison of *Deaf1*, *Ins1*, *GAD67* and *Ins2* relative expression in hepatocytes from pre-diabetic female and male NOD mice. (a) Gene expression analysis by qPCR of native and inhibitory dominant-negative *Deaf1* variants in hepatocytes isolated from 6 week-old female and male NOD mice. Values indicate gene expression fold change relative to *β-Actin*. (b) Gene expression analysis by qPCR of *Ins1*, *GAD67* and *Ins2* in hepatocytes isolated from 6 week-old female and male NOD mice. Values indicate gene expression fold change relative to *β-Actin*. $^{*}P < 0.05$ and n.s. = not significant (unpaired t test). Data are representative of 2 independent experiments (n = 10 per sex; mean and s.e.m.).

Our results suggest a non-significant reduction of native *Deaf1*, *Ins1* and *GAD67* relative expression but show significant reduction of *Ins2* and significant increase of

dominant-negative *Deaf1* relative expression in the hepatocytes isolated from diabetes-prone NOD female mice as compared to diabetes-resistant NOD males already at the pre-diabetic age of 6 weeks.

4.4 Discussion

In this project we have shown preliminary data indicating that hepatocytes express *Deaf1*, a gene coding for a transcription factor recently involved in the regulation of promiscuous gene expression in peripheral lymphoid organs and in the pathogenesis of autoimmunity [9,12,13]. Some of the most characterized PTA-coding genes, in particular *Ins1*, *Ins2*, *Afp*, *Tyr* and *GAD67* genes, are also expressed in hepatocytes. Moreover, our data indicate a possible reduction of the expression levels of native *Deaf1* and *Ins1* and significant reduction of *Ins2* and significant increase of inhibitory *Deaf1* relative expression in the hepatocytes of T1D-prone NOD female mice as opposed to T1D-resistant NOD male mice.

Expression of PTAs has long been considered a unique feature of mTECs to allow the negative selection of potentially auto-reactive thymocytes during their development [1-5]. In recent years, expression of PTAs has been described also in both hematopoietic and stromal cell populations of the LNs and has been shown to play an important role in the maintenance of peripheral tolerance via clonal deletion of PTA-specific $CD8^+$ T lymphocytes [7-12]. In fact, in physiologic conditions, locally expressed antigens are continuously sampled from the extracellular space by immature tissue-resident DCs, which then migrate to regional LNs. In alternative, local extracellular antigens can also be directly drained through lymphatic or blood circulation to regional LNs, where hematopoietic resident APCs (such as DCs) and non-hematopoietic resident APCs (such as LECs) uptake the antigens and present them in the context of MHC class I and II to T lymphocytes [25]. Under non-inflammatory conditions, antigen presentation only provides a suboptimal milieu for antigen-specific T cells to activate and, as a consequence, lymphocytes either die by apoptosis (clonal deletion), acquire an anergic phenotype or develop into suppressive Treg cells [26]. In this scenario, the establishment of peripheral tolerance would be limited to those antigens expressed locally. Promiscuous gene expression has therefore the role to amplify the repertoire of self antigens presented to peripheral T cells in regional LNs, thus increasing the likelihood of auto-reactive T cell deletion [25].

Because of the immunological similarities between certain LN stromal cells, in particular LECs, with non-hematopoietic cells of the liver, in particular LSECs, we hypothesized that promiscuous gene expression could also be part of the tolerogenic mechanisms employed by hepatic cells. Our preliminary findings indicate that hepatocytes are

the only non-hematopoietic cells in the liver and, to our knowledge, the only parenchymal cells in a non-lymphoid organ so far shown to express regulators of promiscuous gene expression (*Deaf1*) and PTA-coding genes. The observation that the relative expression level of all the genes we analyzed is higher in hepatocytes than in thymic cells could be an artifact due to the use of total thymic tissue as opposed to isolated hepatocytes for gene expression analysis. Nonetheless, Deaf1 expression was confirmed both at the RNA and at the protein level in hepatocytes and, most importantly, Deaf1 could be detected in the nuclei of hepatocytes, suggesting transcriptional regulatory activity. Further studies are needed to confirm expression at the protein level also of *Ins1*, *Ins2*, *Afp*, *Tyr* and *GAD67* in hepatocytes and to analyze the expression of other transcriptional regulators and PTAs. Most importantly, we will investigate whether and how such PTAs are transcriptionally regulated by Deaf1, presented on the MHC-I and correlate to tolerance induction.

Autoimmunity results from failure of the immune system to protect self tissues from immune aggression [27]. For example, T1D is a chronic autoimmune disease resulting from aggression of pancreatic insulin-producing β cells by auto-reactive $CD4^+$ and $CD8^+$ T lymphocytes. Genetic susceptibility and exposure to environmental triggers are the major factors involved in T1D etiopathogenesis [28]. In particular, mutations in genes involved in the establishment of both central and peripheral tolerance have been associated with increased T1D susceptibility, as they would lead to defective immune tolerance towards β cell auto-antigens, such as insulin. For example, mutations in the gene coding for AIRE have been found in patients affected by APECED, which is a syndrome characterized by multiple autoimmune manifestations, including T1D [23].

The NOD mouse is a useful model to study the biology and genetics of autoimmunity, as NOD mice spontaneously develop several autoimmune manifestations, among which T1D is the most characterized. Despite relevant differences with human T1D, the NOD mouse model has been extensively used to understand the etiopathogenesis of autoimmune diabetes [24]. Confirming the involvement of altered PTA expression in the development of T1D, previous reports have shown that T cell precursors from the thymus of NOD mice are relatively resistant to negative selection [29] and show similar defects as compared to thymocytes purified from *AIRE*-deficient mice [30]. In addition, reduced insulin expression in the murine thymus has been associated with increased T cell reactivity against insulin in the periphery [31]. Moreover, *Deaf1* and genes coding for several islet-specific antigens, including *Ins1* and *Ins2*, are significantly downregulated in the pancreatic LN of NOD mice at the time of diabetes onset [9]. Interestingly, the expression of a dominant negative form of Deaf1, resulting from alternative splicing and inhibiting the transcriptional activity of

native Deaf1, has been shown in the pancreatic LN of NOD mice. A similar variant of Deaf1 has also been found highly expressed in the pancreatic LN of T1D patients [12].

We hypothesized that if promiscuous gene expression by hepatocytes is relevant in the maintenance of immune tolerance, alterations could be detected in an organism susceptible to autoimmunity, such as the female NOD mouse. When we compared pre-diabetic T1D-prone female NOD mice to age-matched T1D-resistant male NOD mice, we could in fact observe a trend for reduced relative expression of native *Deaf1*, *Ins1* and *GAD67,* significant reduction of *Ins2* and significant increase of dominant-negative *Deaf1* in females, suggesting a possible correlation with their autoimmunity-prone phenotype. Interestingly, we found that the relative expression of the main murine insulin-coding gene, *Ins2*, was significantly reduced by a 171 fold factor in NOD female hepatocytes as compared to NOD male hepatocytes, possibly suggesting that disruption of hepatocyte-dependent promiscuous gene expression could have a primary role in the pathogenesis of autoimmune diabetes. Nonetheless, more solid studies and age-related comparisons are needed to obtain conclusive evidence that altered promiscuous gene expression in hepatocytes has a role in the development of autoimmunity in these mice, especially considering the technical challenges of the NOD mouse model. In fact, diabetes incidence in NOD mice does not reach 100% and environmental variables dramatically affect the onset of autoimmunity [24].

In summary, we suggest that hepatocytes are instrumental in the maintenance of $CD8^+$ T cell peripheral tolerance in the organism by both antigen cross-presentation and direct PTA expression and MHC-I presentation.

Author contributions

M. Damo designed and performed research and analyzed data.

4.5 Materials and methods

4.5.1 Mice

8-10 week old female C57BL/6 mice were obtained from Harlan Laboratories (Gannat, France) and 6 week old female and male NOD/ShiLtJ mice were purchased from Charles River (Saint-Germain-Nuelles, France). Animals were housed in pathogen-free conditions at the animal facility of the Ecole Polytechnique Fédérale de Lausanne and all experiments were performed in accordance with Swiss law and with approval from the Cantonal Veterinary Office of Canton de Vaud, Switzerland.

4.5.2 Cell isolation, flow cytometry and confocal microscopy

Hepatocytes were isolated from the liver of C57BL/6 or NOD/ShiLtJ mice as previously described [15,22]. LSECs were isolated from the liver of C57BL/6 by FACS of liver NPC suspensions by modification of the purification procedure published by Ebraimkhani M. R. *et al*. [15] Briefly, mice were euthanized and livers perfused with 0.5 mg/ml Collagenase D (Sigma-Aldrich) HBSS solution. Livers were then homogenized through a 100 μm cell strainer followed by filtration through a 70 μm cell strainer. Liver cell suspensions were centrifuged for 5 min at 50 *g* at 4°C to collect hepatocyte pellets. For LSECs isolation, the supernatant, containing NPCs, was cleared from hepatocytes by centrifugation at 50 *g* for 5 min repeated for 3 times. The NPC-containing supernatant was spun down for 10 min at 800 *g* at 4°C, stained with Abs specific for CD45 (eBioscience), CD31 (BioLegend) and CD146 (BioLegend) in 2% FBS PBS solution and sorted with a FACSAria cell sorter (BD Biosciences). For flow cytometric analysis, LSECs and hepatocytes stained with Abs specific for CD45 (eBioscience), CD1d (BioLegend) and H-2Kb (BioLegend) were acquired on an LSR II cytometer (BD Biosciences) and data analyzed with FlowJo software (Tree Star). For confocal microscopy, primary hepatocytes were adhered onto 3T3 NIH fibroblast-coated glass coverslips, fixed in 4% paraformaldehyde solution, permeabilized in 3% BSA 0.1% saponin PBS and stained with a primary Ab specific for Deaf1 (Aviva Systems Biology), followed by a fluorescently labeled secondary Ab (Life Technologies) and fluorochrome-conjugated phalloidin (Life Technologies). Samples were mounted using ProLong Gold antifade reagent with DAPI (Life Technologies), imaged with a LSM 700 inverted confocal microscope (Zeiss) and data were analyzed with ImageJ software.

4.5.3 RNA extraction, RT-PCR and gene expression analysis by qPCR

Total RNA was extracted from isolated hepatocytes and LSECs and biopsies of thymic tissue using the RNeasy micro kit isolation protocol (Qiagen) according to manufacturer's instructions. cDNA was obtained by reverse transcription PCR (RT-PCR) of total RNA performed using the SuperScript III First Strand Synthesis SuperMix (Life Technologies) following manufacturer's instructions. Gene expression analysis was performed by cDNA qPCR using TaqMan gene expression assays specific for *AIRE* (Mm00477461_m1), wild-type or native *Deaf1* (Mm00516805_m1), dominant-negative *Deaf1* (custom-made, lot. 1467978) [9], *Ins1* (Mm01950294_s1), *Ins2* (Mm00731595_gH), *Afp* (Mm00431715_m1), *Tyr* (Mm00453201_m1), *GAD67* (Mm04207432_g1) and *β-Actin* (Mm01268569_m1) (Life Technolgies) in a LightCycler 96 System (Roche). Relative gene expression was quantified using the formula (gene expression fold change) = $2^{(\text{Cq } \textit{Actin} - \text{Cq Gene of interest})}$ with *β-Actin* as reference gene.

4.5.4 Statistics

Statistically significant differences between experimental groups were determined by unpaired t test. * $P < 0.05$ and n.s. = not significant. Statistical analyses were performed using Prism software (v6.0f, GraphPad Software).

4.6 References

1. Smith, K. M., Olson, D. C., Hirose, R. & Hanahan, D. Pancreatic gene expression in rare cells of thymic medulla: evidence for functional contribution to T cell tolerance. *Int. Immunol*. **9,** 1355–1365 (1997).
2. Derbinski, J., Schulte, A., Kyewski, B. & Klein, L. Promiscuous gene expression in medullary thymic epithelial cells mirrors the peripheral self. *Nat. Immunol*. **2,** 1032–1039 (2001).
3. Anderson, M. S. *et al*. Projection of an immunological self shadow within the thymus by the aire protein. *Science*. **298,** 1395–1401 (2002).
4. Gallegos, A. M. & Bevan, M. J. Central tolerance to tissue-specific antigens mediated by direct and indirect antigen presentation. *J. Exp. Med*. **200,** 1039–1049 (2004).
5. Avichezer, D. *et al*. An immunologically privileged retinal antigen elicits tolerance: major role for central selection mechanisms. *J. Exp. Med*. **198,** 1665–1676 (2003).
6. Kyewski, B. & Derbinski, J. Self-representation in the thymus: an extended view. *Nat. Rev. Immunol*. **4,** 688–698 (2004).
7. Lee, J.W. *et al*. Peripheral antigen display by lymph node stroma promotes T cell tolerance to intestinal self. *Nat. Immunol*. **8,** 181–190 (2006).
8. Gardner, J. M. *et al*. Deletional tolerance mediated extrathymic Aire-expressing cells. *Science*. **321,** 843–847 (2008).
9. Yip, L. *et al*. Deaf1 isoforms control the expression of genes encoding peripheral tissue antigens in the pancreatic lymph nodes during type 1 diabetes. *Nat. Immunol.* **10,** 1026–1033 (2009).
10. Cohen, J. N. *et al.* Lymph node-resident lymphatic endothelial cells mediate peripheral tolerance via Aire-independent direct antigen presentation. *J. Exp. Med*. **207,** 681–688 (2010).
11. Fletcher, A. L. *et al*. Lymph node fibroblastic reticular cells directly present peripheral tissue antigen under steady-state and inflammatory conditions. *J. Exp. Med*. **207,** 689–697 (2010).

12. Yip, L., Creusot, R. J., Pager, C. T., Sarnow, P. & Fathman, C. G. Reduced DEAF1 function during type 1 diabetes inhibits translation in lymph node stromal cells by suppressing Eif4g3. *J. Mol. Cell Biol*. **5,** 99–110 (2013).
13. Reed, D. E., Huang, X. M., Wohlschlegel, J. A., Levine, M. S. & Senger, K. DEAF-1 regulates immunity gene expression in Drosophila. *Proc. Natl. Acad. Sci. U. S. A.* **105,** 8351–8356 (2008).
14. Diehl, L. *et al*. Tolerogenic maturation of liver sinusoidal endothelial cells promotes B7-homolog 1-dependent CD8+ T cell tolerance. *Hepatology.* **47,** 296–305 (2007).
15. Ebrahimkhani, M. R., Mohar, I. & Crispe, I. N. Cross-presentation of antigen by diverse subsets of murine liver cells. *Hepatology.* **54,** 1379–1387 (2011).
16. Böttcher, J. P. *et al.* Liver-primed memory T cells generated under noninflammatory conditions provide anti-infectious immunity. *Cell Rep*. **3,** 779–795 (2013).
17. Lund, A. W. *et al.* VEGF-C promotes immune tolerance in B16 melanomas and cross-presentation of tumor antigen by lymph node lymphatics. *Cell Rep*. **1,** 191–199 (2012).
18. Hirosue, S. *et al.* Steady-state antigen scavenging, cross-presentation, and CD8+ T cell priming: a new role for lymphatic endothelial cells. *J. Immunol*. **192,** 5002–5011 (2014).
19. Holz, L. E., Warren, A., Le Couteur, D. G., Bowen, D. G. & Bertolino, P. CD8+ T cell tolerance following antigen recognition on hepatocytes. *J. Autoimmun*. **34,** 15–22 (2010).
20. Dubrot, J. *et al*. Lymph node stromal cells acquire peptide-MHCII complexes from dendritic cells and induce antigen-specific CD4+ T cell tolerance. *J. Exp. Med*. **211,** 1153–1166 (2014).
21. Crispe, I. N. Liver antigen-presenting cells. *J. Hepatol*. **54,** 357–365 (2011).
22. Liu, W. *et al.* Sample preparation method for isolation of single-cell types from mouse liver for proteomic studies. *Proteomics.* **11,** 3556–3564 (2011).
23. Pitkänen, J. & Peterson, P. Autoimmune regulator: from loss of function to autoimmunity. *Genes Immun*. **4,** 12–21 (2003).
24. Atkinson, M. A. & Leiter, E. H. The NOD mouse model of type 1 diabetes: As good as it gets? *Nat. Med*. **5,** 601–604 (1999).
25. Zehn, D. & Bevan, M. J. More promiscuity resulting in more tolerance. *Nat. Immunol.* **8,** 120–122 (2007).
26. Kapsenberg, M. L. Dendritic-cell control of pathogen-driven T-cell polarization. *Nat. Rev. Immunol*. **3,** 984–993 (2003).

27. Cho, J. H. & Feldman, M. Heterogeneity of autoimmune diseases: pathophysiologic insights from genetics and implications for new therapies. *Nat. Med*. **21,** 730–738 (2015).
28. van Belle, T. L., Coppieters, K. T. & von Herrath, M. G. Type 1 diabetes: etiology, immunology, and therapeutic strategies. *Physiol. Rev*. **91,** 79–118 (2011).
29. Lesage, S. *et al.* Failure to censor forbidden clones of CD4 T cells in autoimmune diabetes. *J. Exp. Med.* **196,** 1175–1188 (2002).
30. Liston, A., Lesage, S., Wilson, J., Peltonen, L. & Goodnow, C. C. Aire regulates negative selection of organ-specific T cells. *Nat. Immunol*. **4,** 350–354 (2003).
31. Chentoufi, A. A. & Polychronatos, C. Insulin expression levels in the thymus modulate insulin-specific autoreactive T-cell tolerance: the mechanism by which the IDDM2 locus may predispose to diabetes. *Diabetes*. **51,** 1383–1390 (2002).
32. Bendelac, A., Rivera, M. N., Park, S. H. & Roark, J. K. Mouse CD1-specific NK1 T cells: development, specificity, and function. *Annu. Rev. Immunol*. **15,** 535–562 (1997).

Chapter 5

Conclusions

5.1 Final considerations, new scientific questions and future directions

In this Ph. D. thesis aspects of biology and bioengineering were combined to investigate the immune system and its function, either for translational applications (Chapter 2) or for basic studies (Chapter 3 and 4).

The project presented in Chapter 2 describes the development of an improved vaccine suitable for cancer immunotherapy. Since evasion of tumor cells from immunosurveillance has been recognized as a major factor leading to clinical disease [1], several therapies aimed at enhancing anti-tumor immunity have been adopted in the fight against cancer and are now either clinically available or under experimental testing [2]. Unfortunately, clinical data have pointed out the need for more efficacious immunotherapies, therefore much scientific interest, public attention and, more importantly, funding, have been given to the quest for better, safer and more specific therapies [3,4].

When exosomes were first described almost 20 years ago, their employment in cancer research was one of the first applications to be explored. Since then, a plethora of pre-clinical data has indicated that exosomes derived from tumor antigen-loaded DCs could be used as a vaccine to stimulate anti-tumor immunity for the control of tumor growth in murine models [5]. Clinical trials testing DC-derived exosomes for the vaccination of human cancer patients provided useful information on the feasibility and safety of this approach, yet showed limited therapeutic benefits due to weak immunogenicity [6,7].

Because of the experience of our group in the development of vaccines based on nanoparticles, we decided to investigate DC-derived exosomes as cancer immunotherapy. In particular, the aim of our project was to establish a protocol for the production of an exosome vaccine with increased immunogenicity in a murine melanoma model, thus providing an improved alternative to the exosome formulations previously tested on humans. As immunity is the result of antigen presentation in the context of a pro-inflammatory milieu [8], we adapted the procedure for the isolation of DC exosomes in order to couple loading of the DCs with a melanoma lysate, that provided antigens, to maturation of the DCs with poly(I:C), that provided pro-inflammatory danger signals. Exosomes inherit proteins and nucleic acids from the cells of origin, therefore our exosome production protocol resulted in a vaccine capable of inducing potent anti-melanoma immunity associated to significant reduction of tumor growth and prolonged survival of treated melanoma-bearing mice. Our findings suggest that the protocol proposed by our group is a valid and therapeutically promising alternative to the existing pre-clinical and clinical protocols for the production of exosome-based vaccines for cancer immunotherapy.

Even though our vaccine was capable of negatively affecting tumor growth, vaccination did not result in complete tumor eradication and, most importantly, almost half of the experimental mice treated with our vaccine formulation still died of melanoma. Therefore, further improvements are needed. In order to address these issues, we are currently evaluating the use of alternative TLR ligands during exosome production and, among others, we have decided to use MPLA due to the favorable safety and immunogenicity showed in several clinical trials employing MPLA as adjuvant for cancer immunotherapy [9]. In addition, we will also assess whether the combination of two or more TLR ligands could provide additional benefits to increase exosome immunogenicity.

The health of our organism critically depends on the unique ability of the immune system to discriminate self from non-self or mutated-self. Because of the complexity of the subject, a comprehensive understanding of the mechanisms that make this discrimination possible is still missing, even though enormous advancements have been made in recent years. For example, it is now accepted that specific subsets of peripheral non-hematopoietic cells display features of hematopoietic APCs and are therefore capable of presenting antigens to both $CD4^+$ and $CD8^+$ T lymphocytes, significantly contributing to immune tolerance [18-19].

The aim of the project presented in Chapter 3 was to show that the most abundant cell type of the liver, the hepatocyte, is also capable of antigen uptake and processing leading to MHC-I presentation (cross-presentation) and tolerance of antigen-specific $CD8^+$ T cells (cross-tolerance). Our findings suggest that the biggest blood-filtering organ of the organism is not only an essential metabolic compartment of the body but is also instrumental in the maintenance of immune homeostasis. In fact, the multitude of extracellular antigens circulating in the blood and filtered through the liver is directly accessible to both LSECs and hepatocytes. Continuous antigen sampling and presentation by LSECs and hepatocytes could be a major contributor to the maintenance of a tolerant TCR repertoire.

Persistency of hepatic infections, such as HBV and HCV, has been indicated as a drawback of liver tolerogenesis [10]. Our studies indicate that hepatocyte-dependent cross-tolerance can be significantly prevented by blocking PD-1/PD-L1 interactions between $CD8^+$ T lymphocytes and hepatocytes, respectively. We therefore propose that hepatocyte-specific blockade or down-regulation of PD-L1 could be a valid therapeutic alternative for the treatment of chronic viral hepatitis as compared to general and therefore unspecific blockade of PD-1/PD-L1 interactions, which has been proposed for clinical testing [11].

The results described in Chapter 3 prompted us to hypothesize that the liver may have a much more fundamental role in the maintenance of immune homeostasis. Since it has been

recently shown that stromal cells of the LNs contribute to the establishment of peripheral tolerance also by directly expressing and presenting otherwise peripheral tissue-restricted antigens [12-16], the aim of the project presented in Chapter 4 was to investigate whether promiscuous gene expression could also be part of the tolerogenic mechanisms employed by hepatic cells. We analyzed the expression of the two most characterized master regulators of promiscuous gene expression, *AIRE* and *Deaf1*, and observed that hepatocytes, but not LSECs, significantly express *Deaf1* and a list of other PTA-coding genes. In the NOD mouse model, that spontaneously develops T1D as well as other autoimmune manifestations [17], we could observe a trend pointing at a reduction of hepatocyte-dependent expression of *Deaf1*, *Ins1* and *Ins2* in autoimmunity-prone females as compared to autoimmunity-resistant males. Even though preliminary, our data suggest that hepatocytes are capable of promiscuous gene expression. It is therefore tempting to speculate that autoimmune manifestations could result from a multi-organ failure in tolerance development and that the liver could be one of the organs involved.

Many scientific questions are raised by our findings. We are currently performing experiments to investigate whether transcriptional regulators of promiscuous gene expression other than Deaf1 and other PTA-coding genes are expressed in hepatocytes. Most importantly, in order to claim any role for hepatocyte-dependent promiscuous gene expression in the physiology of the immune system and in the pathogenesis of autoimmunity, we first need to prove that PTA genes expressed in hepatocytes are also presented on MHC-I complexes to antigen-specific $CD8^+$ T lymphocytes, leading to tolerance. If the role of Deaf1 as master regulator of promiscuous gene expression in hepatocytes and induction of tolerance are proven, a mouse model of hepatocyte-specific *Deaf1* knock-out could be developed in order to analyze its immune phenotype. In fact, lack or reduction of promiscuous gene expression in the liver may be responsible for profound alterations of immune homeostasis, such as the development of multiple autoimmune manifestations as in NOD mice.

Last, the findings described in both Chapter 3 and 4 suggest that hepatocytes could represent a favorable target for therapeutic strategies aimed at either inducing tolerance, as in the case of autoimmunity or protein-replacement therapies for genetic diseases, or braking tolerance, as in the case of chronic viral infections.

In particular, hepatocyte-targeted delivery of tissue-specific antigens could be exploited to develop cross-tolerance as a prophylactic tolerogenic treatment prior to transplantation of the tissue or organ expressing those antigens. As a proof of concept, experiments of skin transplantation from skin-donor OVA-transgenic mice into wild-type recipient mice are ongoing in order to assess the survival rate of skin grafts in those animals

receiving OVA cross-presenting hepatocytes prior to skin transplantation. Results from these experiments will allow us to propose cross-presenting hepatocytes as an alternative to immunosuppressive drugs in transplantation.

5.2 References

1. Dunn, G. P., Old, L. J. & Schreiber, R. D. The immunobiology of cancer immunosurveillance and immunoediting. *Immunity.* **21,** 137–148 (2004).
2. Zitvogel, L., Tesniere, A. & Kroemer, G. Cancer despite immunosurveillance: immunoselection and immunosubversion. *Nat. Rev. Immunol.* **6,** 715–727 (2006).
3. Caspi, R. R. Immunotherapy of autoimmunity and cancer: the penalty for success. *Nat. Rev. Immunol*. **8,** 970–976 (2008).
4. Mellman, I., Coukos, G. & Dranoff, G. Cancer immunotherapy comes of age. *Nature*. **480,** 480–489 (2011).
5. Pitt, J. M. *et al*. Dendritic cell-derived exosomes as immunotherapies in the fight against cancer. *J. Immunol*. **193,** 1006–1011 (2014).
6. Escudier, B. *et al.* Vaccination of metastatic melanoma patients with autologous dendritic cell (DC)-derived exosomes: results of the first phase I clinical trial. *J. Transl. Med.* **3,** 10-13 (2005).
7. Morse, M. A. *et al.* A phase I study of dexosome immunotherapy in patients with advanced non-small lung cancer. *J. Transl. Med.* **3,** 9-8 (2005).
8. Iwasaki, A. & Medzhitov, R. Control of adaptive immunity by the innate immune system. *Nat. Immunol*. **16,** 343–353 (2015).
9. Steinhagen, F., Kinjo, T., Bode, C. & Klinman, D. M. TLR-based immune adjuvants. *Vaccine*. **29,** 3341–3355 (2011).
10. Knolle, P. A., Böttcher, J. & Huang, L.-R. The role of hepatic immune regulation in systemic immunity to viral infection. *Med. Microbiol. Immunol*. **204,** 21–27 (2014).
11. Barber, D. L. *et al*. Restoring function in exhausted CD8 T cells during chronic viral infection. *Nature*. **439,** 682–687 (2005).
12. Lee, J. W. *et al*. Peripheral antigen display by lymph node stroma promotes T cell tolerance to intestinal self. *Nat. Immunol*. **8,** 181–190 (2006).
13. Yip, L. *et al.* Deaf1 isoforms control the expression of genes encoding peripheral tissue antigens in the pancreatic lymph nodes during type 1 diabetes. *Nat. Immunol.* **10,** 1026–1033 (2009).

14. Cohen, J. N. *et al.* Lymph node-resident lymphatic endothelial cells mediate peripheral tolerance via Aire-independent direct antigen presentation. *J. Exp. Med*. **207,** 681–688 (2010).
15. Fletcher, A. L. *et al*. Lymph node fibroblastic reticular cells directly present peripheral tissue antigen under steady-state and inflammatory conditions. *J. Exp. Med*. **207,** 689–697 (2010).
16. Yip, L., Creusot, R. J., Pager, C. T., Sarnow, P. & Fathman, C. G. Reduced DEAF1 function during type 1 diabetes inhibits translation in lymph node stromal cells by suppressing Eif4g3. *J. Mol. Cell Biol.* **5,** 99–110 (2013).
17. Atkinson, M. A. & Leiter, E. H. The NOD mouse model of type 1 diabetes: As good as it gets? *Nat. Med*. **5,** 601–604 (1999).
18. Böttcher, J. P. *et al.* Liver-primed memory t cells generated under noninflammatory conditions provide anti-infectious immunity. *Cell Rep.* **3,** 779–795 (2013).
19. Hirosue, S. *et al.* Steady-state antigen scavenging, cross-presentation, and cd8+ t cell priming: a new role for lymphatic endothelial cells. *J. Immunol.* **192,** 5002–5011 (2014).

Acknowledgments

Graduate school is a roller coaster of emotions, especially if you live it as I have done: believing it is the beginning of a journey taking you to fulfill your dreams. As in every journey, there have been bright peaks of satisfaction and happiness, but also dark valleys of stress and disillusion. If I am here writing these words today, it is because I have finally reached the top of this mountain.
I must say, the view in front of me now is worth the effort.

This journey would not have been the same without some very special people, and I would like to dedicate a few words to each of them.

Jeff, my Advisor: thank you for trusting my skills, for continuously challenging me and stimulating my scientific interests with your ideas. You made me an independent scientist.

The members of my Ph. D. thesis committee, Prof. Gisou Van der Goot, Prof. Nicola Harris, Prof. Daniel Speiser and Prof. Shannon Turley: thank you for taking time to review my thesis and providing me with helpful scientific advice.

Mamma: non sarei qui se non fosse per il tuo amore incondizionato e gli innumerevoli sacrifici che hai compiuto per me. Sei la donna più forte che conosca. Dedico a te questa Tesi.
Mamma: I would not be here without your unconditional love and the countless sacrifices you made for me. You are the strongest woman I know. This Thesis is dedicated to you.

Papà: anche se separati, la tua presenza è più forte che mai. Ogni giorno cammini al mio fianco.
Papà: we are apart but your presence has never been stronger. You walk with me every day.

Alba & Giorgia: abbiamo sempre avuto un rapporto particolare, ma so per certo che senza di voi sarebbe tutto peggiore.
Alba & Giorgia: our relationship is atypical, but I do know things would be worse without you.

Scott: let's put it in this way, if it weren't for you, your patience, your support, your friendship and your endless help in the lab and outside, I would not be on top of this mountain

now. “Thanks” does not get even close to what I would like to express, but thanks anyway. You know the rest.

Ari & Monica: dopo tutti questi anni siamo ancora noi e siamo ancora insieme. Sono fortunata ad avervi come migliori amiche sin da quando eravamo praticamente bambine. Mi avete sempre dato supporto e volute bene, nei momenti positivi e, soprattutto, in quelli negativi. Grazie, grazie, grazie.
Ari & Monica: after all these years we are still us and we are still together. I feel so lucky for having you as my best friends since we were little girls. You have always supported me and loved me, in good and especially bad moments. Thank you, thank you, thank you.

D!!! Hai reso Losanna una vera e propria avventura: gli orsetti gommosi, le chiacchierate intorno al cactus, le cene a base di salmone e toast…tutto ciò è successo insieme a te. Già a Milano avevo capito che saresti stata l’”Amica fuori di testa” :D Grazie.
D!!! You have made Lausanne such an adventure for me: gummy bears, “cactus talks”, salmon & toasted bread dinners…all happened with you. Already back in Milan I could tell you would be the “Crazy Friend” :D Thank you.

MantiZZZ: gli appunti sono già pronti per la stesura del nostro libro a quattro mani. Sarà senz’altro un successo editoriale strepitoso!
MantiZZZ: I have my notes ready for our book. It will be an amazing editorial success for sure!

Eleo: il tuo contributo si è rivelato preziosissimo in un momento in cui mi sono ritrovata a corto di speranze e d’aiuto. Grazie al tuo aiuto ho pubblicato il mio primo articolo come primo autore. Grazie.
Eleo: your input was priceless in a moment where I really found myself hopeless and helpless. Your help gave me my first first-author paper. Grazie.

Pépette: Merci pour ton optimisme et ta compagnie pendant les longues nuits et les week-ends solitaires dans le labo. Also, you have been the best Britney Spears concert mate ever! We rocked in Vegas :)
Pépette: Merci for your optimism and your company during the long and lonely nights and weekends spent in the lab. Also, you have been the best Britney Spears concert mate ever! We rocked in Vegas :)

Giacomo & Saverio: you have been my favorite LMRP technicians. True you were the only technicians in the lab, but you guys are still my favorite. Your support for all of my *in vivo* experiments has been incroyable. Merci, les gars!

LMRP & LLCB present and past peeps: some of you have helped me a lot with my experiments, some others have been good company in my (unfortunately rare) moments off, but for sure you have all contributed to make my Ph. D. experience unique and positive. Thank you very much.

Alessio: the best tutor I could have been given as a master student. You dedicated your time to me and trusted me in the lab when I could barely hold a pipette in my hand. But, mostly, you showed me how cool it was to be a scientist. So here I am! :) Even though I am afraid I have inherited your "scientific OCD", I am forever grateful for the positive example you still represent to me.

Prof. Naldini & Naldini lab: cool lab with cool scientists working on cool science. I am so thankful I got the chance to start as a student in such a stimulating and friendly environment. I learned most of the things I know about what it means "to do science" from you. Thanks for taking care of my training and education at such an early stage of my career.

Prof. Salvioni, Prof.ssa Pecci, Prof.ssa De Mauri, Prof.ssa Cuzzolin & Prof. Murer: you have inspired the teenager me to become whatever I wanted to be because you believed I could make it. You pushed me to work hard, supported my interests, rewarded my efforts and helped me find my way. Thanks.

Now the journey continues.

I am very looking forward to the people I will meet, the experiences I will live and the places I will see.

Martina Damo

Rue Saint-Roch 5
1004 Lausanne, Switzerland
+41 78 627 97 15

Born 12.01.1986
Italian nationality
martina.damo@epfl.ch

EDUCATION

2011-present **Swiss Federal Institute of Technology (EPFL)**, Lausanne, Switzerland
- **Ph.D. Biotechnology and Bioengineering**, expected graduation: April 2016

2005-2010 **Libera Università San Raffaele**, Milan, Italy
- **M.Sc. Molecular and Cellular Biotechnology**, GPA: 110/110 magna cum laude
- **B.Sc. Medical and Pharmaceutical Biotechnology**, GPA: 110/110

RESEARCH EXPERIENCES

2011-present **Lab. For Regenerative Medicine and Pharmacobiology (LMRP)**, EPFL
- **Ph.D. thesis**
- Exosome-based cancer vaccine immunotherapies
- Liver-dependent mechanisms of immune tolerance
- Thesis director: Prof. Jeffrey A. Hubbell

2010-2011 **Gene transfer and new gene therapy strategies Lab**, San Raffaele-Telethon Institute for Gene Therapy, Milan
- **Research Fellow**
- Pre-clinical development of lentiviral vectors for liver-directed Hemophilia B gene therapy in large animal models
- Advisor: Prof. Luigi Naldini

2008-2010 **Gene transfer and new gene therapy strategies Lab**, San Raffaele-Telethon Institute for Gene Therapy, Milan
- **M.Sc. thesis**
- Optimization of lentiviral vectors for liver-directed Hemophilia B gene therapy
- Thesis director: Prof. Luigi Naldini

2007-2008 **Neuropsychopharmacology Lab**, San Raffaele Scientific Institute, Milan
- **B.Sc. thesis**
- Molecular mechanisms and brain circuits of drug addiction
- Thesis director: Prof. Flavia Valtorta

PEER-REVIEWED PUBLICATIONS

Wilson DS, **Damo M**, Hubbell JA. Synthetic glycopolymer-antigen conjugates induce antigen-specific immune tolerance. *In preparation*

Damo M, Wilson DS, Hubbell JA. Hepatocytes efficiently establish cross-tolerance by inducing deletion and anergy of antigen-specific CD8+ T cells via the PD-1/PD-L1 pathway. *In preparation*.

Damo M, Wilson DS, Simeoni E, Hubbell JA. TLR-3 stimulation improves anti-tumor immunity elicited by dendritic cell exosome-based vaccines in a murine model of melanoma. *Sci. Rep*. **2015**. *In press*.

Lombardo A, Cesana D, Genovese P, Di Stefano B, Provasi E, Colombo DF, Nery M, Magnani Z, Cantore A, Lo Riso P, **Damo M**, Pello OM, Holmes MC, Gregory PD, Gritti A, Broccoli V, Bonini C, Naldini L. Site-specific integration and tailoring of cassette design for sustainable gene transfer. *Nat. Methods*. **2011**;8(10):861-9.

Matrai J, Cantore A, Bartholomae CC, Annoni A, Wang W, Acosta-Sanchez A, Samara-Kuko E, De Waele L, Ma L, Genovese P, **Damo M**, Arens A, Goudy K, Nichols TC, von Kalle C, L Chuah MK, Roncarolo MG, Schmidt M, Vandendriessche T, Naldini L. Hepatocyte-targeted expression by integrase-defective lentiviral vectors induces antigen-specific tolerance in mice with low genotoxic risk. *Hepatology*. **2011**;53(5):1696-707.

CONFERENCE PROCEEDINGS

2015 **American Association for Cancer Research (AACR)** meeting on tumor metastasis, Austin, TX. Improving the immunogenicity of Dexo-based vaccines for the immunotherapy of melanoma. *Poster presentation*.

2015 **European Congress of Immunology (ECI)**, Vienna, Austria. Role of PD-1/PD-L1 interactions in hepatocyte-dependent CD8+ T cell tolerance. *Poster presentation*.

2014 **Biomedical Engineering Society (BMES)** meeting, San Antonio, TX. TLR3 stimulation enhances the immune stimulatory properties of exosome-based vaccines. *Oral presentation*.

2014 **International Society for Extracellular Vesicles (ISEV)** meeting, Rotterdam, the Netherlands. Exosome-based vaccines: a novel TLR-7 agonist enhances immune stimulatory properties of DC-derived exosomes. *Oral presentation*.

TEACHING EXPERIENCES

2015-2016 **Life Sciences and Technology (SV)**, M.Sc. program, EPFL: Project Supervisor

- Supervised EPFL M.Sc. student on engineering exosome-secreting DC cell lines

2014-2015 **Life Sciences and Technology (SV)**, M.Sc. program, EPFL: Project Supervisor
- Supervised EPFL M.Sc. student on characterizing the cross-presentation molecular machinery in primary murine hepatocytes by confocal microscopy

2014 **International Summer Research Program**, EPFL: Tutor
- Supervised undergraduate student from Indiana University on expressing tumor endothelium targeting protein therapeutics

2012-2013 **Life Sciences and Technology (SV)**, B.Sc. program: Teaching Assistant
- Integrated Laboratory in Life Sciences
- Cellular and Molecular Biology III

2012 **Life Sciences and Technology (SV)**, B.Sc. program, EPFL: Project Supervisor
- Supervised EPFL B.Sc. student on purifying tumor cell-derived exosomes

2007 **B.Sc. Medical and Pharmaceutical Biotechnology**, Libera Università San Raffaele: Project Coordinator
- Editorial project "Biotech Book" on cell biology for high-school students

SOCIETY MEMBERSHIPS

2014-present Biomedical Engineering Society (BMES)
2015-present American Association of Immunologists (AAI)

SKILLS

Languages: Italian (mother tongue), **English** (competent spoken and written), **French** (fair spoken and written)

Lab: cell culture; multi-color flow cytometry; bone marrow isolation from mice; HSC isolation from mouse bone marrow; bone marrow transplantation in mice; skin transplantation in mice; total cell, CD4+ and CD8+ T cell isolation from mouse spleen and LN; multi-organ perfusion in mice; liver cell isolation; i.p., i.d. and s.c. injections in mice; BMDC differentiation and maturation; DC-T cell co-culture; antigen-specific and polyclonal T cell activation and restimulation; cell proliferation assay (radioactive and non-radioactive); immunofluorescence; confocal microscopy on cultured cells and tissue sections; transmission electron microscopy; PAGE; western blot; ELISA; DNA gel electrophoresis; southern blot; DNA cloning techniques; DNA plasmid prep; PCR; RNA extraction; RT-PCR; gene expression analysis; lentiviral vector cloning, production and use; P1 and P2 biosafety level work; experience with HBV transgenic

mouse model; experience with Hemophilia B transgenic mouse model; experience with NOD mouse model and glycemia monitoring.

IT: Microsoft Office Package, GraphPad Prism, FlowJo, Adobe Illustrator, Scaffold4.

INTERESTS

Road biking, mountain hiking, international politics, drawing and painting, travelling, ballet, musicals, reading, Latin and Greek classic literature, ancient history.